Review

Graphene derivative based hydrogels in biomedical applications

Journal of Tissue Engineering
Volume 15 1–54

DOI: 10.1177/20417314241282131
journals.sagepub.com/home/tej

Feifei Ni, Yangyang Chen, Ze Wang, Xin Zhang, Fei Gao, Zengwu Shao and Hong Wang

Abstract

Graphene and its derivatives are widely used in tissue-engineering scaffolds, especially in the form of hydrogels. This is due to their biocompatibility, electrical conductivity, high surface area, and physicochemical versatility. They are also used in tissue engineering. Tissue engineering is suitable for 3D printing applications, and 3D printing makes it possible to construct 3D structures from 2D graphene, which is a revolutionary technology with promising applications in tissue and organ engineering. In this review, the recent literature in which graphene and its derivatives have been used as the major components of hydrogels is summarized. The application of graphene and its derivative-based hydrogels in tissue engineering is described in detail from different perspectives.

Keywords

Graphene, graphene oxide, graphene quantum dots, hydrogel, tissue engineering

Date received: 5 June 2024; accepted: 24 August 2024

Introduction

Hydrogel is a type of high molecular polymer with a three-dimensional(3D) network structure. It has strong water absorption and water retention properties and can maintain the stability of cross-linked networks, chain entanglements or crystalline regions. Hydrogel has flexible and adjustable physical and chemical properties, excellent biocompatibility and porous structure, which makes it have important application prospects in biomedicine, bioelectronics, intelligent drive, sustainable energy and water resource utilization.[1]

With the development of science and technology, the application areas of hydrogels are constantly expanding. In the field of vaccines, given the huge challenges posed to global public health by the recent outbreak of COVID-19 coronavirus infection. The development of next-generation vaccine technology to quickly transform wild virus strains into safe and effective vaccines has broad prospects. Live virus vaccines in hydrogels can aggregate immune cells at the injection site. The hydrogel prevents the escape of viral particles and induces strong antigen-specific responses and immune memory in the local inflammatory environment, which can provide effective protection for mice from the attack of deadly viruses, which helps to quickly develop safe and effective vaccines.[2] In the field of tumor treatment, immunotherapy is a revolutionary change. However, limited therapeutic effects and severe immune-related side effects are common challenges. Immunomodulatory hydrogels have the unique

Department of Orthopedics, Union Hospital, Tongji Medical College, Huazhong University of Science and Technology, Wuhan, China

Corresponding authors:
Hong Wang, Department of Orthopedics, Union Hospital, Tongji Medical College, Huazhong University of Science and Technology, Wuhan 430022, China.
Email: chinahust89@163.com

Fei Gao, Department of Orthopedics, Union Hospital, Tongji Medical College, Huazhong University of Science and Technology, Wuhan 430022, China.
Email: 2516067450@qq.com

Zengwu Shao, Department of Orthopedics, Union Hospital, Tongji Medical College, Huazhong University of Science and Technology, Wuhan 430022, China.
Email: ProSHUST@163.com

ability to enhance immune activation and reduce systemic toxicity by encapsulating multiple components such as anti-CD47 antibodies, PD-L1 binding peptides and local administration such as IFN-2b, cyclic dinucleotide, etc. and activating immune cells such as dendritic cells(DCs), macrophages, and cytotoxic T cells. The latest studies have shown that specific CAR-T lymphocytes combined with injectable hydrogels not only significantly enhance the activation, proliferation and migration of T cells, but also the hydrogels can be loaded with a variety of cytokines including IL-2, IL-7 and IL-15 to support the activity of CAR-T cells, thereby maximizing the functional potential of CAR-T cell hydrogel scaffolds.[3–5] Graphene hydrogels also have great application prospects in the field of wearable electronics. Soft, stretchable and biocompatible conductors are necessary for skin and implantable electronics. Studies have shown that a laser-induced graphene/PVA-PA-PPH hydrogel film has super stretchability, ultra-thinness and viscosity, and can be used for skin monitoring and cardiac electrical signal monitoring. In another study, the flow sensor constructed by VGNs/PVA plays an important role in monitoring flow parameters (including flow rate, speed, direction and rotation frequency). It has high sensitivity and can detect tiny frequencies and flow rates.[6–8] The test results in the 3D printed vestibular system show that the sensor has the ability to develop a new generation of artificial vestibular implants, and its function is closest to vestibular hair cells. Therefore, these studies have greatly enriched the application field of graphene-based hydrogels.

With the improvement of people's requirements for a high quality of life continue to promote the development of new fusion technologies. 3D printing technology, also known as additive manufacturing, rapid prototyping, and solid freeform manufacturing is based on computer-aided design (CAD)[9,10], 3D model data, and integrates cutting-edge technologies in the fields of digital modeling technology, electromechanical control technology, information technology, material science, and chemistry. It adopts a layer-by-layer manufacturing method, which has unique advantages such as high efficiency, speed, and no need for combination and assembly.[11–13] It has been applied in various fields including tissue engineering, regenerative medicine, aerospace engineering, and robotics engineering.[14,15] There is high application potential for 3D printing in the medical field; 3D bioprinting can be used to accurately distribute loaded cells, rationally manufacture structured scaffolds to control cell behavior and promote tissue development, and construct complex 3D functional living tissues or artificial organs. It is helpful in solving the problems of organ and donor shortages in the medical field.[16–18] In aerospace, the introduction of nano-nucleating agents that control solidification during the 3D printing process can overcome the unbearable microstructure of large columnar grains and periodic cracks caused by the melting and solidification dynamics during the printing process. This method manufactured high-strength aluminum alloy has a crack-free, equiaxed (i.e. the length, width and height of the grains are approximately equal), fine-grained microstructure, making the material strength comparable to that of deformed materials, significantly improving the materials strength, fatigue life and Fracture toughness.[19] In the field of electronics, the structure and surface area of fused deposition modeling 3D printed electrodes are significantly more flexible than copper, aluminum and carbon electrodes. At the same time, 3D scaffolds based on highly conductive nanocomposites are significantly better than hot-pressed solid scaffolds in terms of electromagnetic interference (EMI) and fluid sensing.[20] However, existing materials have advantages and disadvantages; therefore, there is an urgent need to develop more effective 3D bioprinting materials for soft and hard tissues.

Carbon is one of the most widely distributed elements in nature and many allotropes form carbon materials with unique structures. Graphene is a two-dimensional carbon nanomaterial that is peeled from graphite and is composed of carbon atoms in sp2 hybrid orbitals, forming a hexagonal honeycomb lattice. This is the thinnest one-atom thickness of any known material.[21,22] Graphene oxide (GO) is an oxide of graphene. After oxidation, the number of oxygen-containing functional groups such as carboxyl, hydroxyl, and epoxy groups increases, making it more active than graphene and having good hydrophilicity, physical and chemical properties. The performance of hydrogel-GO composites composed in different forms not only overcomes the limitations of individual components (poor mechanical properties and low biocompatibility, respectively). It also has excellent in vitro and in vivo biocompatibility, angiogenesis, cell growth effects, antibacterial properties, conductivity and adsorption capacity. Therefore, it has a bright future in the fields of drug delivery, wound healing, bone tissue engineering.[23] About rGO, graphene oxide uses chemical, thermal or electrochemical methods to reduce some of the oxygen-containing groups on the surface of graphene oxide under the action of a reducing agent to generate reduced graphene oxide. Compared with GO, it has a stronger conductivity due to the sharp reduction of oxygen-containing functional groups. It has excellent thermal stability, adsorption, large surface area, high photocatalytic activity, etc. After combining with hydrogel, the hydrogel has good conductivity and flexibility, especially in the fields of nerve and heart repair and environmental engineering has broad application prospects.[24–26] GQDs refers to a hot material in the graphene family with a graphene sheet size of less than 100nm and a sheet number of less than 10 layers. GQDs plays an important role in the biomedical field due to its 3D porous structure, large specific surface area, good biocompatibility and low toxicity. GQDs hydrogel can effectively promote bone healing, antibacterial, wound healing,

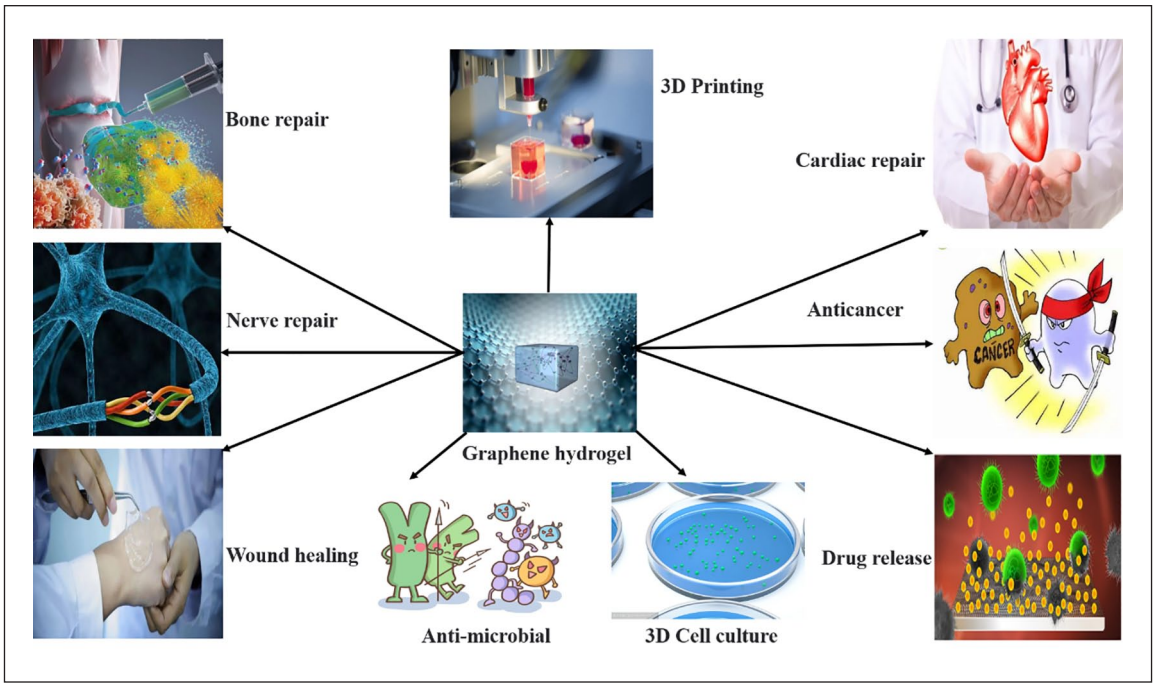

Figure 1. Medical applications of hydrogels composed of graphene and its derivatives.

and nerve repair.[27,28] However, since GQDs is a relatively new member of the graphene family, its performance and potential applications have not been fully understood, and it is necessary to conduct in-depth research on it.

Graphene is considered a revolutionary material owing to its excellent optical, electrical, and mechanical properties and good biocompatibility, which have important application prospects in materials science, energy, biomedicine, and other fields has important application prospect.[29,30] For example, studies have shown that a surface plasmon resonance sensor (SPR) based on graphene film, when combined with catalytically inactive CRISPR-associated protein 9 (dCas9), achieves excellent sensing performance and can be used to analyze recombinant plasmids with only three base mutations, and can achieve rapid, accurate, sensitive and specific detection for the diagnosis of Duchenne muscular dystrophy with two exon deletions, different variants of SARS-CoV-2, and early diagnosis of lung cancer. At the same time, this plasmon resonance (SPR) biosensor framework integrates DNA origami and DNA scissors technology. This method combines the accuracy of DNA origami probes with the inherent single-base resolution of DNA scissors, achieving ultra-sensitive diagnosis of early lung cancer at the single-base level, systematically solving the limitations of traditional SPR technology and improving detection accuracy.[31–34] Graphene derivatives such as graphene oxide (GO), reduced graphene oxide (rGO), and other derivatives have a wider range of functions and application prospects than original graphene. Three-dimensional scaffolds containing graphene can appropriately simulate in vivo conditions to promote cell adhesion, proliferation, and differentiation owing to their unique characteristics such as good porosity and wrinkles, which are conducive to cell-to-cell and cell-to-scaffold interactions. Moreover, graphene and its derivatives have been used in the pharmaceutical, genetic engineering, antibacterial, biological imaging, tissue engineering (Figure 1), and 3D cell culture fields, among others.[35,36] Therefore, graphene has great potential for applications in the field of tissue engineering. In this review, we summarize the applications of hydrogels composed of graphene and its derivatives in biological tissue engineering.

Graphene and its derivative based hydrogels as 3D bioprinting bioinks

With the emerging 3D printing technology, various complex and personalized structures can be accurately realized. Due to its excellent specific surface area, rich functional groups, excellent electrical/thermal conductivity and outstanding mechanical properties, graphene-based hydrogels can be used as ideal inks for printing complex 3D structures with high stacking and high shape fidelity. This new strategy greatly enriches the construction of advanced hydrogels with good mechanical properties and complex shapes, and expands its application in the field of tissue engineering.

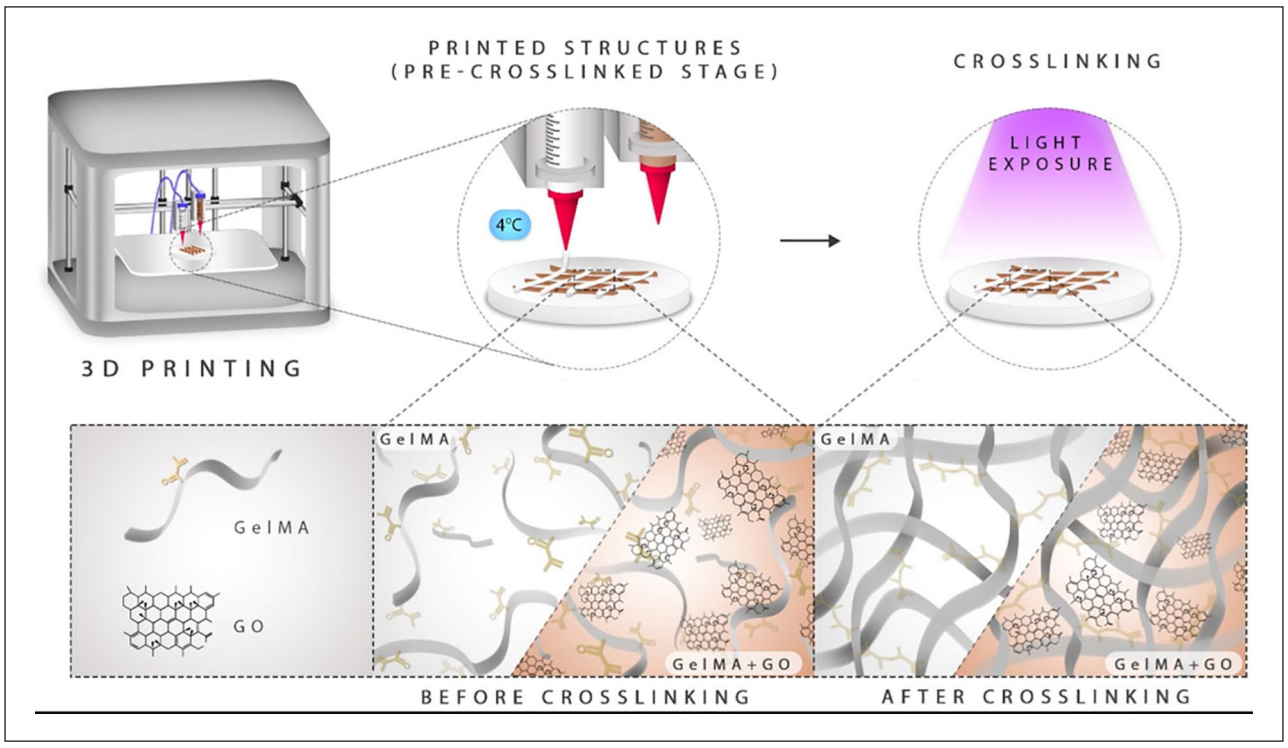

Figure 2. Graphical representation of the extrusion printing process of the hybrid electroactive hydrogel composed of gelatin methacryloyol (GelMA) and graphene oxide (GO).[38]

GO

Research has found that GO can be combined with various hydrogels to produce bioinks with different printing characteristics. Fe3+-assisted crosslinked GO ink with excellent rheological properties and printing performance was used to print scaffolds at room temperature using microextrusion 3D printing technology, and they exhibited good filament spacing and diameter. The dynamic energy storage modulus G" and loss modulus G" of Fe3+-modified GO hydrogels were both increased by 1.7 orders of magnitude compared to pure GO hydrogels. In addition, GO has a controlled porous structure conducive to enhanced oxygen and nutrient transport. GO ink has low cytotoxicity, and HepaRG cells showed good viability and attachment behavior on it, regardless of whether the scaffold was superficial or internal.[37] Gelatin methacryloyl alcohol (GelMA) and GO hydrogels have been used for 3D printing and are electroactive. The addition of extremely small amounts of GO to 5% w/v GelMA hydrogels resulted in an approximately 35-fold decrease in impedance at 1 Hz compared with GelMA alone, whereas a more than 6-fold increase in charge injection capacity was attributed to the increased electroactive surface area of GO, which also enabled the 3D printed structure to exhibit higher electrical activity than the non-printed structure. The addition of GO improved the mechanical properties of the hydrogel by approximately twofold, while also enhancing the rheological properties of the composite. Compared with pure GelMA, GelMA-GO improved the shape fidelity and integrity of the 3D printed structure, significantly increased PC-12 cell viability, and enhanced metabolism on the GO hydrogel.[38] The hydrogel was directly mixed with MSCs as a bioink for 3D scaffold printing for bone regeneration and repair. The introduction of GO had no effect on the cell printing activity or printability of GelMA. MSCs secrete more actin fibers in response to GO, thereby promoting osteogenesis. Compared with cells cultured in GelMA alone, GO scaffolds stimulated osteogenic differentiation, and the expression of osteoblast-related genes and proteins, such as OPN, OCN, and RUNX2, was increased. In summary, the composite bioink enhanced cell proliferation, adhesion, and osteogenic differentiation properties[39] Figure 2.

Phenol-rich gelatin (GHPA) and GO constitute bioinks that mimic the ECM with high fidelity and viability of loaded cells. GO nanoparticles were successfully incorporated into GHPA without any adverse effects on its microstructure and mechanical properties and with improved thermal stability. The 3D scaffold provided a suitable microenvironment for C2C12 myoblast differentiation, and promoted cell attachment, migration, and proliferation, as well as growth in the printing direction. GO can induce spontaneous myogenesis in C2C12 myotubes by

enhancing the adsorption of fibronectin and albumin and accelerating intercellular signaling. In addition, the appropriate shear stress generated by 3D printing and the biochemical effects of GO can synergistically induce the directional alignment of C2C12 cells for myocyte maturation.[40] Furthermore, the SISMA-GO bioink made of acellular small intestinal submucosa (SISMA) and GO was successfully embedded in hADMSCs to mimic the ECM. The addition of GO enhanced the conductivity of the ink without affecting its rheological and shear-thinning properties, which could be used for electrical stimulation and extrusion 3D bioprinting. When GO was added, the stem cells extended more filopodia to promote cell adhesion and the proliferation rate increased. The stem cells retained high viability on the scaffold after 1 week.[41] Other studies have found that GO composite inks based on photocrosslinked alginate, gelatin, and chondroitin sulfate can be used to mimic the ECM of cartilage. GO enhances printability and improves the shape fidelity and resolution of printed scaffolds. In addition, the liquid crystalline nature of GO enables the 3D printed scaffold to produce an anisotropic structure that helps to obtain an ordered cell distribution. The hADMSC proliferation experiment showed that, compared with the pure hydrogel, the GO scaffold exhibited a uniform distribution and high proliferation ability and could guide the cells to proliferate along the direction of the 3D printed line. In contrast, the direction of the cells in the pure hydrogel was random. In addition, the results showed that 3D printed scaffolds containing GO induced chondrogenic differentiation in the absence of exogenous chondrogenic factors after 28 days of culture, and GO significantly improved the ECM deposition of cells on 3D printed scaffolds.[42] Similarly, the new bioink composed of collagen, chitosan, and GO could provide a good cartilage microenvironment and significantly enhance chondrogenic ability. The new cartilage of the 3D printed scaffold containing GO was thicker, and the expression of collagen type 2, Rank, OP-1, and MMP13 was higher than in other scaffolds. The chondrocytes of the 3D printed scaffold containing GO expressed Rank, whereas the cells of the 3D printed scaffold without GO did not. Therefore, GO scaffolds may play a protective role in cartilage tissue via the Rank/Rankl/OPG signaling pathway.[43] A higher GO concentration (1 mg/ml) improved bioprintability, fidelity, biodegradability, neuroconductivity, and cell-to-cell interactions in bioinks made of alginate gelatin and GO. Compared with the 2D environment, the microenvironment created by the 3D printed structure was more conducive to the neural differentiation of WJ-MSCs, and the expression of neural differentiation markers was higher. This ink was mixed with hMSCs to make a biological ink. GO (1 mg/ml) caused the highest degree of osteogenic differentiation in hMSCs and upregulated the expression of osteogenesis-related genes (ALPL, BGLAP, and PHEX). A cell-loaded 3D GO bone-defect scaffold was successfully printed using a mouse skull model, and after 42 days of culture, micro-CT and histological staining confirmed that 1 mg/ml GO ink maintained the best printed scaffold fidelity and the highest mineralization formation. Compared to pure hydrogels, GO composite bioinks exhibit better 3D bioprinting capabilities.[44,45] In composite hydrogels formed of 3 wt% chitosan and 0.5 wt% GO (CH-GO), GO significantly increased the printability, fidelity, and viscoelasticity of the hydrogels. The nerve cells cultured on the CH3GO-5 scaffold were evenly spread and well differentiated, whereas those on the CH3GO-0 scaffold remained undifferentiated after 20 days of observation. Electron microscopy revealed that CH3GO-5 had larger pores; an increased pore area promotes the diffusion of nutrients and oxygen, making it easier for cells to attach and differentiate. This suggests that GO promotes the neuronal differentiation of SH-SY5Y cells.[46]

Alginate-GO (Alg-GO) composite hydrogel has been used as a bioink and GO significantly improved the viscosity and shear-thinning characteristics of the ink. Bioink containing 3% Alg and 0.5 mg/ml GO exhibited the most balanced characteristics, including printability and structural stability. This type of GO bioink exhibited the highest calcium deposition, ALP activity, and expression of osteogenic markers during the osteogenic culture of hMSCs. hMSCs on 3D printed scaffolds showed good proliferation and survival rates, which may be due to the antioxidant activity and protein adsorption of the GO components. The cells were minimally damaged by shear stress during printing and remained viable for up to 7 days[47] Figure 3. The ink also showed good compatibility with ADSCs seeded onto 3D scaffolds or wrapped in GO-containing ink for direct 3D printing. Compared with the GO-free printed scaffold, the 3D scaffold containing GO showed better cell viability and morphology, and especially protected the cells from shear stress during extrusion, indicating that GO has a protective and proliferative effect on the cells. GO scaffolds have larger pores and more cell-anchoring sites for cell growth.[48] In addition, GO-glucan hydrogels can be used for microfluidic 3D printing. GO concentrations in the range of 4–7 mg/ml showed excellent 3D printing adaptability, fibers were uniform and stable, and rheological tests showed that a DEX/GO solution exhibited suitable shear-thinning and shear-yield behaviors. A live/dead experiment showed that NIH3T3 cells maintained a normal morphology, and cell viability increased significantly after 3 days of hydrogel culture. Furthermore, the microfibers exhibited excellent electrical conductivity owing to the incorporation of GO.[49,50] With the development of science and technology and economy, people have higher requirements for wearable devices. Based on the combination of DEX/GO hydrogel and microfluidic 3D printing technology, a series of complex 3D wearable devices have been generated. They have good conductivity, self-healing ability, flexibility and responsiveness to deformation, and

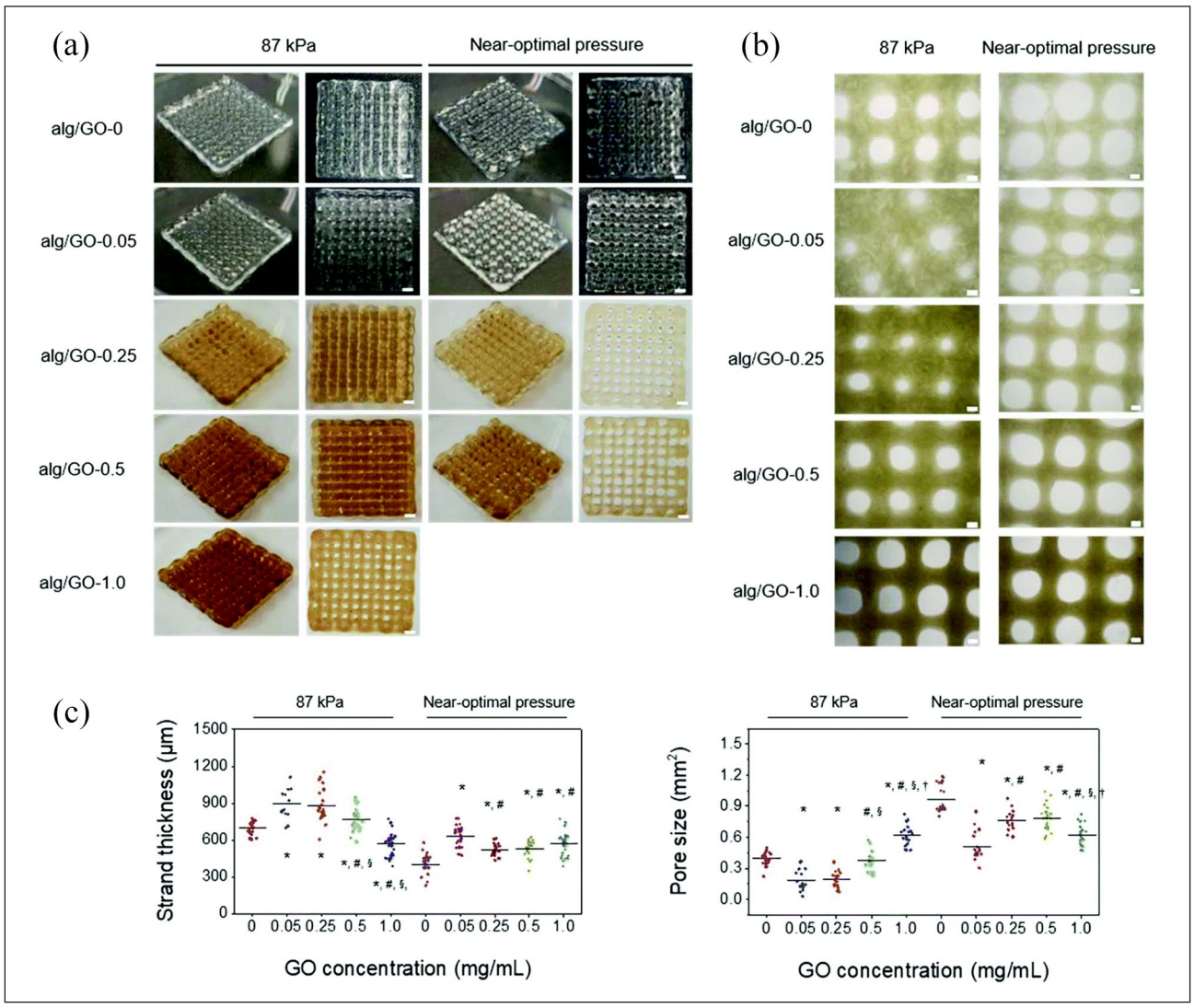

Figure 3. 3D printing of various alg/GO bioinks. (a) Photographs of the printed scaffolds (scale bars = 2 mm). (b) Optical micrographs of the top view of the printed scaffolds. Scale bars = 300 μm. (c) Dimensions of the strand thickness and pore size of the printed scaffold with each ink. *, #, §, † indicate significant differences with the alg/GO-0, alg/GO-0.05, alg/GO-0.25, and alg-GO/0.5 respectively ($p < 0.05$).[47]

can sense various movements of the human body. In addition, the ability to monitor subtle throat movements during speech and convert these stimuli into resistance signals shows their potential in the field of flexible electronics and provides a potential printing method for building functional materials for various applications. However, there are many types of hydrogels that can be used for 3D printing, and their functions are also different. There are also many types of 3D printers. In the future, our researchers should focus on commercialization rather than just applying it to laboratories, allowing consumers to choose bioinks and 3D printers according to their different preferences, and pay more attention to the application from theory to practice, so that this technology can truly enter thousands of households.

A printable composite hydrogel composed of GelMA, neural stem cells, and graphene nanoparticles was constructed using stereolithography 3D bioprinting technology. The porous GelMA hydrogel provides a biocompatible microenvironment for the survival and growth of neural stem cells. The addition of graphene did not affect cell growth and promoted neuronal differentiation. The printed structures were clear and the cells were evenly distributed. After 2 weeks of culture, neural stem cell(NSCs)within the printed constructs showed neuronal differentiation and neurite extension.[51] Hydrogel prepared from methyl methacrylate chitosan (ChiMA) and graphene nanosheets was suitable for 3D solution printing. The addition of graphene increased the G′ and G″ of ChiMA, which behaves as a viscous fluid, with G″ being more dominant than G' to

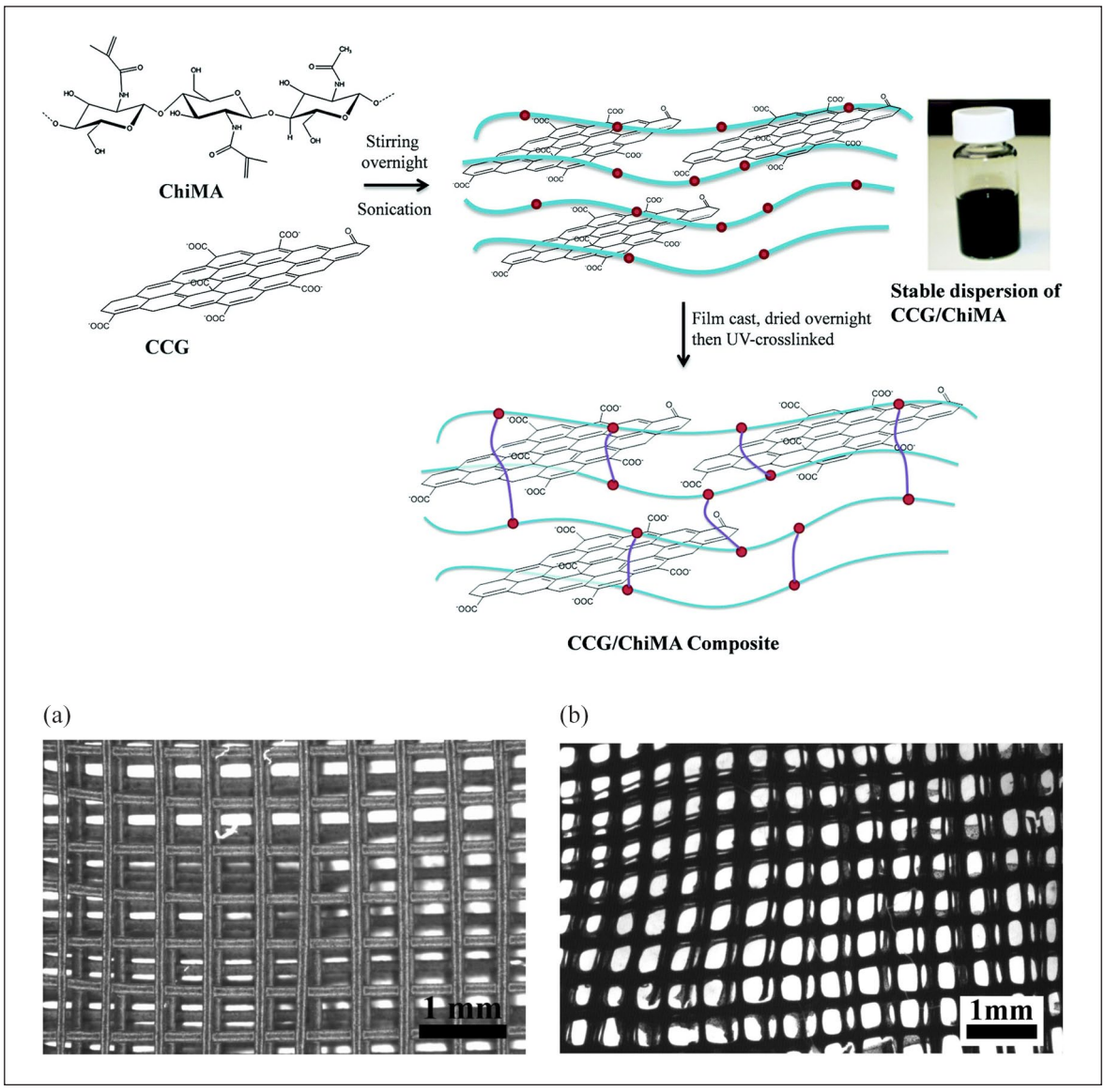

Figure 4. Schematic depicting the preparation of a CCG/ChiMA composite with the resulting stable dispersion shown (inset). ChiMA 3CCG scaffolds fabricated by extrusion printing (a) after printing in isopropanol, and (b) after UV-crosslinking and soaking in PBS for 10 days.[52]

maintain the printed shape. The performance of the composite was significantly better than that of ChiMA alone, with more than 57% improvement in tensile strength and several orders of magnitude improvement in electrical conductivity. The addition of graphene also improved the adhesion, proliferation, and spreading of L929 fibroblasts. The printed scaffolds remained structurally intact after 10 days of immersion in PBS[52] Figure 4. Graphene-polyurethane nanocomposite hydrogel has suitable rheological properties for 3D printing and survival of NSCs. Polyurethane is sufficiently degradable to cover the graphene surface to make the bioink relatively non-toxic, and its dispersion undergoes a sol-gel transition at near human body temperature. The addition of a very low concentration (25 ppm) of graphene significantly enhanced oxygen metabolism (increased 2–4 times), cell viability, and neural differentiation of NSCs, and increased GFAP, β-tubulin, and MAP2. The mechanism of graphene regulation of oxygen metabolism may be that sp2 on the surface of graphene provides a stable resonance structure for free π electrons. It has the characteristics of a short gelling time (850 s) and long extrusion operation window. In addition, the hydrogel provides a suitable 3D environment for the proliferation and differentiation of NSCs.[53]

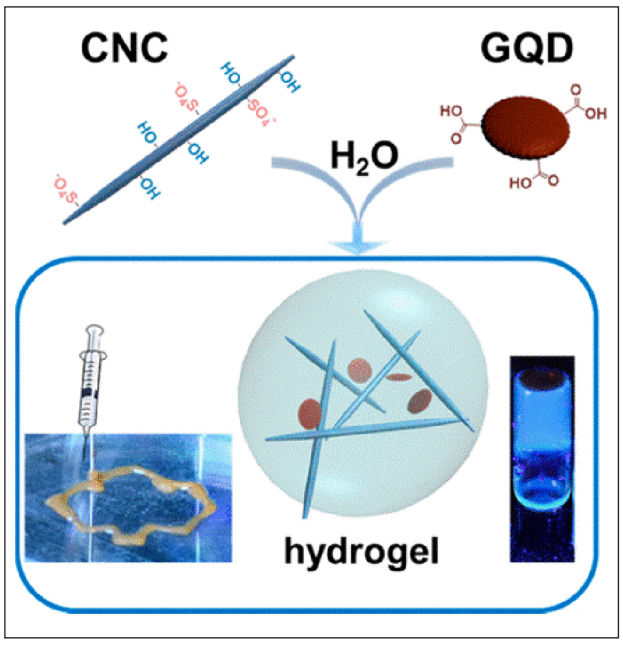

Figure 5. Schematic of the formation of the CNC-GQD hydrogel.

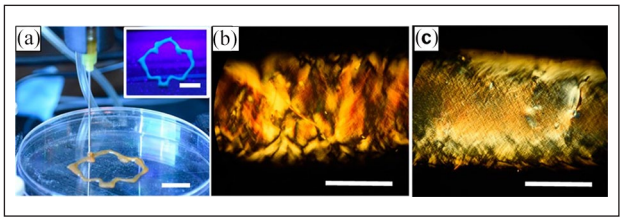

Figure 6. (a) 3D printing of the CNC-GQD hydrogel formed at CCNC = 50 mg/ml and CGQD = 10 mg/ml. The scale bar is 1 cm. Inset: Optical fluorescence microscopy image of the hydrogel thread. λexc = 365 nm. The scale bar is 1 cm. (b and c) Polarized optical microscopy images of the hydrogel thread and a dry thread, respectively, formed as in (a).[54]

Graphene quantum dots (GQDs)

A multifunctional hydrogel was formed from cellulose nanocrystals (CNCs) and GQDs. The formation of hydrogels is due to the hydrogen bond between the carboxyl group of the GQDs and the hydroxyl group of the CNCs and the hydrophobic interaction between the surface of the GQDs and the hydrophobic region of the CNCs. This overcomes the electrostatic repulsion between the negatively charged carboxyl group of the GQDs and the semi-ester sulfate group of the CNCs and produces a physically cross-linked hydrogel with controllable mechanical properties. Owing to their shear-thinning behavior, the CNC-GQD hydrogels can be used as injectable materials for 3D printing. Hydrogels have anisotropic nanofiber structures that are essential for cell guidance, proliferation, and differentiation[54] Figures 5 and 6. We also made a direct comparison between these different formulations of GO-based hydrogels in Table 1.

In summary, In the rapidly developing field of biotechnology, 3D printing technology has become a ray of hope for solving key medical problems such as organ transplantation, tissue engineering, drug testing and development, nerve regeneration, and disease modeling. Bioprinting technology has the potential to subvert modern medicine and is increasingly receiving close attention from all walks of life. The excellent mechanical properties of graphene-based hydrogel can significantly improve mechanical properties such as tensile strength and elastic modulus. Ultra-large specific surface area and high carrier mobility can be used for 3D printing of flexible electronic devices. Graphene-based hydrogel has good biocompatibility and antibacterial properties. 3D printing is used to prepare biological scaffolds to enhance the wear resistance of artificial bone tissues and joints. Although 3D printing graphene-based hydrogels has broad application prospects, there are still some challenges in practice. (1) The cost of 3D printing materials is still relatively high, which limits the application of 3D printing technology in some fields. (2) Develop high-precision and high-performance 3D printing graphene technology; (3) Expand the application potential of 3D printing graphene-based hydrogels. Although there are some challenges and limitations in practice, with the development of technology and reduction of costs, the accuracy and efficiency of 3D printers will continue to improve, allowing them to be applied in more fields, from medical equipment to industrial manufacturing. From personalization to sustainable development. Through continuous innovation and improvement, 3D printed graphene hydrogel will help create a more personalized, efficient and sustainable future.

Graphene and its derivative based hydrogels as 3D scaffolds for cell culture

3D cell culture provides a physiological environment closer to that of cells in vivo, including cell-cell interactions, cell-matrix interactions, cell-blood, cell-oxygen, and so on. Such culture conditions closer to the real environment can better simulate the growth and function of cells in human body.

Hydrogels are materials with a 3D network structure. Two-dimensional (2D) cell cultures gradually lose their original properties with proliferation in vitro, and cell morphology also changes. There are limitations in simulating the physiological and pathological environments of cells. Graphene and its derivatives have good biocompatibility and safety and can transmit biochemical information from 2D surfaces to 3D culture systems.[55] That's because, the polar functional groups such as hydroxyl and carboxylic

Table 1. A direct comparison between these different formulations of GO-based hydrogels.

Bioink composition	Method	References
FeCl3·6H2O/GO hydrogel	micro Extrusion-based Printing	Lu et al.[37]
GelMA/GO	Extrusion-based Printing	Xavier Mendes et al.[38]
GelMA/GO/MSCs	Extrusion-based Printing	Jiang et al.[39]
GHPA/GO	Extrusion-based Printing	Kang et al.[40]
small intestine submucosa (SISMA)/GO	Extrusion-based Printing	Rueda-Gensini et al.[41]
ALG/CS/GE/GO	micro Extrusion-based Printing	Olate-Moya et al.[42]
collagen type I solution/GO	micro Extrusion-based Printing	Cheng et al.[43]
alginate/gelatin/GO/MSCs	microextrusion-based two-syringe cell bioprinter	Zhang et al.[44]
Alginate/Gelatin/GO/MSCs	pneumatic-driven Extrusion-based Printing	Zorba Yildiz et al.[45]
CH/GO	Extrusion-based Printing	Marapureddy et al.[46]
alginate/GO/MSCs	Extrusion-based Printing	Choe et al.[47]
Alg/Gel/GO	Extrusion-based Printing	Li et al.[48]
Histidine/dextran/GO	microfluidic 3D printing	Ding et al.[49]
Silk Fibroin/GO	Digital light processing (DLP) printing	Ajiteru et al.[50]
GelMA/GO	Stereolithography based 3D bioprinter	Zhu et al.[51]

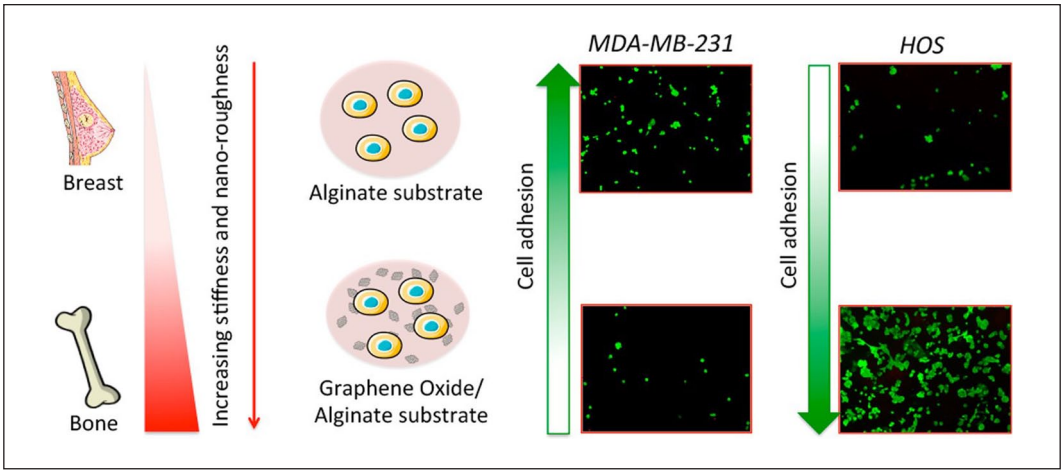

Figure 7. GO functionalized hydrogel-based surfaces, biomechanically and structurally more similar to the tumor environment, selectively inhibits malignant breast cancer cell adhesion efficiency and spreading area, while promotes HOS and 3T3 adhesive processes.

acid on the surface of graphene or GO in hydrogels can interact well with nutrients and exhibit different biological functions to cells. The unusually high adsorption capacity of graphene for dexamethasone and β-glycerophosphate can be attributed to the π-π stacking between the aromatic rings in biomolecules and the graphene base plane. Therefore, graphene promotes the osteogenic differentiation of MSCs. However, denaturation of insulin through strong π-π interactions and the dissolution of its 3D configuration can inhibit the adipogenic differentiation of MSCs. The hydrogen bonding and electrostatic interactions of GO enhance its binding ability with insulin, thereby promoting the adipogenic differentiation of stem cells. Therefore, the surface properties of 2D materials effectively affect the fate of stem cells in 3D hydrogel culture systems.[55,56]

GO

Studies have used alginate (Alg) and GO hydrogels loaded with a human osteosarcoma (HOS) cell line and healthy mouse fibroblasts, and their mechanical properties simulated the cellular microenvironment (Figure 7). The addition of GO promoted the adhesion of HOS and 3T3 cells, and the number of living HOS and 3T3 cells cultured on GO/Alg for 7 days was significantly higher than that in pure Alg. GO addition also significantly increased the expression of vinculin and actin in 3T3 and HOS cells. These proteins are involved in protein anchoring, cytoskeletal attachment, and hemidesmosome formation[57] (Figure 8). Simultaneously, it was found that gelatin (GH) can simulate the extracellular matrix (ECM) very well, and GO mixed with GH can enhance mechanical properties and

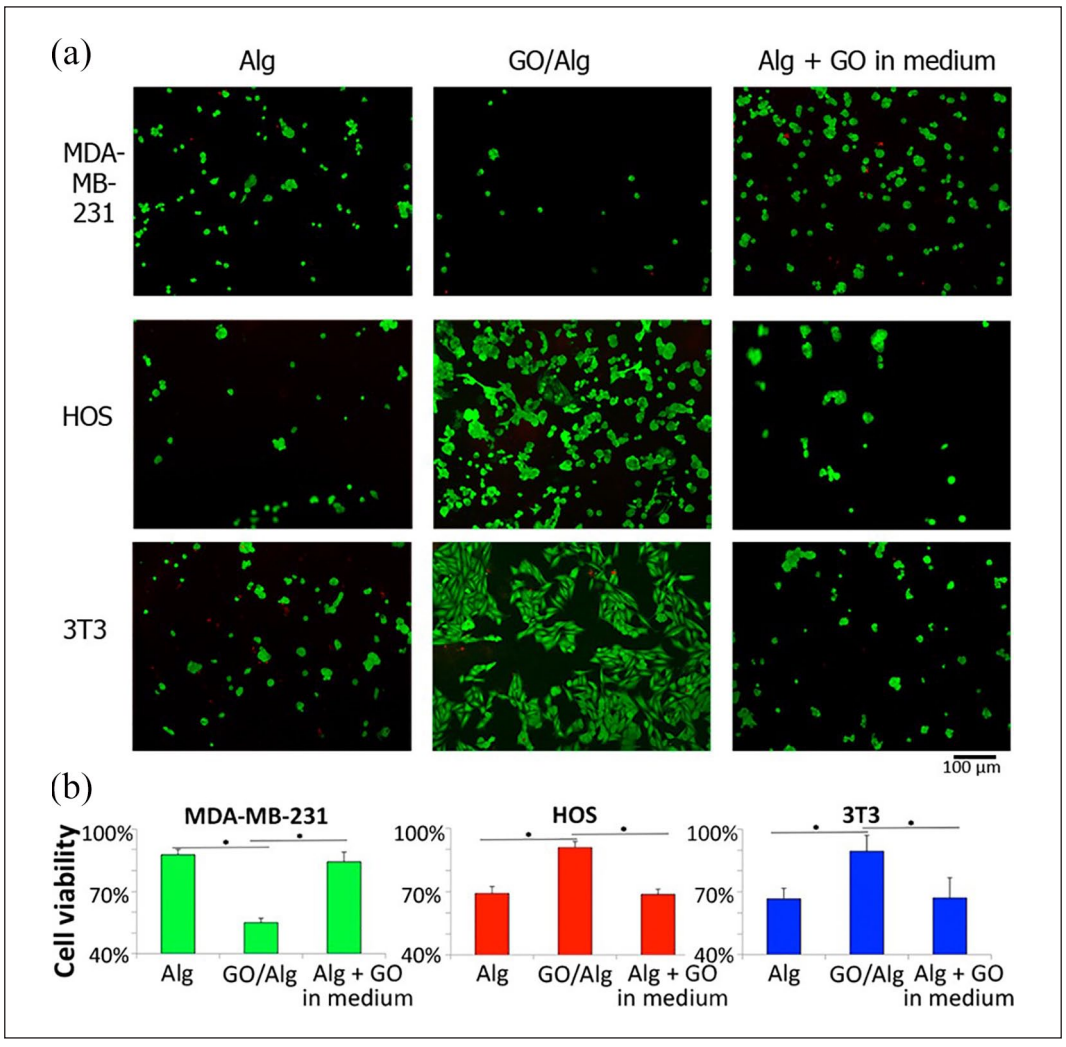

Figure 8. (a) Cell viability measured by live/dead staining of the three cell lines cells after 24 h of culture over each hydrogel-based substrate (Alg, GO/Alg, and Alg with GO nanosheets dispersed in the medium). (b) Quantitative analysis assessed through Presto Blueassay of viable cells adhering on the substrates for the three cell lines.[57]

adhesion. The proliferation rate of human dermal fibroblasts increased by 117%, 517%, and 661%[58]compared with that of a control group after 3, 5, and 7 days of culture, respectively. At 2.0 mg/ml GO and 15 wt% N-isopropyl acrylamide (NIPAM), a 3D GO hydrogel scaffold with an adjustable pore size and morphology was created by utilizing the near-infrared response of GO and the thermal response of the NIPAM hydrogel, allowing suspended human hepatoma cells to be subjected to a controlled compressive force generated by dynamic scaffold contraction. A compact and uniform 3D sphere could be quickly formed, and it was found that, in contrast to the spindle cells grown in conventional 2D flat porous plates, the edges of the cells in scaffolds were smoother and more three-dimensional, similar to in vivo morphology, and the cells inside and outside the sphere were alive and vigorous. More importantly, a 3D multilayer coculture system consisting of hepatocytes and fibroblasts wrapped in endothelial cells was established by sequentially accumulating different cells in the scaffold. This multicellular system significantly improves liver function. These properties enable the use of scaffolds in artificial biological liver applications.[59]

When crosslinking chitosan (CS) and GO at different concentrations (0.1, 0.5, and 1.0 wt.%) to form 3D hydrogel scaffolds, the addition of GO improved the structure of CS hydrogel scaffolds, promoted the formation of a 3D spatial network structure, and facilitated cell growth and proliferation. Co-culturing of human endothelial progenitor cells with the prepared 3D scaffolds promoted the proliferation and lumen formation of EPCs; the lumen formation ability of the 0.5% GO group was the strongest, and the expression of CD34, VEGF, MMP9, and SDF-1 in EPCs was significantly upregulated. Moreover, GO may

Figure 9. Schematic diagram of GO-3D mesh synthesis for further use in cell culture.[61]

regulate the angiogenic capacity of EPCs via the SDF-1/VEGF signaling pathway.[60] Similar studies, such as those on a combination of polyethylene glycol (PEG) and GO, led to the development of GO-based 3D hydrogel scaffolds in which the hydrogel exhibits a microporous 3D structure. Vascular endothelial cells and fibroblasts grown on the 3D scaffolds adhered closely to each other. Confocal imaging showed morphological characteristics similar to those of blood vessels in vivo; namely, the two types of cells fit closely in the scaffold, often located at the edge of the scaffold or inside the pore, forming a capillary-like structure. This indicated that the scaffolds provided a suitable 3D microenvironment for the growth of different vascular cells[61] Figure 9.

After 5 days of fibroblast culture in methacrylate capacarrageenan dopamine functionalized graphene oxide, the proliferation and spread of fibroblasts increased by 2.5 times and 5.7 times. With an increase the content of the hydrogel, the cytoskeleton expanded and the cells formed pseudopods on the hydrogel, leading to the formation of interconnecting bridges between fibroblasts. This is because the PD-modified catecholic groups on the GO surface can effectively increase adhesion sites and attract proteins in the medium through electrostatic interactions, thus improving cell attachment, diffusion, and nutrition.[62] TMSCs (Tonsil-Derived Mesenchymal Stem Cells) were cultured in a GO-polypeptide 3D composite system. Compared with the simple P system, the GO/P system significantly increased the expression of lipid markers, such as PPAR γ, CEBP-α, LPL, AP2, ELOVL3, and HSL, and the GO-polypeptide system produced more lipid pellets and deeper oil red O staining. GO, which has polar surface functional groups such as hydroxyl and carboxylic acids, has a high affinity for insulin; therefore, it can adsorb insulin in nutrient solutions and effectively interact with it, thus promoting the lipid differentiation of TMSCs. The GO-polypeptide composite system provides a good platform for the 3D culture of tonsil-derived mesenchymal stem cells for lipid differentiation.[55] We also made a direct comparison between these different formulations of GO-based hydrogels Table 2, the advantages and disadvantages of various hydrogels can be visualized.

rGO

The effect of 3D scaffolds prepared using polyacrylamide (PAAm) and rGO on the growth of skin fibroblasts was studied and compared with that of the control PAAm hydrogel. Cells were collected at 1, 7, 14, 21, and 28 days, and cell viability and proliferation significantly improved. Even after 28 days, cell viability was 83%.[63] rGO and l-cysteine form porous hydrogels in which human osteoblasts exhibit good cell adhesion and growth abilities; human osteoblasts are spherical and grow well over time.[64] Other studies have shown that 3D hydrogel scaffolds prepared using magnetically modified reduced graphene oxide (m-rGO) and collagen not only simulate the natural ECM of nerve tissue, but also have an anisotropic structure. Under the action of a low external magnetic field, m-rGO is oriented along the direction of the magnetic field and assists in the directional gluing of collagen fibers, with good biocompatibility and electrical conductivity. Throughout the experiment, the survival rate of the cells in the 3D scaffold exceeded 95%. SH-SY5Y cells in the scaffold showed unidirectional growth, axons extended along the direction of the magnetic field, and calcium signals propagated along the direction of the cell arrangement. In contrast, in pure hydrogels, the orientation of the collagen fibers is random; therefore, there is a lack of spatial orientation. Cell growth is multidirectional, F-actin filaments extend in all directions, and calcium signals propagate randomly. The neurite lengths in the m-rGO hydrogel group were $143.90 \pm 45.2\,\mu m$ and $181.05 \pm 35.8\,\mu m$. The m-rGO scaffold promoted growth and differentiation of SH-SY5Y cells.[65] A new type of hydrogel composed of GO, rGO, NF, and Gel has been used as a 3D cell culture platform. rGO-Gel-NF had a higher degree of cell spread than GO-Gel-NF, which was attributed to the hydrophobicity of rGO and its stronger protein adsorption ability. In both hydrogels, α-SMA was highly expressed in fibroblasts but mainly around the nucleus and not in the cytoskeletal region of mature myoblasts. This indicated that fibroblasts were at an early stage of differentiation, suggesting that fibroblast differentiation could be induced even without the provision of inducible factors. In particular, in rGO-Gel-NF, there were more filamentous pseudopods on the leading edge of the fibroblast cell membranes, which anchor to scaffolds and contribute to more mature muscle fiber differentiation[66] Figure 10. We also made a composition of graphene-hydrogel, strengths and weaknesses Table 2.

Table 2. The composition of graphene-hydrogel, strengths and weaknesses.

Hydrogels composition	Strengths	Weaknesses	References
Poly(ethylene glycol)-poly(Lalanine) (PEG-PA) and GO	The unique surface properties of GO can regulate the behavior of stem cells. The temperature sensitive hydrogel composite system is conducive to insulin adhesion and promotes the expression of adipogenic markers of stem cells. The surface properties of GO 2D materials provide a three-dimensional cell culture environment for the differentiation of TMSCs into adipocytes	The simple hydrogel does not have binding sites for insulin, resulting in a limited amount of insulin to be accommodated in the composite hydrogel	Mokhtari et al.[62]
Alginate (Alg) and GO	The GO functionalized hydrogel surface is biomechanically and structurally closer to the tumor environment. The addition of GO selectively inhibited the adhesion efficiency and spreading area of malignant breast cancer cells, while promoting the adhesion process of HOS and 3T3.	Since the presence of GO can lead to hardening of the effective matrix surface to some extent, which hinders cell adhesion, the effect of the hydrogel to GO ratio on cells needs to be further studied.	Narayanan et al.[63]
Gelatinhydroxyphenyl propionic acid(GH) and GO	GO incorporation enhances mechanical properties through additional interactions between the hydrogel and tissue or within the hydrogel network, and enhances tissue adhesion	Although the addition of GO slowed down the degradation rate of GH hydrogel, it was still too fast (about 3 days). Too fast degradation was not conducive to tissue healing. As GO concentration increases, free radicals are generated, resulting in prolonged gelation time of GH hydrogel.	Wang Y et al.[64]
N-isopropylacrylamide and GO	Combined with microfluidic technology, the preparation of porous structures with interconnected adjustable pore sizes and remote light-controlled capacity responsiveness can realize a 3D multi-layer co-culture system of hepatocytes with encapsulated fibroblasts and endothelial cells, which can simulate the functional units of liver tissue	GO concentration is not easy to control. Too high or too low will affect the contractile properties of composite hydrogels. It can only simply simulate the microenvironment of liver tissue	Santhosh et al.[65]
Chitosan(CS) and GO	CS/GO hydrogel scaffolds had better network structure and mechanical strength. The addition of GO improved the pores of chitosan hydrogel to be more uniform, and enhanced the proliferation activity and angiogenesis ability of EPCs	Firstly, the specific mechanism of CS and GO cross-linking has not been comprehensively investigated. Secondly, there are few detailed studies on the molecular mechanism of CS/GO hydrogel scaffolds regulating EPC angiogenesis. Third, since in vivo experiments were not performed, it was not possible to verify the role of this scaffold material in repairing bone defects in vivo	Kim et al.[66]
Poly(ethylene)(glycol) (PEG) and GO	The stable three-dimensional structure of the micropore mesh, with an increased number of pores and good connectivity, can be used to study cell-cell and cell-microenvironment interactions. Vascular endothelial cells and perivascular fibroblasts growing on the mesh are tightly attached	The cell adhesion ability of the hydrogel was affected to a certain extent, and the cell proliferation ability was affected. When the porosity exceeds 90%, pores with irregular shape and reduced connectivity are formed, and the 3D mesh is fragile. Therefore, the porosity needs to be controlled during gelling	Feng et al.[67]

(Continued)

Table 2. (Continued)

Hydrogels composition	Strengths	Weaknesses	References
MethacrylateKappa-carrageenan (KaMA)-dopamine(PD) and GO	It has good mechanical properties, injectability and self-repair. The catecol groups of PD on the GO surface could effectively increase adhesion sites, resulting in significant improvement in compressive strength and toughness, 2.5-fold increase in fibroblast proliferation and 5.7-fold increase in spreading.	At higher GOPD content, the chemical cross-bridge between the methacrylate groups of KaMA is inhibited, resulting in a reduction in the compression modulus K-G4. There is a lack of animal experiments for further verification.	Hu et al.[68]
Polyacrylamide (PAAm) hydrogels and rGO	It could mimic the extracellular matrix and facilitate the efficient proliferation of skin fibroblasts. After 28 days of culture, the cell viability was still as high as 83%. The pore size of the composite hydrogel can be adjusted by the addition of rGO.	The gelling concentration of rGO makes the composite hydrogel have a certain cytotoxicity	Saravanan et al.[69]
L-cysteine and rGO	The graphene-composite hydrogel layered structure increases the conductivity by four–five orders of magnitude. The conductive rGO hydrogel can promote cell adhesion and growth by electrical stimulation	The cells on the composite hydrogel can adhere and proliferate well, but the survival rate needs to be further improved.	Pathmanapan et al.[70]
Collagen hydroge and magnetic- rGO	It has good biocompatibility and electrical conductivity, and the encapsulation of SH-SY5Y can control the differentiation of neurons and axon orientation. The differentiated neurons in the hydrogel show spontaneous electrical activity and unidirectional calcium signal propagation.	Further verification by in vivo animal experiments is lacking	Céspedes-Valenzuela et al.[71]
Gelatin and rGO	To simulate a 3D model of tissue fibrosis in vitro, encapsulated dermal fibroblasts exhibited highly variable phenotypic changes	The increased rGO made the composite hydrogel insufficiently permeable	Qi et al.[72]
Laminarin hydrogel (LAgel) and Graphene	With the photocrosslinking property, the composite hydrogel has better toughness. It can promote the adhesion and spreading of hMSCs and realize the transport of biological signals to regulate cell behavior. It has good electrical conductivity and good biocompatibility	Pure GF is prone to fracture or collapse due to its rigidity and brittleness	Khorshidi and Karkhaneh[73]
Collagen hydrogel and Graphene	It has excellent electrochemical sensing performance and can monitor reactive oxygen species released by microglia in collagen matrix in real time	The long-term survival rate of cells in the composite hydrogel system needs to be further verified, and there is a lack of further verification in vivo animal experiments	Liu et al.[74]

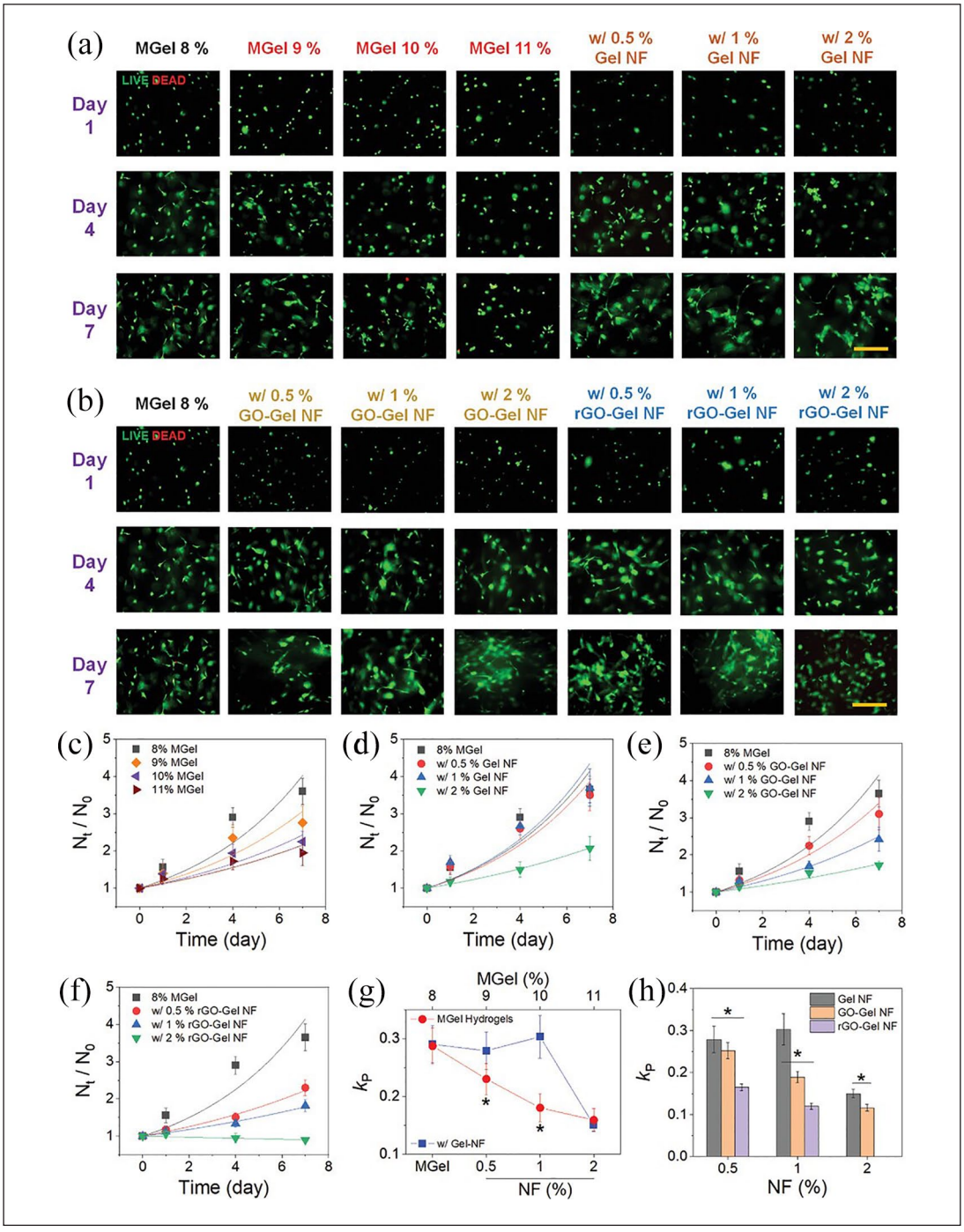

Figure 10. (a and b) Fluorescent images of fibroblasts encapsulated in MGel hydrogels at various MGel concentrations, Gel NF hydrogels, GO-Gel NF hydrogelsand rGO-Gel NF hydrogels at various nanofiber concentrations (scale: 100 μm). The cells were fluorescently labeled to visualize live (green) and dead (red) cells. (d–f) The plots of normalized number of live cells (Nt/N0) versus time were obtained for the encapsulated fibroblasts. (g and h) Proliferation rates (kP) of fibroblasts obtained by fitting the plots in (c–e) with Equation 1.[66]

Graphene

A 3D composite scaffold composed of graphene foam (GF) and LAgel showed good flexibility and a 3D interconnection network. Three-dimensional GF can promote the adhesion and diffusion of human bone marrow mesenchymal stem cells (hMSCs). Immunostaining after 7 days of culture showed that hMSCs remained round in the LAgel system, which may affect the growth of the cells because they were confined in a rigid covalent connection

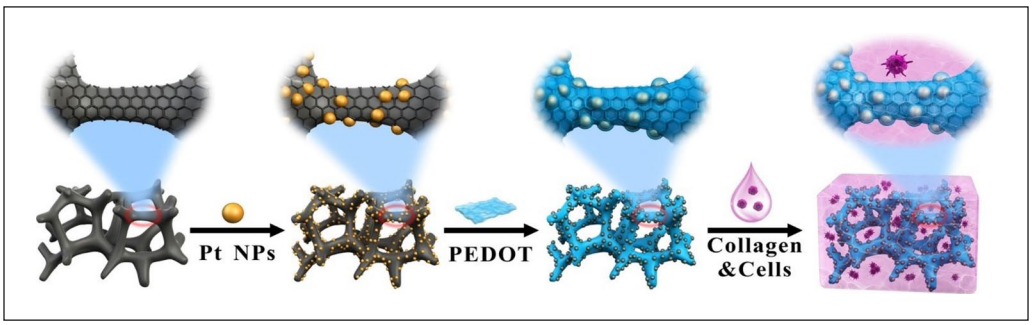

Figure 11. Schematic illustration of the fabrication processes of the 3D GF/Pt NPs/PEDOT electrochemical sensor and collagen hydrogel integrated platform.[68]

network. However, the hMSCs cultured in GF-LAgel exhibited a fully spread morphology, showing a slender spherical shape.[67] Functional 3D GF and hydrogels prepared with type I collagen have also been used for 3D culture of microglia cells. In 2D culture dishes, cells are individually spindle-shaped, while in a 3D scaffold, cells are spherical and in a state of agglomeration. This morphological difference reflects the advantage of 3D cell culture[68] Figure 11.

In summary, studies have shown that hydrogels can improve cell behavior by mimicking the microenvironment in the body. Graphene oxide itself can serve as an artificial extracellular matrix. Its structure has unique properties, including surface functionalized groups, ultrathin topology, hydrophilic nature, and appropriate size, which are more suitable for cells that promote proteins in the culture medium or cell secretions, thereby improving cell interaction. The overall interaction of the hydrogel makes it have good biocompatibility and significantly promote cell proliferation, differentiation and gene expression. 3D cell culture technology has shown its potential in multiple application fields. In the field of drug screening, 3D models can provide more predictive toxicity data and help reduce the failure rate of preclinical drug development. In regenerative medicine, 3D culture provides a platform for tissue and organ regeneration and is expected to solve the problem of donor organ shortage. However, standardization and large-scale production of the technology remain key obstacles to achieving widespread adoption. In addition, regulatory approval standards for 3D cell culture products are constantly evolving. With the continuous advancement of technology and the growth of market demand, 3D cell culture technology will continue to play an important role in the field of biotechnology. Future research will focus on improving the efficiency of cell culture, developing new biomaterials and improving automation. At the same time, interdisciplinary collaboration will help solve the challenges faced by 3D cell culture and promote the application of this technology in a wider range of fields. Given the various advantages of graphene hydrogels, it is expected to make greater contributions to disease treatment and the advancement of biotechnology in the future.

Medical tissue engineering applications of hydrogels composed of graphene and its derivatives

Repairing large-sized bone defects remains a medical problem. The osteoconduction and osteoinduction processes of biomaterials are the key to repairing large-sized bone defects. Hydrogels have a unique highly hydrated 3D polymer network and can be designed into bionic materials with physical and chemical properties close to those of bone matrix, providing stem cells with adhesion, support, sustained release and other carrier functions, promoting better survival and osteogenic differentiation of stem cells. The addition of graphene and its derivatives significantly improves the mechanical strength, degradability, and viscoelasticity of hydrogels. At the same time, loading different nutritional factors in hydrogels improves the osteogenic microenvironment, significantly promotes angiogenesis and osteogenesis, and inhibits osteoclastogenesis. Therefore, graphene-based hydrogels are expected to provide a new and effective treatment strategy for clinical critical-sized bone defects.

Bone

GO. GO hydrogels can mimic the ECM, and the hydrogel formed by GO, isopropylacrylamide (PNIPAAm), and chitosan (CS) exhibits good compressive strength and biocompatibility and can provide a biomimetic ECM microenvironment. It significantly promotes the proliferation and differentiation of MSCs into osteoblasts. Hydrogels containing 0.5% GO, glycerol phosphate (GP), and chitosan (CS) showed similar results. The hydrogel exhibited good biocompatibility and metabolic activity in MSCs. The -COOH and -OH groups of GO attract Ca2+ and promote the precipitation of hydroxyapatite by attracting

PO43-, which significantly promotes osteogenic proliferation and mineralization. Moreover, under osteogenic conditions, the main components in GO interact with dexamethasone via π-π interactions. Furthermore, the upregulation of Runx2, ALP, COLL1, and OCN can promote osteogenic differentiation of mouse MSCs and improve bone tissue repair.[69] In the hydrogel scaffold formed by fibrin and GO, GO had a large surface area, which enhanced the structural integrity and stability of the scaffold, while the production of ROS was reduced owing to the interaction of carboxyl groups, thereby improving cell viability. An in vivo study of bone defects in mice showed that a hydrogel filled with GO showed significantly increased deposition of collagen, calcium, and phosphorus.[70] ChiMA and GO formed a composite hydrogel that functioned as a cell physiological medium, with a cell survival rate higher than 80%. This hydrogel enables the effective aggregation of platelets because platelets promote osteoblast migration and proliferation and increase blood vessel formation. Experiments have shown that GO hydrogels can evenly distribute the load, and enhance bone induction and conduction through the bone-bone interface to promote bone repair, and have good effects on oblique and transverse femoral fractures. Simultaneously, a study found that the composite hydrogel formed by sericin methacryloyl (SerMA) and GO has a high pressure stress close to that of normal bone tissue. The expression of OCN, CoLL1, and Runx 2 in BMSCs co-cultured with the composite hydrogel was significantly higher than that in the pure hydrogel. In a rat skull defect model, the bone mineral density and bone volume of the composite hydrogel group were significantly higher than those of the pure hydrogel group at 4, 8, and 12 weeks after surgery. RNA sequencing has shown that composite hydrogels promote BMSC migration and osteogenic differentiation via the activation of MAPK, TNF, and chemokine signaling pathways.[71,72] Similarly, a composite hydrogel scaffold composed of GO, an oxidized polysaccharide, and gelatin in an optimal ratio can also simulate the microenvironment of the bone matrix. After the addition of GO, the gel surface exhibits nanoscale roughness, and cells tend to adhere, diffuse, and migrate on a rough surface more than on a smooth surface. Composite hydrogels promote the adhesion, proliferation, and morphological maintenance of human osteoblast-like cells.[73] Furthermore, the OiECM, GO, and COL composite hydrogels exhibited a porous and unique rough structure owing to the addition of GO. The synergistic effect of the ECM and GO increased the proliferation rate and osteogenic ability of the BMSCs cultured on the composite hydrogel. After 14 days of culture, the expression of the osteogenic genes COLL (7.51 times), BMP-2 (26.25 times), and OCN (1.76 times) was significantly higher than that in the control group. In vivo experiments showed that OiECM-GO-COL implantation in rats with severe skull defects significantly increased bone volume and OCN-positive cells 12 weeks after treatment, whereas the control group showed limited bone formation.[74] In addition, the roughness of the inner wall of the composite hydrogels prepared with GO, carboxymethyl chitosan (CMC), and polyethylene glycol diacrylate (PEGDA) increased after the addition of GO, which was conducive to cell adhesion. The mechanical properties of the composite hydrogel scaffold were better than those of the pure gel scaffold, providing sufficient mechanical support to the cellular microenvironment. This promoted new bone formation and tissue repair.[75] When GO was added to a SA−CS−Coll hydrogel, hydrogen bonds were formed between the −OH and −COOH functional groups on the surface of GO, and the hydroxyl group of SA formed a brick mortar structure with a significant effect on the modulus of the hydrogel. The modulus of the hydrogel strongly matched those of human collagen, cervical spine components, ligaments, and bones. In addition, the proliferation and differentiation of the osteoblasts attached to the GO scaffolds significantly increased. GO increases the ionic cross-linking between polymer chains and GO particles, acting as a calcium ion in the chemical cross-linking process, which can induce osteogenesis and calcium ore deposition.[76] Another study found that silk fibroin, hydroxyapatite and GO hydrogels promoted rBMSC osteogenic differentiation and collagen deposition owing to the good porous structure of the hydrogel. GO also reduced the gel-water contact angle (40%) and greatly improved water absorption (5790%) and retention (2750%). Water retention capacity is critical for fluid absorption and transport of cellular nutrients and metabolites, and rBMSC-loaded scaffolds have been shown to significantly increase new bone regeneration and collagen deposition.[77] The study found that GO, collagen and hydroxyapatite (HAP) composite hydrogels with pore sizes ranging from 80 μm–150 μm ensured good cell infiltration and nutrient exchange inside the hydrogel, promoting the growth of rBMSCs. The addition of GO provides more biologically active sites for HAp deposition and protein adsorption. It also promotes cell adhesion, proliferation, and expression of osteogenic factors such as ALP, OCN, and COLL1. In skull and mandibular defect models, micro-CT showed that the skull defect in the composite hydrogel group was almost completely filled with new dense bone tissue 12 weeks after implantation, and the amount of bone tissue in the mandibular defect was significantly greater than that in the other groups[78] Figure 12.

GO hydrogels can mimic the ECM and promote angiogenesis. A new hydrogel (GOG) formed by combining GO and gelatin can mimic the ECM. In addition, GOG-mediated BMSCs can promote osteogenesis and angiogenesis by activating the Erk1/2 and AKT pathways, which are conducive to bone repair. In the repair of skull defects in vivo, the initial hypoxic microenvironment constructed by the GOG can gradually relieve hypoxic tension and then transform into a

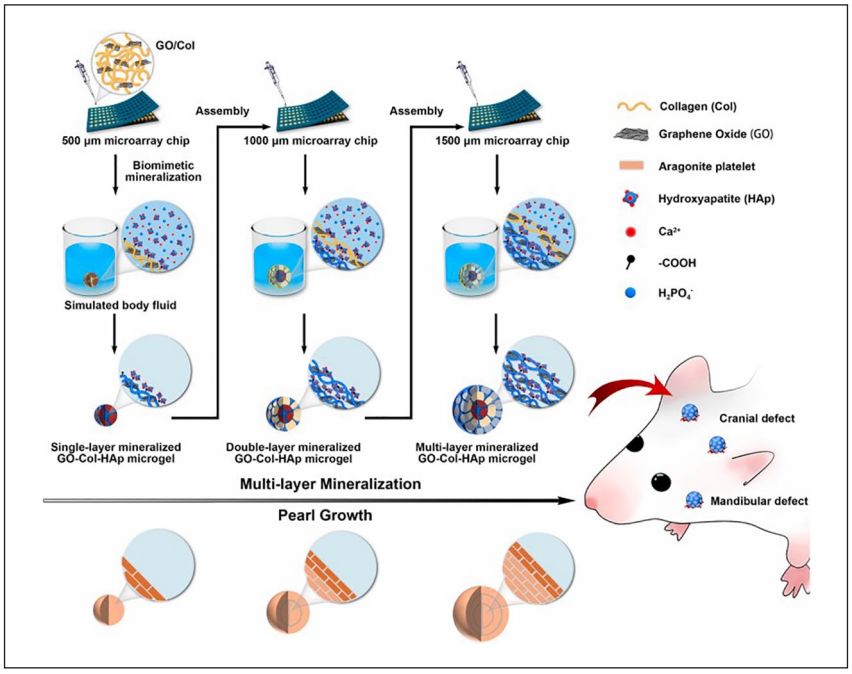

Figure 12. Schematic illustration of the preparation of multi-layer mineralized GO-Col-HAp microgels with uniform HAp deposition and their applications in rat cranial defect and mandibular defect repair.[78]

good vascular stable state, which simulates the process of bone healing and achieves rapid bone regeneration.[79] As the rapid repair of large bone defects has always been a clinical problem. The hydrogel composed of GO and gelatin in this study can simulate the extracellular matrix and has the functions of bone repair and angiogenesis, and can simulate the entire process from the initial inflammation stage to the subsequent bone remodeling stage. Animal experiments show that the repaired bone is composed of mature trabecular bone mesh and new blood vessels formed around and inside the new bone, which has rapid and excellent repair performance. At present, a large number of studies focus on the single function of hydrogel for bone repair. In fact, the bone repair process is a complex process involving bone formation and osteolysis. Different animals and animals at different ages have different responses to hydrogels, and the final results obtained are also different. Therefore, our future research direction should be to construct a multifunctional hydrogel system, such as involving inflammation, immunity, angiogenesis, osteoclasts, microenvironment, etc., comprehensively considering the needs of different stages of bone repair in the body, so as to achieve precise repair. At the same time, we must also consider the clinical transformation of research results. The ultimate goal of biological experimental research is to serve the clinic. The commercialization of hydrogel products for bone repair in the future needs to attract our attention.

The hydrogels composed of GO and hydroxyapatite (GO-HAP), and gelatin methacrylate and gelatin polyethylene glycol diacrylic acid (GelMA/PEGDA) have a 3D sponge-like structure. It was found that less than 1 μg/ml GO stimulated cell proliferation and created a favorable immune environment for osteogenesis and angiogenesis. Therefore, the hydrogel promoted HUVEC migration and tube formation, and the vascularization was conducive to osteogenesis. The expression of osteogenic differentiation- and osteogenesis-related genes (ALP, COL-Il, BMP-2, and Runx2) was significantly higher in the BMSC-loaded cultures. Simultaneously, it was shown that HAP nanoparticles were uniformly distributed on GO nanosheets because of the oxygen functional groups on the GO surface, which are conducive to interface bonding and uniform dispersion and continuously release Ca2+ to promote recognition and adhesion between the cytoskeleton and the ECM[80] Figure 13.

The conductivity of GO is beneficial for bone regeneration. SEM images showed that, in a GO hydroxyapatite gel, the HAP nanoparticles uniformly deposited on the GO were well interconnected, had good conductivity, and could transmit electrical signals from the surrounding bone, which is beneficial for bone regeneration.[81] GO-HAP nanocomposite hydrogels exhibited good compatibility with BMSCs. The mechanical and electrical coupling properties of GO hydrogels can change the morphology of adherent cells, and regulation of the cytoskeleton under electrical stimulation can further promote the osteogenic differentiation of BMSCs. Studies have confirmed that GO hydrogels, in addition to good biocompatibility, rheology,

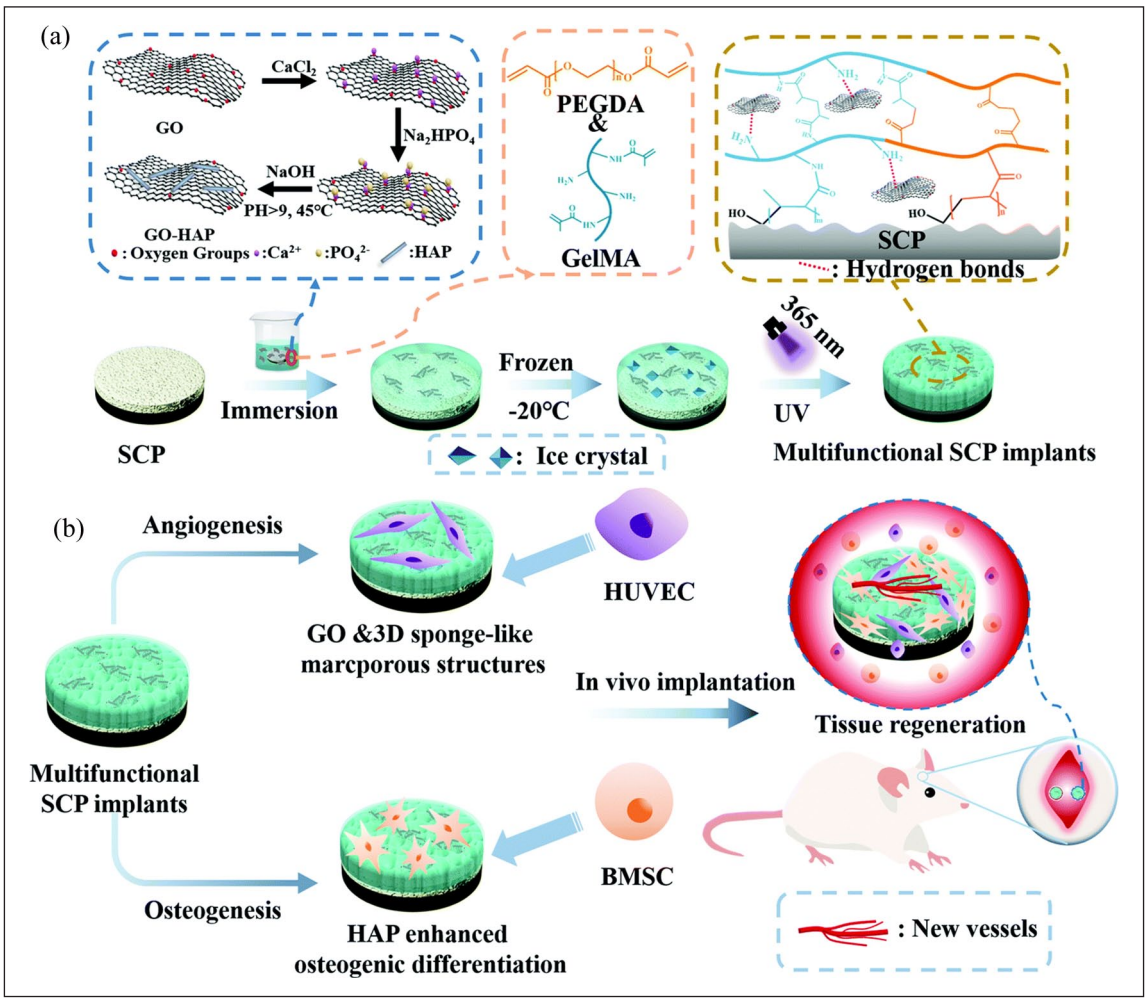

Figure 13. (a) The modification procedures on the sulfonated LCFRPEEK surface and (b) its biological functions: angiogenesis and osteogenesis.[80]

and viscoelasticity, also possess osteoinductive and osteoconductive activities, which can provide a suitable 3D microenvironment for BMSCs to promote cell proliferation and osteogenic differentiation.[82,83]

rGO. The π-π interactions between rGO layers was used to construct a chitosan (CS) and rGO hydrogel, and the interface adhesion between CS and rGO was strong and cell compatibility was good. After 14 days of culture with MG-63, isolated calcium phosphate particles were observed on the surface of the material. After 28 days of incubation, a dense continuous layer of osteoid apatite formed on the surface of the material.[84] However, in the Gel-rGO hydrogels, the residual hydroxyl and carboxyl groups of rGO and other gelatin molecules are linked by hydrogen bonding and electrostatic attraction. rGO incorporation resulted in increased contact angle and hydrophobicity, which were conducive to cell attachment and proliferation. Furthermore, enhanced osteoinductive and bone-conduction properties were observed. MG63 cells cultured for 14 days showed significantly increased ALP activity, mineralized nodules, and significantly increased COLL and OPN expression.[85] Other studies found that functionalized graphene has good biocompatibility and promotes bone regeneration without causing significant inflammation.[86] Gelatin methacrylate (GM), acryloyl β-cyclodextrin (Ac-CD), and β-cyclodextrin (β-CD) were functionalized with rGO to prepare hydrogels. The introduction of rGO resulted in good electrical conductivity of the composite hydrogel. rGO can enhance the electrical conductivity and simulate the electrophysiological microenvironment of bone tissue, which is conducive to signal transduction between cells. Intracellular Ca2+ can accelerate calcium deposition in response to exogenous or endogenous electrophysiological microenvironments. Due to the ability of -OH group-based protein adsorption 55 and strong π-π binding ability, rGO can adsorb osteotrophic factors. The hydrogel promoted the proliferation of MC3T3 cells, expression of osteoblast-related proteins COLL, OCN, and Runx2, and the deposition of calcium

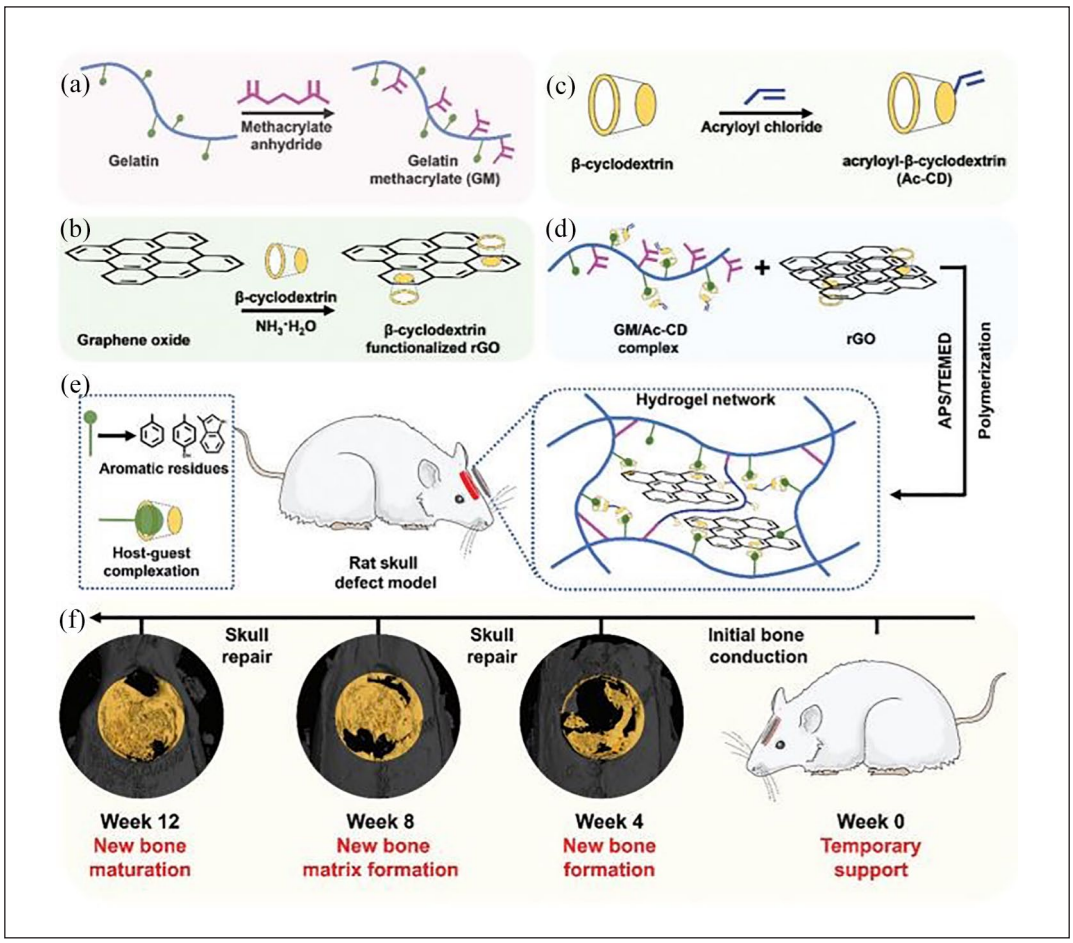

Figure 14. Scheme of the fabrication of GM/Ac-CD/rGO hydrogels. The synthesis of GM (a), rGO (b), and Ac-CD (c); (d) the schematic diagram of the GM/Ac-CD/rGO hydrogel network constructed by double-bond radical polymerization and host–guest complexation; (e) the application of the hydrogel patch as an implant in initial bone conduction; (f) skull bone repair in a rat skull defect model.[87]

salt. In vivo, the expression of Col I, OCN, and Runx2 in the GM/Ac-CD/rGO hydrogel group was significantly higher than in the control group after 8 and 12 weeks of treatment. In the coronal and sagittal views of the skull, the new bone thickness was closer to that of a normal skull[87] Figure 14.

In addition, the rGO hydrogel not only has electrical conductivity but also has good photothermal and osteogenic effects, which play an important role in the repair of large tumor-related bone defects. After 20 min of IR laser irradiation, only 8% of the co-cultured MG-63 cells survived in a nano-hydroxyapatite (nHA) and rGO hydrogel, indicating a strong inhibitory effect on the transplanted tumors in mice. The laminar structure of rGO promoted cell adhesion. Live/dead cell staining and CCK-8 assays showed that the rBMSCs had good proliferation ability and ALP activity in the hydrogel. Micro-CT and histological analyses confirmed that the hydrogel promoted osteoblast mineralization and collagen deposition in a rat skull defect model.[88]

Graphene. Multilayer graphene hydrogel (MGH) films mimic natural cancellous and cortical bone to some extent. Its unique multilayer nanostructure facilitates protein adsorption, cell adhesion, and apatite deposition, functions that promote osteoblast development. MGH membranes can completely block cell transport but allow the entry of fluid and small trophic molecules to successfully maintain the bone space, promote early osteogenesis, and accelerate mineralization. In vivo experiments showed that MGH membranes promoted the osteogenic differentiation of cranial plate stem cells and bone matrix deposition. At 8 weeks after surgery, the bone volume fraction and mineral density of the MGH film group were higher than those of the control group. New bone formation and mature lamellar bone structure were observed in almost all defect areas[89] Figure 15. Another study found that self-supporting graphene hydrogel (SGH) membranes promoted osteogenic differentiation of human adipose-derived stem cells (hADSCs). The film itself can stimulate the osteogenic differentiation of hADSCs independent of other chemical inducers, which is

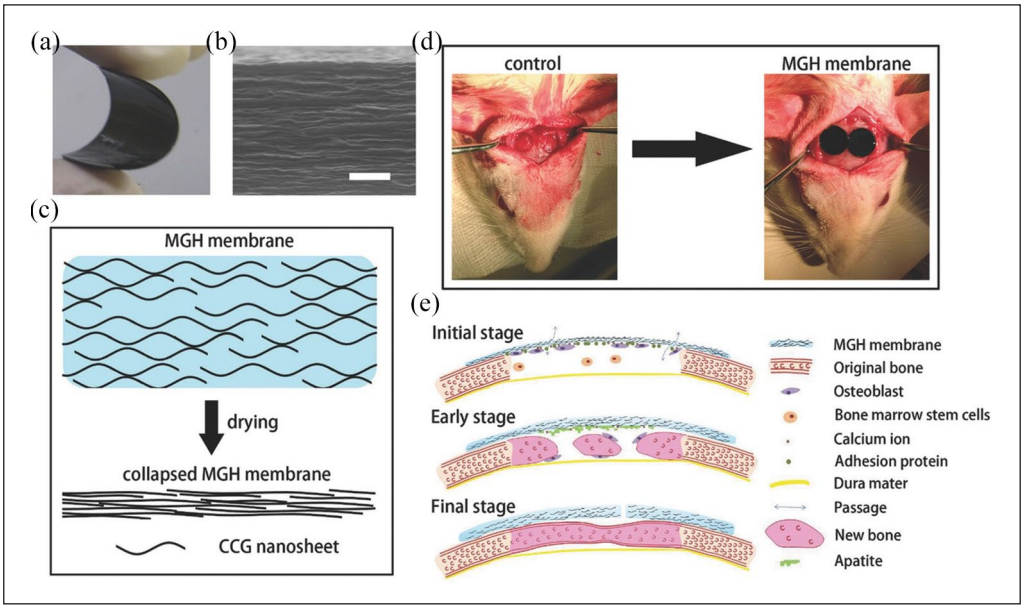

Figure 15. The structure of the CCG based membranes and schematics of the MGH membranes on GBR model of calvarial defect of rat. (a) Photograph of the flexible MGH membrane; (b) SEM image of the cross-section of a freeze-dried MGH membrane; scale bar, 1 μm. (c) Schematic of the cross section of the MGH membrane showing that water molecules are trapped in between CCG layers. After drying, the multilayered nanoarchitecture of MGH membrane collapses to form a highly densified structure. (d) Schematic of the surgical operation that places the MGH membranes to seal off the calvarial defects of rat; (e) proposed GBR healing process of a calvarial defect using the MGH membranes as a barrier membrane. At the initial stage after bone trauma (from immediate to 1 d), the MGH membrane absorbs calcium ions, proteins, and osteoblasts, promoting the activity of bone formation cells, the deposition of bone matrix, and early bone formation. From 1 to 4 weeks (early stage), the membrane accelerates mineralization and the formation of apatite. The new bone formation appeared in both the lateral margin and the center region. At the final stage (after 8 weeks of operation), the newly formed bone with mature lamellar bone structure can be found across almost all the defect areas.[89]

closely related to its remarkable physical properties, including specific nanostructures, surface morphology, strong cell adhesion, good hydrophobicity, and high protein absorption rate. After the addition of graphene, hADSCs could adhere tightly to the SGH membrane and spread in a spindle shape.

Immunofluorescence analysis showed that the cells on SGH membranes had stronger fluorescence for OCN, BMP2, and Runx2 than those on carbon fibers. In addition, hADSCs on SGH membranes had higher calcium accumulation levels after 21 days of culture.[90]

However, traditional bone repair methods, such as autogenous bone and allograft bone transplantation and repair of large bone defects, are difficult to meet the challenges of bone reconstruction and suffer from multiple complications. The mechanical properties of pure hydrogel are suitable for soft tissue repair, but it is difficult to meet the needs of repairing large bone defects. In order to solve this problem. We combined graphene with hydrogel to enhance the porous structure of the composite scaffold, improve the gelation time, adsorption of nutrients, porosity and other biological properties, and provide a microenvironment for osteoblast attachment. At the same time, the presence of graphene makes the composite hydrogel both conductive and promotes bone formation by simulating the ECM of bone tissue through controllable degradation and osteoinduction. In vivo tibial defects showed that defects filled with graphene composite hydrogel scaffolds showed better healing ability than graphene-free scaffolds, suggesting that this scaffold would be an ideal bone tissue engineering scaffold for use in bone defects. Whether graphene hydrogels modulate bone regeneration through immune pathways is an interesting topic that merits further investigation. Graphene hydrogels provide a promising strategy for the future development of tissue engineering in the field of bone defect repair.

Cartilage

Articular cartilage is an avascular and flexible connective tissue located on the bone surface of biarticular joints. With the rapid development of cartilage tissue engineering, functionalized hydrogels have become promising cartilage matrix substitutes due to their good biomechanical properties, water content, swelling capacity, cytocompatibility, biodegradability and lubrication behavior. In order to make hydrogels more suitable for local treatment of cartilage, the mechanical properties of hydrogels are one of

the most important parameters, including: youngs modulus, fracture stress, fracture strain, friction and wear properties and swelling ratio. The addition of graphene and its derivatives can significantly improve these parameters and effectively promote cartilage repair.

GO. Hydrogels formed from ethylenediamine, GO, and chondroitin sulfate are conducive to chondrogenesis. The addition of GO rendered the hydrogel porous, promoted chondrogenic differentiation and collagen matrix deposition of hMSCs, and activated the signaling pathway of cartilage repair. ALP staining and imaging of hMSCs revealed no ALP expression, indicating that hMSCs could form a stable cartilage phenotype.[91] Some studies have found that GO hydrogels can improve chondrogenic differentiation of MSCs without the use of exogenous growth factors in GO or polylactic acid-polyethylene glycol (PDLLA) hydrogels. GO-PDLLA-coated hBMSCs showed higher levels of cartilage matrix gene expression such as sox9, aggrecan, and collagen II, and produced more GAG and collagen than hBMSCs coated with PDLLA hydrogel. In the nontoxic range, the prochondrogenic effect of GO was enhanced with increasing GO concentration, probably due to the large surface area of GO and its ability to efficiently adsorb peptides and proteins, as well as other macromolecules, through physical interactions such as π-π stacking, electrostatic interactions, and hydrogen bonding. Immunohistochemistry showed that GO-enhanced chondrogenesis of hBMSCs was associated with insulin enrichment, which is essential for the chondrogenesis of hBMSCs via hydrogen and electrostatic interactions.[92] In the hydrogel-simulated articular cartilage, GO as a dopant improved the lubrication properties of the cartilage surface layer without any signs of wear, which could reduce the friction of the articular cartilage. Owing to the presence of GO, the energy dissipation was higher and a dense and stable crosslinking network was formed, which had better mechanical properties than the pure hydrogel. Wear tests confirmed that GO hydrogels can withstand up to 100 000 physiologically relevant stresses with a toughness close to that of native AC.[93] The amino group protonation of gelatin and the carboxyl group protonation of GO were subjected to hydrogen bonding and electrostatic forces to form a composite hydrogel. With moderate surface roughness and adhesion, hydrogels transitioned from hydrophilic to hydrophobic, providing a suitable microenvironment for cell attachment and growth Figure 16. The hydrogel showed good cell-material interactions when cocultured with SW1353 cells and BMSCs. In the hydrogel group, HE, alcian blue, and Safranin O staining showed the presence of bone lacunae, proteoglycans, GAG, and collagen type 2, which formed new healthy hyaline cartilage and grew well after 8 weeks of treatment[94] Figure 17. Simultaneously, GO and the growth factors exerted synergistic effects. GO was incorporated into poly-D, l-lactic acid/

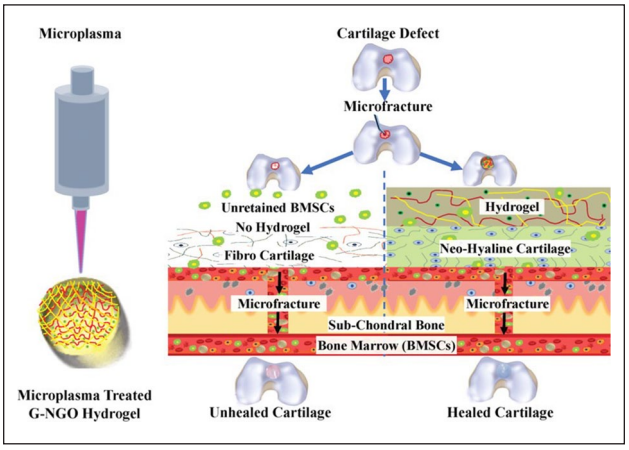

Figure 16. Schematic of G-NGO hydrogel synthesized by the Ar-NT microplasma process.[94]

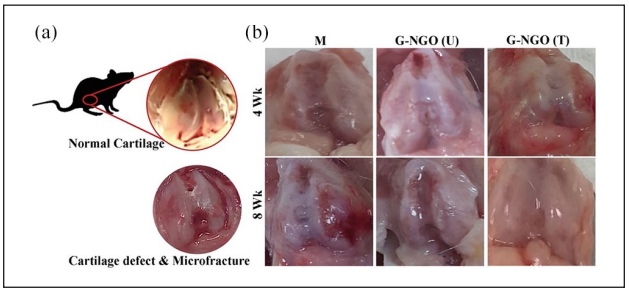

Figure 17. (a) Gross morphology of the normal rat knee joint and (b) knee joints of different in vivo experimental groups such as the M group with no implant, microfracture followed by G-NGO (U) implant, and G-NGO (T) Ar-NT microplasma-treated hydrogel implants on Day 0 and at 4 and 8 weeks.[94]

polyethylene glycol (PDLLA) hydrogels. hBMSCs loaded with TGF-β3 showed higher viability and promoted chondrogenic gene expression, including aggrecan, COLLII, and SOX9, as well as cartilage matrix production, compared to GO-free scaffolds containing the same amount of TGF-β3. Alcian blue-positive staining increased, and GO alone enhanced COLLII expression. Thus, GO-mediated retention of growth factors is enhanced, and GO and TGF-β3 have a synergistic effect on chondrogenesis. After subcutaneous implantation in vivo, the novel hydrogel showed better cartilage matrix generation than the GO-free TGF-β3/PDLLA hydrogel.[95]

Some GO hydrogels are also suitable for AC replacement. In a composite hydrogel composed of GO and polysulfobetaine methacrylate (PSBMA), the compressive stress of the PSBMA hydrogel was enhanced by approximately five times, and its surface was covered by GO, which resulted in less elastic deformation of the hydrogel, lower energy dissipation during sliding, and a significantly reduced coefficient of friction. The synergistic interaction between GO and PSBMA resulted in a higher hydrogel

loading capacity. The ultrathin layered structure of GO further improves the lubrication properties during sliding by mimicking the cartilage function.[96] The tensile strength and elongation at break of a chondroitin sulfate and GO hydrogel film containing 5 wt% GO were 5.35 MPa and 193.5%, respectively. The hydrogel film had a pearl-like brick mortar microstructure, which endowed it with excellent mechanical properties that exceeded those of AC. The GO lamellae and chondroitin sulfate chains were entangled with each other, resulting in a high and firm cross-linking density. These characteristics make it a promising candidate for applications in artificial cartilage.[97]

Intervertebral disc (IVD) degeneration begins in the central nucleus pulposus (NP) and leads to inflammation, degradation of the ECM, and progressive loss of IVD height. The octapeptide FEFKFEFK (F8; F = phenylalanine, E = glutamic acid, K = lysine) and GO were used to prepare hydrogels for NP cells and IVD regeneration. When GO was introduced into F8 hydrogel, the peptide nanofibers were adsorbed on the GO surface through π-π stacking and hydrophobic interaction, and the GO peptide hydrogel exhibited similar mechanical properties to the NP.[98] Further studies found that the hydrogel improved the viability and metabolic activity of NP cells and promoted the expression of the NP cell-specific genes ACAN, COL2A1, SOX9, FOXF1, and PAX1. Two key components of the ECM of NP cells, aggrecan and collagen II, were simultaneously produced and deposited. In addition, GO was found to be in contact with the NP cell membrane and protrusions into the scaffold were observed, indicating that the cells actively explored their interaction with the surrounding environment. The scaffold was remodeled by cells through endocytosis, which was beneficial for promoting IVD regeneration.[99,100]

Graphene. A hydrogel for cartilage tissue engineering based on polyvinyl alcohol (PVA)/ AGAR/graphene (PAG) has the 3D network structure of graphene and can undergo elastic deformation during the tensile process, thus effectively assisting the strain energy dissipation of the AGAR/PVA network. The good interaction between the polar surface of graphene and the hydroxyl group of the polymer increases the compatibility between the materials, with the characteristics of high strength, toughness, and self-healing.[101] A further study found that graphene elastic hydrogel (GEH) scaffolds can simulate the porous structure of cartilage tissue. The highly elastic porous structure (porosity 95.66 ± 3.16%, pore size 140–180 μm) increases the interaction between the material and chondrocytes, which is conducive to the diffusion of nutrients and metabolic waste. It provides an active microenvironment for the growth of chondrocytes. The growth of chondrocytes on the surface of GEH scaffolds is accelerated and stable, and the expression of type II collagen and SOX9 can be selectively promoted. The mechanism is related to the activation of the Rho/ROCK pathway. Matrix metalloproteinases MMP8 and MMP13 and their inhibitors TIMP1 and TIMP3 were significantly up-regulated and in dynamic equilibrium, indicating that the scaffold provides an environment that promotes cartilage matrix remodeling. In vivo cartilage regeneration studies showed that cartilage ECM was uniformly aligned and phenotypically stable along the highly ordered porous GEH scaffold, whereas the cartilage-specific matrix was not neatly aligned in the control group without graphene, indicating the importance of an open porous structure on the outer surface of the scaffold in promoting cartilage remodeling[102] Figure 18. We list all quantitative data in Table 3, Help deepen our understanding

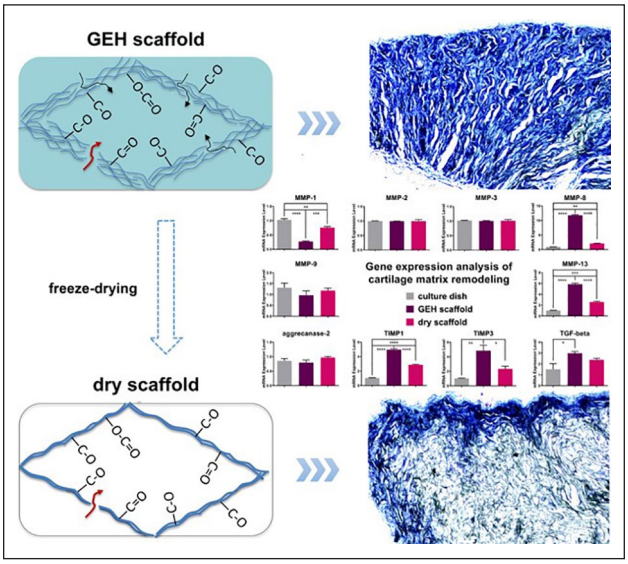

Figure 18. General pictures and schematic diagram of the GEH and dry scaffolds.[102]

In summary, there are two distinct pathways in bone formation: intramembranous osteogenesis (IMO) and endochondral osteogenesis (ECO). From a bone developmental physiology and clinical perspective, long bone development and fracture healing in the limbs are mainly carried out through ECO.[103] Therefore, the development mode of the skull is mainly IMO. Studies have shown that different graphene hydrogels can significantly promote both endochondral bone osteogenesis and intramembranous osteogenesis. These results confirm that functionalized GO hydrogel composites have great application potential in promoting bone repair, but this review found that the models of graphene hydrogel promoting bone repair are mainly animal skull defect repair models, so the repair method is mainly IMO to achieve bone repair. This may be because the skull defect model is easy to model, the technology is mature, and it is widely used by everyone. recognition. For most craniofacial and long bones, the IMO pattern often results in avascular necrosis

Table 3. All quantitative data in section 4.2.2.

Agar/PVA/Graphene	Quantitative data	References
Self-healing	10 min	Samadi et al.[101]
Strength	1157 kPa	
Strain	500%	
Toughness	2610 kJ/m3	
σf	881 kPa	
XRD peak	19.4°	
Graphene elastic hydrogel	**Quantitative data**	
Porosity percentage	95.66 ± 3.16%	Lyu et al.[102]
Pore size	140–180 μm	
Compressive modulus	3.8 kPa	
XRD peak	25°	

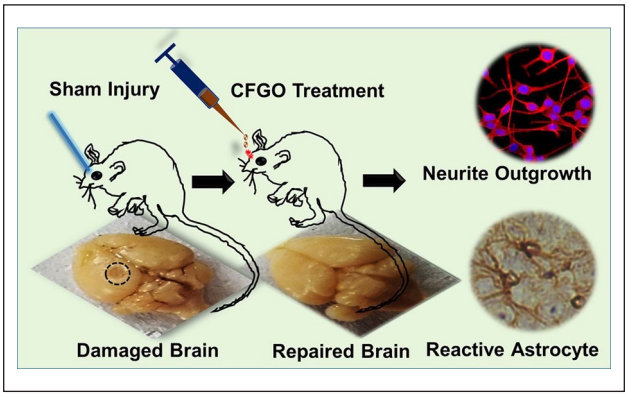

Figure 19. Synthesis and characterization of CFGO-based hydrogel.[107]

and degradation in the central region due to insufficient angiogenesis and poor nutrient perfusion, especially in a harsh microenvironment. In contrast, the ECO pattern is a time-dependent process that begins with an initial cartilage template, followed by hypertrophy and mineralization, and is extremely tolerant to avascular and hypoxic microenvironments due to early chondrogenesis. Therefore, it is very attractive to develop graphene hydrogels with endochondralization and osteogenic functions in the future. Moreover, GO hydrogels with different functions have greatly enriched people's choice of bone defect repair materials.

Nerves

Spinal cord injury is one of the most serious public health problems due to its high morbidity and disability. In the process of spinal cord injury, the central nervous system has limited spontaneous regeneration capacity, including limited axonal regeneration and myelin regeneration, and nerve regeneration and repair are still urgent problems in the central and peripheral nervous systems. Based on the ideal properties and various advantages of hydrogels, it is undoubtedly a suitable carrier system for nerve repair. How to construct functional hydrogel carriers so that they can be better used in the repair of various types of nerve injury is the mainstream direction of nerve repair at present. Graphene and its derivatives-based hydrogels have good conductivity, flexibility, mechanical stability and permeability, which can not only imitate nerve tissue, but also effectively promote nerve regeneration.

GO. Studies have shown that hydrogels with good stability and conductivity can endow surrounding cells with biological current signals, which can effectively recruit and stimulate the specific differentiation of BMSCs into neural-like cells.[104] A GO/polyacrylamide (PAM) composite hydrogel containing 0.4 mg/ml GO exhibited the best performance in promoting the adhesion and proliferation of Schwann cells. In addition, cells on the 0.4 mg/ml GO hydrogel showed higher biological factor release and greater matrix adsorption. This could effectively promote the secretion of neurotrophic factors NGF, BDNF, and CNTF by Schwann cells. After 5 days of culture, Schwann cells on the pure PAM hydrogel spread poorly. In contrast, cells on GO/PAM hydrogels were more widely distributed.[105,106] Acetylcholine-functionalized GO (CFGO) and polyacrylic acid composite hydrogels also promoted nerve growth, and GO and choline had synergistic neuroprotective effects. After culturing primary rat cortical neurons on the CFGO hydrogel for 14 days, the expression of some key neuronal markers, such as GAP43, Tuj1, and MAP2, increased, demonstrating that CFGO promoted the growth of cortical neurons Figures 19 and 20. CFGO also stabilizes neuronal cytoskeletal filaments, microtubules, and actin, contributing to neuronal structural maintenance and axonal transport. Therefore, composite hydrogels are important for nerve repair.[107,108] Ammonia-functionalized GO hydrogels also contribute to axonal regeneration,[109] The addition of GO contributes to the electrical conductivity of the hydrogel, and the GO content makes silk fibroin (SF) hydrogels have both soft and hard properties, thereby affecting the growth of Schwann cells. The softer 1 kPa-GOM hydrogel resulted in the highest mRNA expression of BDNF, NGF, and CNTF after 1 and 3 days of culture, as determined by PCR. In contrast, the harder 10 kPa-GOM hydrogel significantly downregulated the expression of these markers. This suggests that a soft microenvironment supports the expression and secretion of neurotrophic factors.[110]

rGO. Some studies have reported the tendency of SH-SY5Y cells to form extended 3D cell networks on rGO-based hydrogels. After 2 days of culture, the neurosphere structure of SH-SY5Y cells self-assembled and formed a structure very similar to that of organoids. With the extension of culture time, cell proliferation and migration increased and possibly differentiated, whereas the

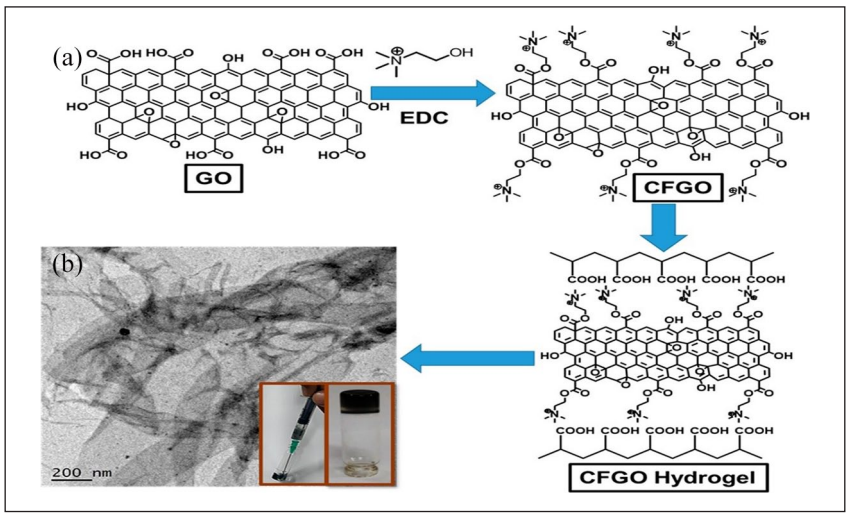

Figure 20. (a) Synthetic scheme for preparation of CFGO hydrogel. (b) TEM image of CFGO hydrogel. (inset, right) Hydrogel formation and (inset, left) the injectable property and repairing of sham injury in the mice brain with the treatment of CFGO hydrogel.[107]

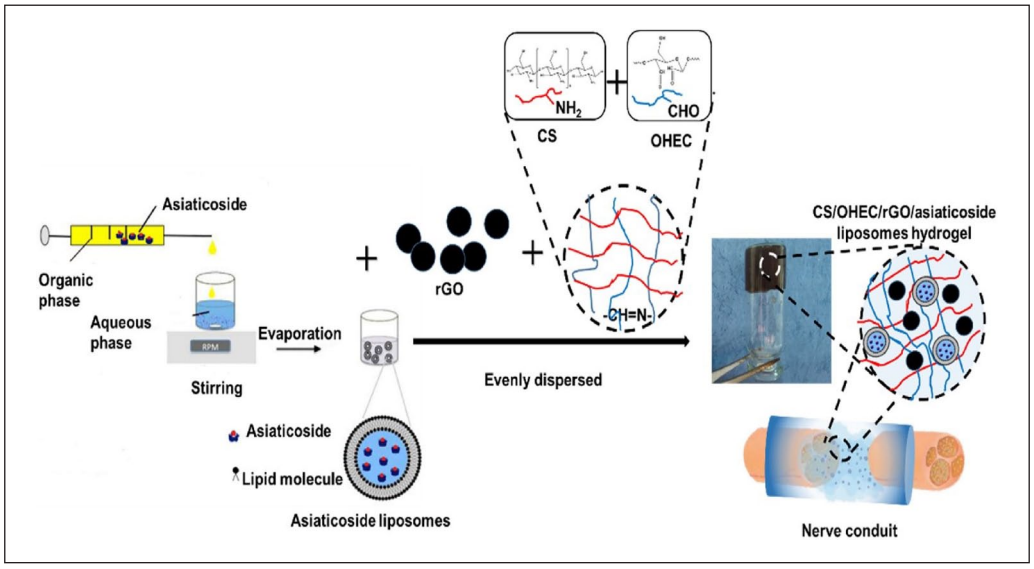

Figure 21. CS/OHEC hydrogel with rGO and asiaticoside liposomes was prepared, by Schiff base cross-linking between -NH2 on CS and –CHO on OHEC, to develop suitable microenvironment that can inhibit scar formation and provide electrical stimulation for nerve repair.[112]

hydrogel allowed nutrient diffusion and promoted the migration of SH-SY5Y cells in the hydrogel. The cells exhibited high interpore penetration.[111] Chitosan oxidized hydroxyethyl cellulose (CS/OHEC) hydrogel loaded with asiaticoside liposomes and conductive rGO, can be used to modify the peripheral nerve regeneration microenvironment. Asiaticoside and rGO synergistically promote the functional recovery of damaged peripheral nerves. After the addition of rGO, electrical stimulation in 3D hydrogel culture conditions can promote the differentiation and proliferation of PC12 nerve cells and accelerate nerve regeneration; the cells are assembled into networks owing to axonal connections compared to monolayer culture conditions[112] Figure 21. This may be the result of cell-material interactions, including interactions between cells and the rGO-based microenvironment, hydrogel surface roughness, elasticity, and hardness, upregulated expression of genes involved in the calcium signaling pathway, and higher rGO electron transport capacity.[113]

Nerve-guided conduits (NGCs) are promising substitutes for peripheral nerve regeneration. rGO and brain-derived neurotrophic factor (BDNF)-loaded GelMA was

used to prepare hydrogel NGCs. Owing to the biocompatibility of the GelMA hydrogel and the electrical conductivity of rGO, the hydrogel improved cell-to-cell communication, enhanced cell orientation, and promoted an increase in the axon length of PC12 cells and neural stem cells. In addition, successfully obtained NGCs effectively promoted the functional regeneration of axons, nerves, and muscle tissue during the repair of 10 mm sciatic nerve defects in rats.[114] The other hydrogel neural guide tube is composed of graphitized carbon nitride (g-C3N4) and rGO. rGO addition greatly enhanced the surface charge, with good anisotropy and electrical activity. Hydrogels have the most suitable mechanical stiffness for peripheral nerve regeneration and support the proliferation and differentiation of PC12 cells. Neural differentiation in the rGO hydrogels (1 and 3 mg/ml) was significantly higher than that in the control group. The neurite length of PC12 cells differentiated on the g-C3N4/rGO3 (3 mg/ml) hydrogel was 47% greater than that on the g-C3N4 hydrogel, indicating that rGO was beneficial for nerve recovery.[115]

Graphene. Studies have shown that graphene can affect the growth of nerve cells and be used in 3D cultures of neurons when incorporated into hydrogels.[116] When hippocampal neurons were seeded onto a PAM hydrogel, they did not attach to the hydrogel and barely grew. PAM allows neurons to grow and develop after the addition of small amounts of graphene.[117] Compared to the pure hydrogel, the graphene hydrogel adhered well to the spinal cord tissue. Histological evaluation showed robust tissue growth around the graphene hydrogel, with ingrowth of connective tissue components, blood vessels, neurofilaments, and Schwann cells, which easily adhered to the graphene nanohydrogel scaffold and provided a scaffold for regenerating axonal ingrowth after spinal cord injury.[118] A composite hydrogel prepared using graphene and sodium alginate (GR-SA) can simulate the in vivo microenvironment, which is conducive to the enrichment and release of nutrients. Owing to the good electrical properties of graphene, the electrical conductivity of the hydrogel increased by 148%, which was similar to the conductivity of natural brain tissue, and could promote the aggregation of cells around axons. Simultaneously, the hydrogel had a porous structure that promoted the growth of neurotrophic factors. Both SA and graphene can significantly promote the expression of growth-related factors S100, NF160, MBP, and β3-tubulin and reduce the expression of inflammatory factors in the sciatic nerve, which has a synergistic effect.

Compared to SA, the expression of tyrosine hydroxylase (TH), a key dopaminergic neuron marker, in N27 cells was significantly increased in GR-SA hydrogels, and the increase in TH expression is beneficial for nerve growth. Results from a mouse model showed that the regenerated sciatic nerves in the GR-SA hydrogel group were denser, with a more uniform myelin sheath size, and contained a higher density and number of axons than those in the SA hydrogel group.[119,120] In contrast, elastic MGH membranes showed almost no inflammatory reaction 8 weeks after implantation in the rat sciatic nerve. When used as nerve stimulation electrodes, MGH membranes can provide a rich ionic surface with a charge injection capacity 1–2 orders of magnitude higher than that of conventional platinum-based membranes, which can be used to treat nerve injuries.[121] In citric acid-functionalized graphene and alginate composite hydrogels, the addition of graphene provides a rough surface conducive to the adhesion and diffusion of PC12 cells on the surface. Growing neurites and axons are almost interconnected and exhibit good electrical conductivity, which is conducive to signal transmission between cells. Roughness promotes the adsorption of serum proteins, which is favorable for nerve growth. Cells with neurites were numerous (64% vs 41%) and had longer neurites (195 vs 53 μm). The negatively charged pure alginate chains repel negatively charged PC12 and have low roughness, which is unfavorable for adhesion.[122] GO can also enhance the nerve guide tube function. GelMA/silk fibroin hydrogel functions as a nerve guide tube. In vivo experiments showed that the addition of graphene not only improved the mechanical strength of the conduit but also significantly promoted the remyelination of the injured nerve and the growth of the gastrocnemius muscle owing to its good electrical conductivity. Compared to the simple hydrogel, the microvessel density of the graphene group was doubled, indicating a good pro-angiogenic effect. Blood vessels are the bridge for nerve regeneration and provide the necessary nutrients for nerve regeneration; therefore, composite hydrogels can be used for nerve repair.[123] A 3D graphene tube can be used to fill hydrogels with good electrical conductivity. In vitro studies have shown that graphene tube containing hydrogels can support the proliferation and alignment of RSC96 nerve cells better than pure hydrogels, and the alignment of Schwann cells can guide cell migration and axonal extension in the appropriate direction, which is important for nerve regeneration.[124] The amino-functionalized graphene-crosslinked collagen hydrogel, which also has good electrical conductivity, increased the ATP paracrine of BMSCs under electrical stimulation, contributed to neuronal regeneration and immune regulation, and enhanced the expression of MAP-2 kinase and β-tubulin III, indicating neural differentiation. Immunohistochemistry demonstrated the differentiation of BMSCs into neurons in the hydrogel. When the 0.5% graphene collagen hydrogel was cultured with adult rat spinal cord sections, spinal cord cells proliferated from the spinal cord into the porous hydrogel, which helped establish neural connections and facilitated spinal cord injury recovery.[125] Schwann cells were seeded onto silk fibroin (SF)–graphene and pure SF hydrogels. In the in vitro cell culture, BDNF, CNT, and

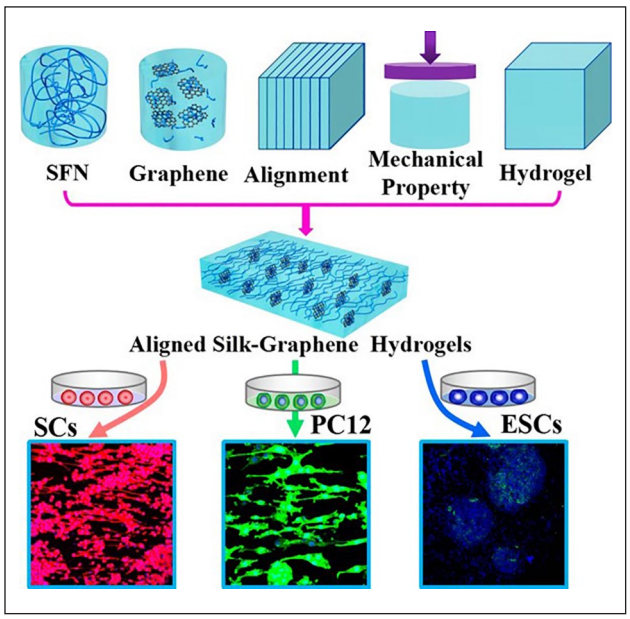

Figure 22. Aligned silk fibroin (SF)-graphene hydrogels with preferable stiffness were developed through arranging SF nanofibers and SF-modified graphene sheets under an electric field. The desired adhesion, proliferation, differentiation, extension, and growth factor secretion of multiple nerve-related cells was achieved on these hydrogels.[126]

NGF secretion significantly increased in the SF hydrogel, and the expression of these factors was further enhanced after graphene introduction. The longer PC12 axons and higher GAP43 gene expression levels on the hydrogel with higher graphene content indicate that the composite hydrogel containing more graphene can promote PC12 cell differentiation and neurite outgrowth induction[126] Figure 22.

In summary, in recent years, the development of neural tissue engineering technology has provided new ideas for related treatments. In recent years, studies have reported that graphene nanomaterials can promote the proliferation of various stem cells and their differentiation into nerve or neuron-like cells, ultimately promoting the formation of functional neural networks. At present, the possible mechanisms of graphene-based hydrogel nerve repair include: (1) Promoting neuronal electrical activity by realizing the electrical coupling reaction between neural stem cells and scaffolds through their own good electrical and thermal conductivity and mechanical strength. (2) Improving the immune microenvironment by promoting angiogenesis, inhibiting inflammatory responses, and scavenging free radicals. (3) Increasing the activity of enzymes related to nerve repair. (4) GO's large specific surface area and oxygen-containing functional groups are conducive to the adhesion of nerve cells, thereby providing a stable environmental basis for the growth and proliferation of nerve cells, which is a feature that previous neural scaffold materials did not have. The characteristics of graphene-based hydrogels effectively inhibit the formation of glial scars, clearing the obstacles for axon regeneration and achieving rapid repair of axons. Although graphene-based hydrogels have great potential in treating nerve damage, more long-term and short-term in vivo research results are still needed to further evaluate the long-term biosafety and effectiveness of graphene materials in animals before formal clinical use.

Wound healing

Poor wound healing after trauma and surgery is a pressing global medical problem that affects millions of people each year and poses a huge challenge to medical staff. Hydrogels have excellent abilities in hemostasis, anti-inflammation, and hypoxia relief. Polymer hydrogels can maintain good hydrophilicity, hygroscopicity, moisture retention, and have adjustable physical and biocompatibility. They are considered to be the most promising wound dressing candidates, which can accelerate healing and significantly improve healing quality. Graphene-derived hydrogels have high porosity, self-healing, shear-induced thinning, increased cell proliferation and migration, which are beneficial to promote wound hemostasis, inflammation, cell proliferation, and tissue reconstruction.

GO. GO exhibits good biocompatibility and mechanical properties, making it a potential wound-dressing material. Go (0.03 wt% and 0.09 wt%) was successfully integrated into a bacterial nanocellulose (BNC)/poly(acrylic acid) (P(AA)) network to prepare a BNC/P(AA)/GO composite hydrogel. Increasing GO concentration in the hydrogel led to a decrease in crosslink density and an increase in pore size, promoting nutrient transport and substance exchange, and simultaneously leading to an increase in water vapor permeability, which can prevent secretion accumulation in the wound and promote healing. The significant swelling ability of the 0.09 wt% GO hydrogel is due to a high density of hydrophilic functional groups such as COOH, CO, OH, and CO C groups on the GO surface. The interaction between GO and BNC/P(AA) endows the composite hydrogel with a water-locking effect, enhances water loading, improves swelling properties, and absorbs excess wound exudates, thereby promoting healing. The biocompatibility of GO-coated hydrogels was improved, and cell adhesion and proliferation of human dermal fibroblasts were significantly enhanced. Similarly, the introduction of GO in a composite CS and GO hydrogel resulted in an interconnected porous structure conducive to wound healing. This compound promoted fibroblast adhesion and proliferation. A rat wound model showed that the GO-containing composite hydrogel significantly accelerated wound healing; the wound closure rate reached 92.2% after 21 days, and the collagen fibers were arranged in an orderly manner. The scar closure rate of the pure hydrogel

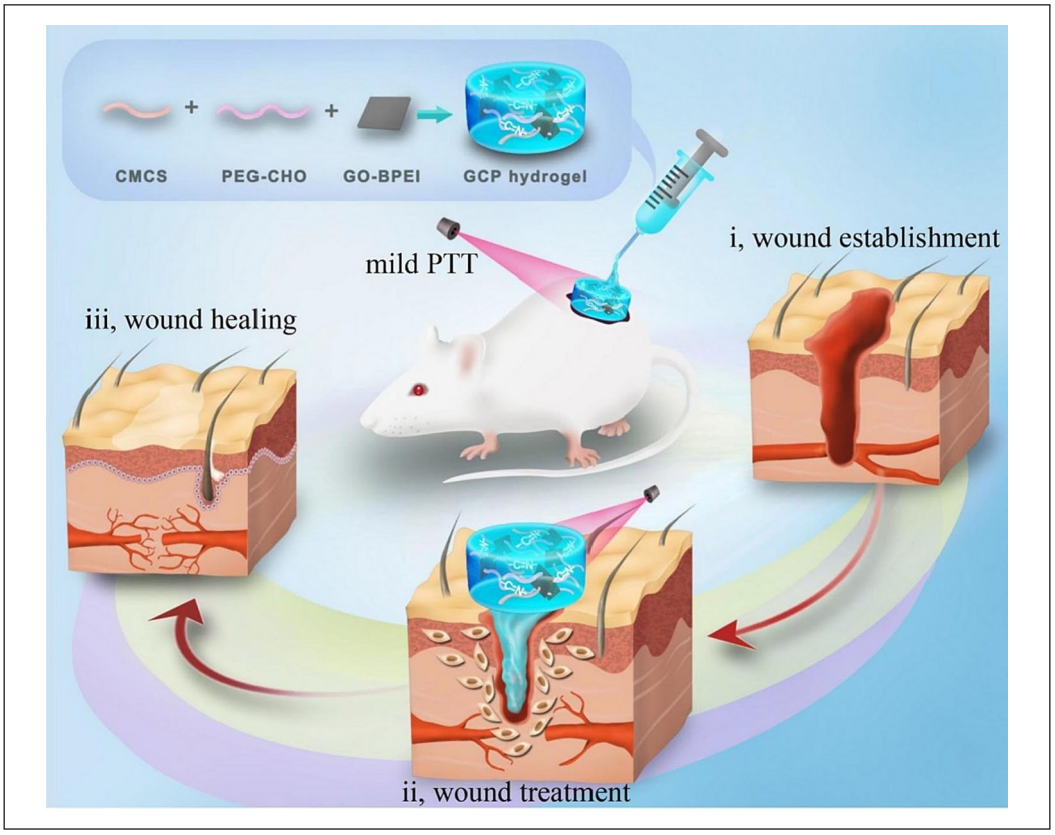

Figure 23. Schematic illustration of GO-BPEI/CMCS/PEG-CHO hydrogel and its application in promoting wound healing.[131]

control group was only 77.3%, and a large amount of immature granulation tissue was observed.[127–129] Previous studies confirmed that CS hydrogels supplemented with metformin (Met) and GO exhibit synergistic effects. In a rat type II diabetic foot model, the synergistic effect of Met and GO promoted angiogenesis to promote wound repair in vivo and has been shown to promote the healing of chronic diabetic wounds.[130]

The photothermal effects of GO promote wound healing. Studies have found that a hydrogel containing branched-chain polyethylenimine (BPEI) combined with GO (GO-BPEI) improved the absorption of near-infrared radiation, and the photothermal conversion performance was significantly improved. On day 14 of the rat wound model, the wounds of rats in the GO-BPEI infrared irradiation group were completely closed, while the wounds of rats in the pure hydrogel group healed slowly. Masson staining showed that infrared irradiation with GO-BPEI significantly improved collagen fiber deposition, promoted re-epithelialization and granulation tissue regeneration, and significantly accelerated wound healing, indicating that local thermal stimulation promoted fibroblast proliferation Figure 23.[131] A hydrogel composed of GO and dextran (DEX/GO) also exhibited a photothermal effect. The in vivo wound model showed that wound healing in the DEX/GO5 group was more apparent than that in the pure DEX and PBS groups owing to the photothermal effect of GO after 2 days of treatment.[132]

The CSGO hydrogel prepared using chitosan and GO has good water absorption ability and can maintain a moist environment in the wound, which is beneficial for hemostasis and wound healing. The abundant functional groups on GO lamels endow them with a specific attraction to biomolecules, cells, and tissues, increasing the potential of CSGO in wound healing. In a full-thickness skin defect model, HE staining showed that the wounds in the CSGO hydrogel group were almost completely healed compared with those in the pure hydrogel group. The distance between the granulation tissues in the blank control group was approximately 822 μm, while the distance between the granulation tissues in the CSGO group was significantly reduced to 480 μm[133] Figure 24. The composite hydrogel prepared using BNC with polyvinyl alcohol (PVA) and GO also showed water absorption, and the best performance was in that containing 0.04 mg GO, which helped absorb more wound exudate, maintain burn and chronic wound healing, exhibited excellent mechanical properties, and ensured sufficient strength to resist swelling after absorption of the wound exudate.[134] GO-loaded GelMA also showed significant wound healing potential, especially at 2% GO concentration, demonstrating the ability to promote keratinocyte proliferation and migration

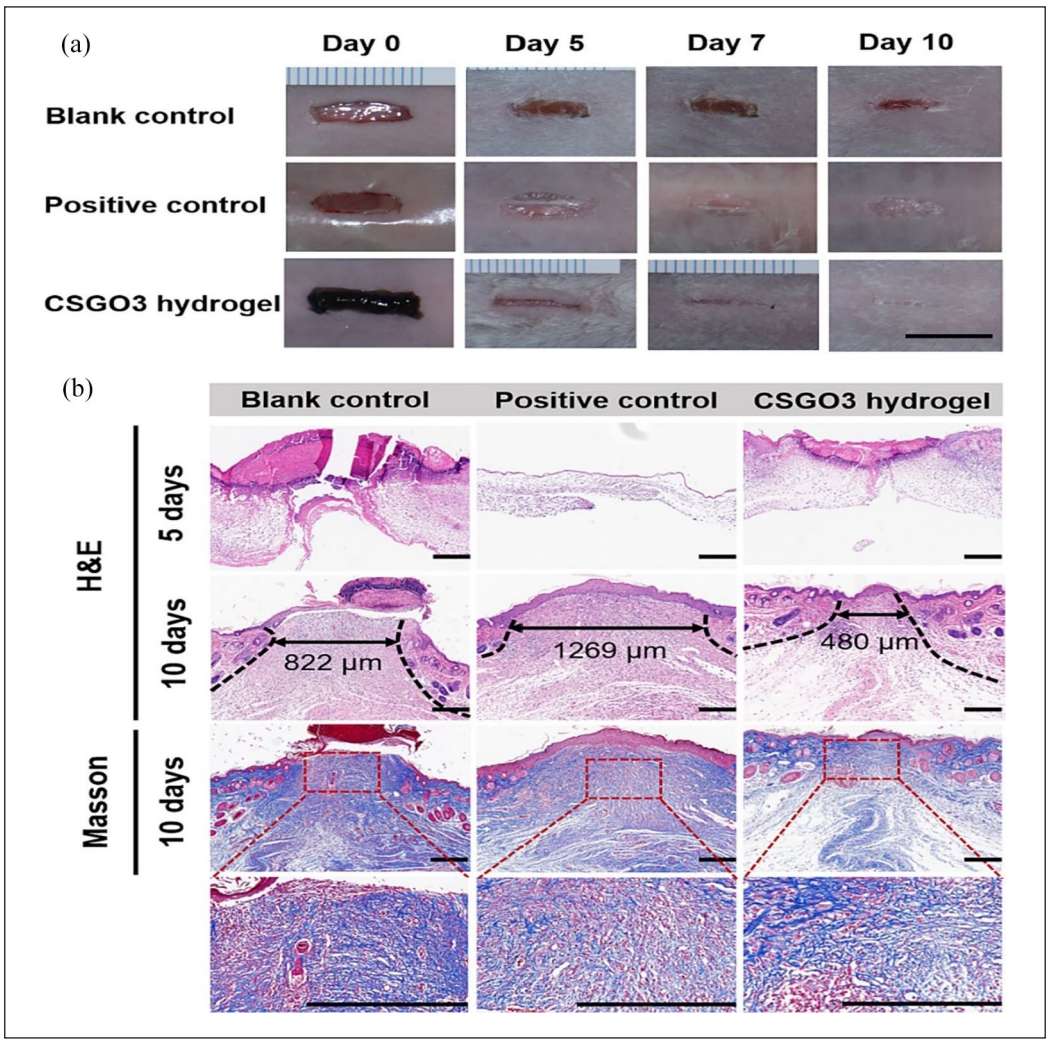

Figure 24. In vivo wound healing performance. (a) The wound healing sites of different treatment groups on day 0, 5, 7, and 10. Scale bar: 1 cm. (b) H&E staining images of wound tissues at fifth day and 10th day. The distance between the two ends of the black arrow indicates the distance between mature granulation tissues. And Masson's trichrome staining of wound healing on 10th day. The shades of blue represent the collagen fiber in the tissues. Scale bar: 240 μm.[133]

without cytotoxicity. A scratch assay showed that 2 wt% GO GelMA-treated cells migrated almost twice as much as in blank GelMA hydrogels.[135] Cell migration to the wound edge is a key step in wound healing. GO was impregnated into a genipin hydrogel to control its release by enzymes. Human adipose-derived mesenchymal stem cells (ADMSCs) and fibroblasts grew well on the hydrogel. After 12 h of incubation, the migration of human fibroblasts in the 1 wt% GO hydrogel group was significantly enhanced compared to that in the pure hydrogel group, and the scratch wound was completely closed at 24 h.[136] GO also promotes wound healing via hemostasis. Studies have shown that a hybrid hydrogel of peptides and GO has almost complete hemostasis when the GO content of the hydrogel is 0.5 wt%, the minimum blood loss is 1.4%, and the fastest hemostasis time is approximately 12 s, showing superior hemostasis ability. It has been found that GO activates platelets and induces thrombosis to stop bleeding, thereby accelerating the coagulation process. HE staining of a full-thickness skin defect model in rats showed that the GO 0.5-containing hydrogel caused less inflammation, whereas commercially available Tegaderm caused strong and prolonged inflammation which delayed wound healing.[137] Hydrogels prepared using chitosan oligosaccharide-modified GO (CG) and calcium alginate foam gel dressing (CGCD) promote wound healing by hemostasis. Studies have confirmed that the presence of CG makes the CGCD pore distribution uniform and pore size medium, which provides a stable platform for blood coagulation to form 3D reticulated thrombus and is conducive to accelerating the hemostasis process. CG in the hydrogel has a strong interaction with platelets, which enables the wound dressing to stop bleeding rapidly within 10 s. Owing to the large number of hydrophilic groups in

CG, the water retention ratio of the dressing was significantly increased after loading CG, which not only ensured the drainage of wound fluid, but also showed good fluid retention ability and created favorable external conditions for wound healing. The in vivo wound healing experiment showed that the wound covered with the 1% CG hydrogel almost completely healed within 12 days. Histological morphology showed that the hydrogel significantly accelerated wound healing by reducing inflammation and promoting vascular remodeling, whereas the control group without CG had less granulation tissue and more surrounding inflammatory areas.[138] A mouse skin defect model was used to evaluate the in vivo functions of a PEP (PDLLA-PEG-PDLLA) modified GO hydrogel (PEP@GO). Treatment with PEP@GO for 14 days significantly accelerated diabetic wound healing and epidermal regeneration compared to other trial treatments. HE and Masson staining of the wound tissue showed the presence of an intact epithelial barrier and a large amount of collagen production in the PEP@GO group. Other groups showed extensive inflammatory cell infiltration, sparse collagen fibers, and epithelial barrier disorders.[139]

rGO. GelMA hydrogels loaded with different concentrations of rGO exhibited sufficient porosity, permeability, and degradability. Live/dead experiments confirmed that the hydrogel had good biocompatibility with 3T3 cells, EA.hy926, and HaCa, without toxic effects. MTT and scratch assays showed that the hydrogel containing 0.002% w/w rGO significantly increased cell proliferation and migration, indicating that the optimal concentration of rGO could enhance the wound healing process by promoting the migration of different cell types. In vivo chick embryo angiogenesis (CEO) tests indicated that the slow release of rGO from the hydrogel may stimulate cell proliferation and ultimately promote new blood vessel formation and maturation.[140]

Studies on hyaluronic acid-dopamine and rGO (HA-DA/rGO) hydrogels have found that their mechanical properties are similar to those of human skin. In a mouse wound model, addition of a conductive component rGO@PDA accelerated wound closure and improved angiogenesis, while significantly enhancing vascularization by down-regulating the pro-inflammatory factor TNF-α and up-regulating CD31. It improved granulation tissue thickness and collagen deposition, promoted wound closure, and was more effective than the commercially available Tegaderm membrane. The enhanced conductivity of rGO helps transfer electrical signals between wounds, excites skin cells, and promotes the wound healing process[141–143] Figure 25.

GQDs. Citrate-crosslinked GQDs were used to prepare composite hydrogels (TA/KA-GQDs). In a rat wound healing model, the TA/KA-GQDs group showed faster wound healing than the TA/KA group, and almost 100% wound closure was observed in the TA/KA-GQDs group on day 16. Immunochemical staining showed that blood vessels, hair follicles, collagen fibers, and sebaceous glands were clearly visible in the wound. The wound-healing activity of TA/KA-GQDs is mainly related to the large surface area of GQDs, which can absorb more body fluids and do not form crusts. In addition, GQDs exhibit enhanced cell growth activity, reduced cytotoxicity, and new skin and tissue regeneration capacities[144,145] Figure 26.

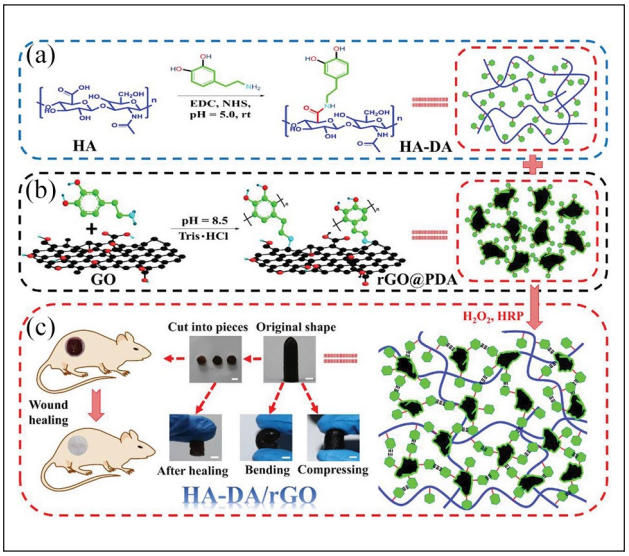

Figure 25. Diagrammatic sketch of HA-DA/rGO hydrogel preparation. (a) Preparation scheme of HA-DA polymer and (b) rGO@PDA, (c) scheme of HA-DA/rGO hydrogel and the original, bending, compressing, self-healing representation, and the application in wound healing.[141]

Similar results were obtained for hydrogels using GQDs and bacterial cellulose (BC). Invitro analysis showed that, compared with BC alone, the application of the GQD-BC hydrogel significantly increased the migration of human fibroblasts, and the gene expression of endothelial nitric oxide synthase, vascular endothelial growth factor A, matrix metalloproteinase 9, and vimentin was significantly upregulated, which promoted angiogenesis and tissue repair. The less dense binding of BC to the GQDs gives the hydrogel good wound fluid absorption and water-retention properties. In addition, the peak of GQD-BC for the WFA after 48 h was 117.7%, while that of the control group was 67.4%. Therefore, GQD hydrogels can be used as potential wound dressings.[28]

In summary, with the improvement of people's living standards, people have higher and higher requirements for skin scar healing. The healing process of skin wounds involves the collaborative efforts of growth factors, ECM and different tissues and cells. Although the skin has strong regenerative potential, so far, people still cannot achieve true scar-free healing and can only suppress the size of

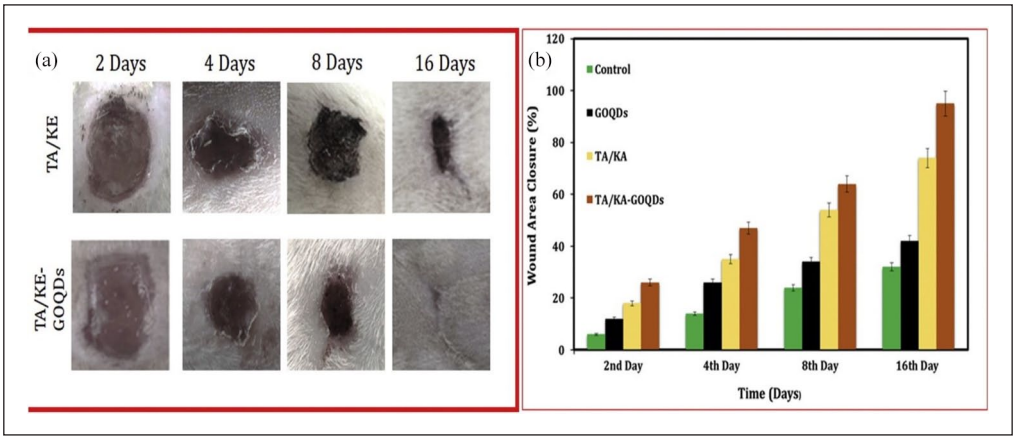

Figure 26. (a) Macroscopic appearances of the skin wounds treated with the prepared samples at the end of 2, 4, 8, and 16 days post-wounding; (b) Histogram comparing the wound closure percentages of the wound dressings of prepared samples at the end of 2, 4,8 and 16 days post-wounding.[145]

scars to a certain extent. The large number of carboxyl groups, hydroxyl groups and epoxides on GO sheets can form complex non-covalent interactions with the primary amines and hydroxyl groups of the hydrogel, including but not limited to electrostatic attraction and hydrogen bonds. The combination of the two makes the hydrogel have excellent water absorption properties, enhanced shear thinning and self-healing properties. This enables the hybrid hydrogel to absorb a large amount of water immediately after being attached to the wound surface, and maintain a moderately moist environment on the wound surface. At the same time, it can better adhere to the wound, effectively promote epidermal cell proliferation and skin regeneration, and achieve scar-free skin. repair. One study showed that blocking TGFβ signaling can reduce tissue fibrosis and scarring, but systemic inhibition of TGFβ may cause significant side effects and inhibit wound epithelialization. However, a pulse release platform based on light-induced imine cross-linked hydrogels, Pulse release of TGF-β inhibitors within a specific period of time after the wound appears has successfully achieved scarless wound healing in a mouse model. In view of the optical, electrical and thermal properties of graphene, the light of graphene hydrogel can be used in a timely manner.[146] electrical and thermal properties, causing the pulse release of TGFβ, which can also promote scar-free skin repair and even achieve better results. Therefore, based on the different physical and chemical properties of graphene and realizing its maximum potential by combining different methods, graphene hydrogel will have broad space for scar-free healing of skin wounds in the future.[147]

Drug release

In recent years, local drug therapy has received increasing attention due to the toxic and side effects of certain drugs when used in large doses throughout the body. Local drug therapy can not only reduce the systemic toxicity that may be caused by large doses of drugs, but also improve the local bioavailability of drugs. After loading drugs, hydrogels can use their good tissue adhesion properties to prolong the duration of local drug action and reduce the adverse effects that may exist when using local drugs. However, the drug loading capacity of hydrogels is limited, and the release is not slow enough to achieve sufficient long-term treatment. Graphene and its derivatives can be used as efficient drug carriers through hydrophobic interactions and π-π stacking of surface functional groups and huge specific surface area, and are conducive to the targeted release of drugs.

GO. Physical effects: In a carboxymethylcellulose and GO (CMC/GO) composite hydrogel, the π-π interaction between DOX (doxorubicin) and GO and the strong interaction between the amine group of DOX and the carboxyl group of GO led to higher DOX loading and sustained release in the hydrogel. The increased GO content in the GOC/MC-DOX complex resulted in greater cell-killing activity. It is possible that the percentage of DOX loading increases with increasing GO content[148] Figure 27.

CS and GO-Ag composite hydrogels can also be used for the controlled release of anticancer drugs DOX. There are hydrogen bonds and attractive electrostatic interactions between GO-Ag and DOX, which make drug loading highly efficient. CS hydrogel loaded with DOX showed burst release behavior after 30 min. However, the release path of DOX was prolonged in the hydrogel containing GO-Ag; therefore, the initial burst release of DOX significantly decreased, which in turn slowed the release of DOX. The addition of GO abolished the initial burst release of gemcitabine from the hydrogel, increased the loading capacity, controlled the release rate, and prolonged the

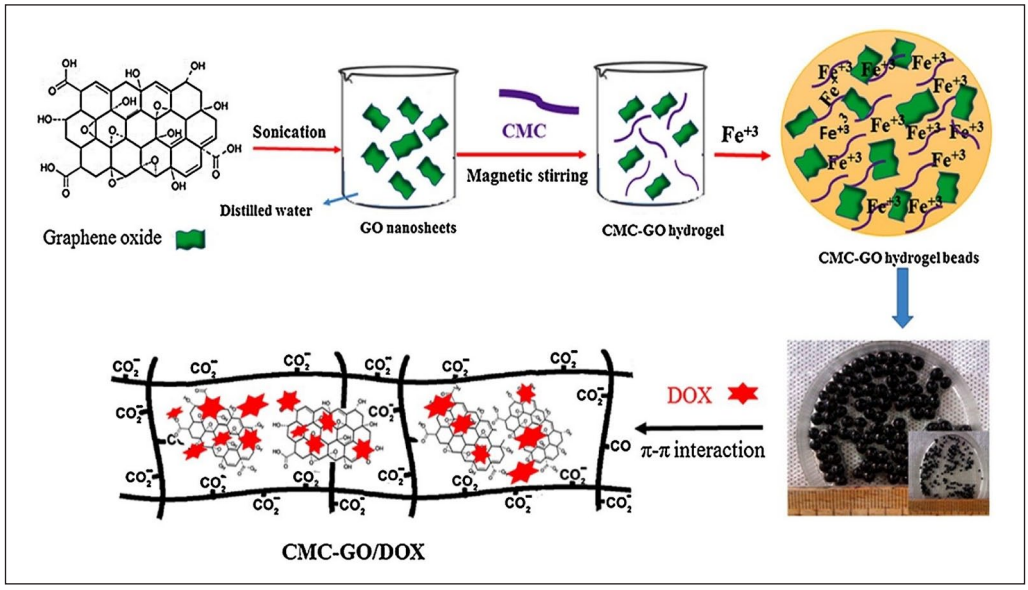

Figure 27. The schematic picture describing the chemical structure of the created dosage.[148]

action time of gemcitabine.[149,150] Similarly, a calcium alginate hydrogel containing GO that can be encapsulated can eliminate the disadvantage of the rough edges of GO and reduce damage to normal cells. DOX has a high loading rate of 89% on GO via π-π interactions, and the hydrogen bonding and electrostatic forces of DOX on GO lead to slow release. The ionic complexation of GO and LH is key to improving the loading capacity and controlling the release of the hydrogel. After 120 h, the LH release rate of SA hydrogel was 62.73 ± 0.70%, while that of GO-SA was only 51.10 ± 0.44%, and GO-SA had no burst release phenomenon. This shows good sustained-release performance. Moreover, when injected subcutaneously into mice, the hydrogel was maintained for more than 1 week, and dissection revealed no infection or inflammation in the surrounding internal organs.[151,152] Another hydrogel synthesized from hyaluronic acid (HA) and GO controls the sustained release of SenA, an emerging drug candidate for the treatment of occlusive vascular diseases, with strong hydrogen bonding and π-π superposition and hydrophobic interaction between the drug and GO resulting in a loading efficiency of more than 90%. The optimal GO:SenA ratio was 4:1, which maintained the continuous delivery of SenA for 21 days. It can be used to treat vein graft failure in occlusive vascular disease.[153] The huge π-binding layer on the GO surface was used to load cyclosporine into the GO-containing hydrogel contact lens via hydrophobic interactions. The non-covalent interaction of cyclosporine with the GO surface prevented local precipitation of the drug in the hydrogel. The surface and edges of GO are rich in oxygen-containing functional groups, which can retain water molecules by forming hydrogen bonds; thus, improving the swelling properties of GO is conducive to the sustained release of cyclosporine. Drug release studies in rabbit eyes have shown that GO contact lenses containing cyclosporine significantly improve the mean retention time of cyclosporine, improve swelling, and reduce total protein deposition compared to eye drops.[154] In addition, the π-π interaction between the drug and GO is beneficial to the use of sustained-release bimatoprost in the treatment of glaucoma. The simple immersion method leads to low drug uptake, swelling of the lens, and changes in light transmission, which limit the application of the drug. The incorporation of GO into hydrogel contact lenses resulted in the controlled release of bimatoprost. The water-holding properties of GO improved the swelling of the lens, whereas the uniform dispersion of bimatoprost on the GO surface prevented local precipitation of the drug, thereby improving the lens transmittance.[155] The π-π stacking or hydrogen bonding between tetracycline and GO can also be used for sustained release of tetracycline. A mesoporous polydopamine (MPDA) cross-linked cellulose nanofibril (CNF) hydrogel containing GO was successfully coated on the outer surface of MPDA-TH to control the drug release time and burst release behavior; the longest drug release time was 72 h. The drug release time of MPDA@GO/CNF was 3 and 7.2 times longer than that of polydopamine/CNF and CNF alone, respectively[156] Figure 28.

Photothermal effect: Using the rapid photothermal conversion of GO, the uniform embedding of GO in the composite hydrogel network of hyperbranched polyglycidol (HbPGL) and poly(AM-ran-2-AAPBA) ensured the near-infrared photothermal response of the hydrogel. With an increase in GO content, the photothermal conversion of the material accelerated. The maximum temperature reached was higher, and the temperature of the hydrogel could be maintained between 36.6°C and 41.0°C. The

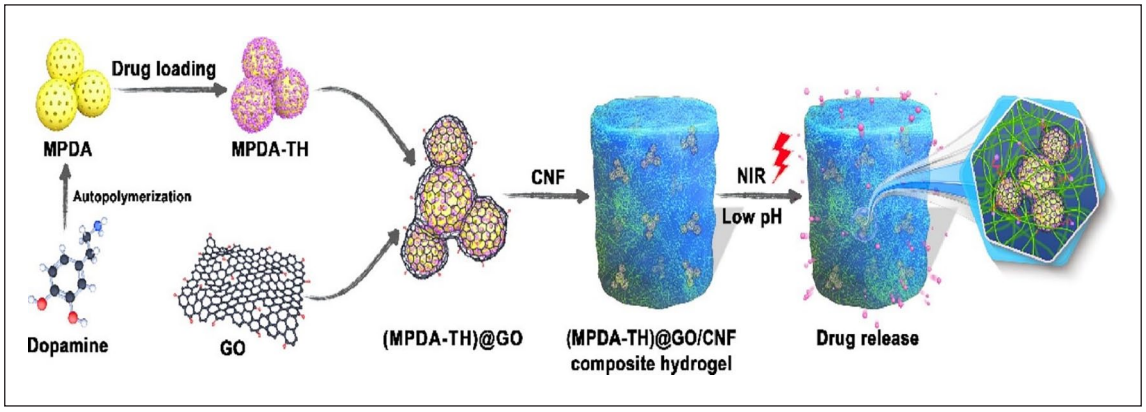

Figure 28. Schematic illustration of the preparation of the MPDA@GO/CNF composite hydrogel and its mechanism of drug release by a combination of multiple stimuli (pH change and NIR light irradiation).[156]

composite hydrogel was found to be suitable for thermal responsive control of niacin delivery at a GO concentration of 6.6 mg/ml.[157] Polystyrene (PS), poly(N-isopropylacrylamide) (PNIPAm), and GO were used to prepare novel hydrogels photonic crystal hydrogels (PCHs). GO is a black light-absorbing substance with photothermal effects. It absorbs incoherent scattered light, which reduces the reflectivity of PS@GO and improves its color contrast. When the temperature increased from 25°C to 40°C, the structural color changed from yellow to blue within 120 s, while when the temperature decreased from 40°C to 25°C, the structural color changed from blue to yellow. The sustained release of cisfloxacin was easily monitored by observing the corresponding color changes in real time.[158] PEGDA, GO, and pNIPAM were used to synthesize a new hydrogel, and the amount of drug released was predicted based on the color of the hydrogel. The hydrogel exhibited the best photothermal conversion efficiency and thermal response at a GO concentration of 4 mg/ml. Simultaneously, with the extension of near-infrared irradiation time, the released fluorescence intensity of FITC-dextran in the hydrogel gradually decreased, and the color of the hydrogel gradually changed from red to orange, yellow, green, cyan, and blue.[159]

pH: PVA/GO composite hydrogel is sensitive to pH. At low pH (1.7), the GO layer size changes owing to the electrostatic repulsion between the GO sheets in the composite hydrogel, which provides an internal driving force for the controlled release system and makes VB12 move to the low-concentration region after the change in the GO structure. Thus, controlled release of VB12 was achieved. However, in a neutral environment, the internal structure of the gel did not change significantly, and the gel dissociated a small amount of the drug. This demonstrates the ideal controllability of drug release in a simulated gastric environment.[160] However, when loaded with curcumin (CUR), the opposite effect was observed, and the π-π superposition between GO and the phenyl moiety of CUR was conducive to CUR loading. In acidic environments, GO tended to form compact aggregates, limiting the diffusion of CUR, of which the release was less than 10% within 24 h at pH 1.2. However, an increase in pH to 6.8 and 7.4 resulted in a significant increase in further ionization and the release of carboxylic acid groups on GO, which exceeded 20% and 50%, respectively. Therefore, the composite hydrogel was able to protect CUR during its passage through the stomach and small intestine into the proximal colon, which favored the action of CUR in the colon.[161,162] A composite hydrogel prepared from Pluronic modified with GO and oligo-lysine effectively hosted 5-FU owing to the hydrophobicity, crosslinking, and network density of the GO surface. Simultaneously, the GO surface was pH sensitive. Under acidic conditions, the degree of ionization of the carboxyl groups at the edge of the GO lamellae is reduced, leading to the easy destruction of the hydrogel, and rapid release of 5-FU, improving its therapeutic effect.[163] In xanthan gum, polyacrylic acid, and GO (XG-g-PAA/GO) composite hydrogels, the adsorption capacity of GO to diclofenac potassium (DCFP) decreased with an increase in pH, and the higher the pH value, the stronger the electrostatic repulsion between DCFP-ionized anions and GO, which favored the release of DCFP. In vitro, the cumulative release of DCFP in simulated intestinal fluid (68.41%) was higher than that in simulated gastric fluid (34.57%) after 96 h, avoiding side effects in the stomach.[164]

rGO. In the Pluronic®F127 rGO hydrogel loaded with ondansetron, the π-π stacking was enhanced as the rGO content in the hydrogel increased, and the drug release rate decreased proportionally. The pH of the hydrogel was within the normal range of skin (4–6.5), and the hydrogel did not irritate the skin when applied topically.[165] Studies have shown that hydrogels can also be loaded with cyclosporine for the treatment of psoriasis; however, the thick stratum corneum poses challenges for topical application.

The hydrogen bond formed by the hydroxyl and carboxylic acid groups of rGO increases the interaction with cyclosporine and the previous π-π interaction, leading to the sustained release of cyclosporine from the rGO hydrogel. The size of rGO was 361 nm, which is sufficiently small to make it highly permeable. In mouse models, hydrogels have been shown to be effective in the treatment of psoriasis by minimizing side effects encountered during oral administration.[166] Simultaneously, the high permeability of the hydrogel could be used to maintain the sustained release of the bronchial drug tulobuterol. In vitro release data showed that the hydrogel maintained the release of tulobuterol for 72 h due to the strong π-π interaction between the drug and rGO, and the hydrophobic and electrostatic nature between the drug and rGO. Similar results were obtained in a rat model. This may avoid complex inhaler administration, frequent dosing, and poor adherence.[167] Another Pluronic®F68 rGO hydrogel is an excellent carrier for sustained drug release. Due to the strong π-π interaction between rGO and lidocaine, its release time is extended to 10 h. Compared with commercially available lidocaine ointments, hydrogels have been shown to have a sustained anesthetic effect in radiant heat tail flick tests and sciatic nerve block models for effective pain management.[168] The sustained and stable release of triptolide was also achieved by exploiting the properties of Pluronic®f68 rGO, and the release time was extended up to 14 h. Owing to the high surface area of rGO and the disruption of the poor cell membrane structure by Pluronic®F68, the relative bioavailability of Pluronic®F68 rGO increased 3.3-fold, the drug was absorbed more rapidly, and the drug plasma concentration significantly increased at all time points. Anti-rheumatoid models suggest that composite hydrogels are effective in relieving swelling and pain in rheumatoid arthritis and can be used as an alternative to tablets and intravenous injections.[169] This property of the hydrogel also improved the sustained release of flurbiprofen axetil, increased drug penetration, and sustained release for up to 72 h, which was superior to that of the rGO-free hydrogel and other commercially available patches. Moreover, rGO entrapment of flurbiprofen axetil did not cause skin irritation, significantly inhibited edema, significantly enhanced anti-inflammatory activity, improved the short half-life of tablets and parenteral injections, reduced the need for frequent administration, and reduced abdominal discomfort.[170] Another characteristic of rGO is its large surface area and high loading capacity for aromatic compounds due to π-π stacking between the graphene surface and the aromatic compounds. The electrostatic interaction between polyanionic HA and the cationic rGO hydrogel can limit the diffusion of loaded drugs and prevent rapid release. Paclitaxel release was sustained for 104 h.[171] Additionally, the near-infrared properties of rGO can be used to control sustained drug release. Some studies have found that rGO has a stronger light-absorption capacity than GO in the near-infrared region. Therefore, the thermoactive hydrogel formed by carboxyl-reduced GO (rGO-COOH) and metformin hydrochloride is beneficial for improving metformin release.[172] In CMC-functionalized rGO, the intercalation effect of CMC-rGO improves the distribution of rGO in the 3D hydrogel, which helps to improve the near-infrared absorption and photothermal performance of the composite hydrogel. Heat from near-infrared irradiation does not cause DOX burst release or damage healthy cells. The hydrogen bonding and electrostatic interactions between DOX and rGO lead to high DOX loading, and the hydrogel can release DOX more effectively in an acidic environment than in a physiological environment, while the acidic microenvironment of tumor tissue can trigger active drug release, which is beneficial for antitumor activity[173] Figure 29.

Graphene. Increasing the concentration of graphene in a chitosan-graphene hybrid hydrogel increased the porosity and surface roughness of the hydrogel, which was beneficial to the loading of methotrexate (MTX). The initial burst release of MTX decreased from 24.7% to 5.32%, and the cumulative release of MTX decreased, which made the release slower and more controllable. MTX-loaded hydrogels inhibit the growth of MCF-7 breast cancer cells without harming normal cells.[174] The thermal effect of graphene can also modulate the release of diclofenac. Thermally triggered hydrogels synthesized from polyacrylic acid, agarose, and graphene can improve the release of diclofenac. Diclofenac can inhibit COX expression to exert anti-inflammatory effects. The strong interaction between the aromatic group of diclofenac and the π orbital of graphene leads to the physical adsorption of the drug on graphene. The thermal π-π effect between graphene and the drug during diffusion can be used to regulate the release of diclofenac via temperature. The interaction between diclofenac and graphene does not affect the therapeutic properties of diclofenac.[175]

The composite hydrogel composed of graphene and poly (N-isopropyl acrylamide) containing polydopamine nanoparticles (PDANPs) showed good electrical conductivity. DOX was used as the loading drug. When the hydrogel was irradiated using a near-infrared laser for 1 min, the DOX in the hydrogel was released, and the amount released increased sharply. When the near-infrared laser was turned off, drug release stopped, indicating that the drug release ability of hydrogels can be effectively controlled by light.[176] Studies have shown that specific interactions between graphene and the appropriate polymer can trigger the release of hydrophobic drugs. Graphene-diaminotriazine (G-DAT) composite hydrogels, owing to DAT hydrogen bonding and π-π stacking of graphene and hydrophobic microdomains formed by interaction with graphene's NH2, partially disrupt DAT-DAT stacking. The

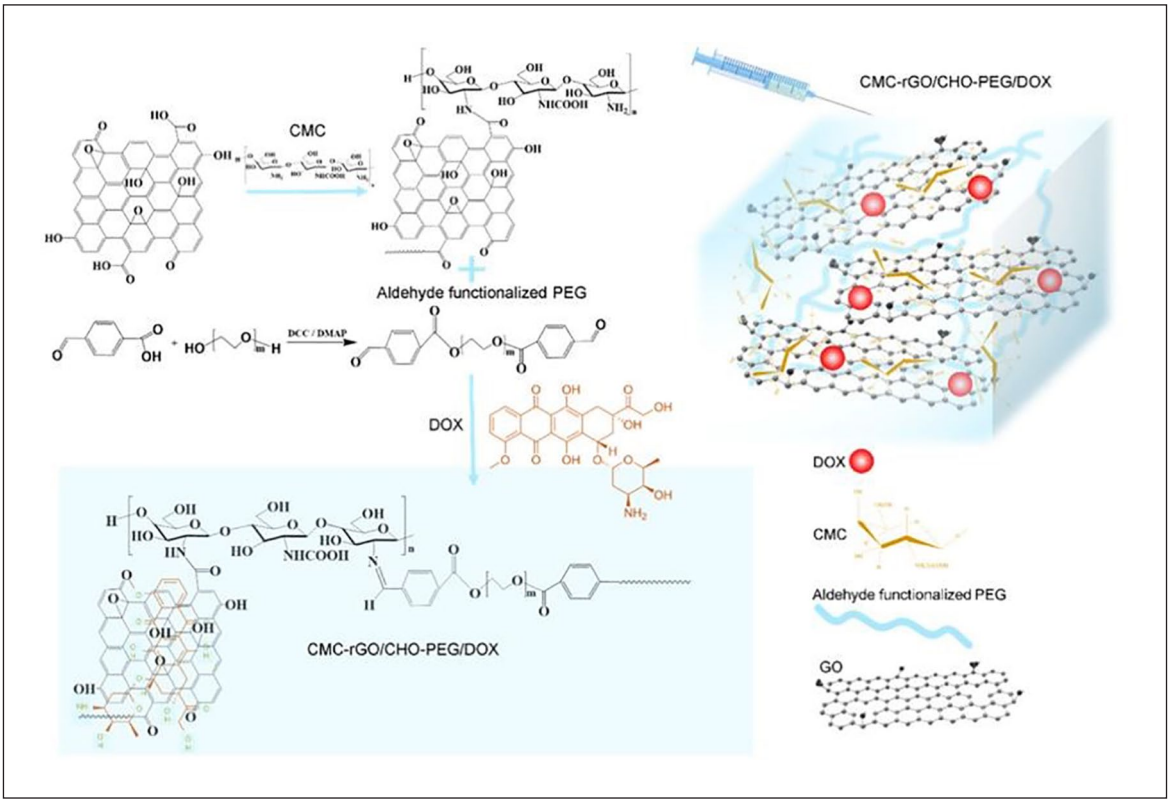

Figure 29. Illustrations of the CMC-rGO/CHO-PEG hydrogel fabrication and drug loading processes.[173]

affinity of the hydrogel for hydrophobic drugs was improved. Graphene also exhibits enhanced swelling properties and improved loading and release capabilities. The hydrophilic drug metronidazole had a lower drug loading of approximately 15%. In contrast, imipramine, which is more hydrophobic, had a higher drug loading of more than 35%[177] Figure 30. **G**-DAT hydrogel also exhibits a microwave radiation response, which can enhance skin permeability and release hydrophobic drugs. The graphene in the hydrogel acts as a radiator to avoid overheating of the scaffold during microwave radiation, and the graphene-conjugated π-structure allows efficient microwave absorption. The 0.5 -G-DAT hydrogel is not easy to overheat and has the best effect on sustained release of imipramine.[178]

GQDs. Graphene quantum dot nanoparticles incorporated into carboxymethyl cellulose (CMC) hydrogels exhibit pH sensitivity and can be used for the controlled release of DOX. The electrostatic attraction and π-π stacking between DOX and GQDs at pH 7.4 and 4.5, respectively, play a major role in adsorption. Moreover, the swelling rate at pH 4.5 was lower than that at pH 7.4, and a low swelling rate was detrimental to drug release. Thus, a low PH can release DOX slowly and continuously, and slower drug release can minimize drug loss and side effects. An MTT assay showed that the hydrogel had a significant inhibitory effect on K562 cells and induced apoptosis without any apparent toxicity.[179] GQDs also play important roles in analgesia. The dextran/polyisopropyl acrylamide (Dex/PNIPAM) composite hydrogel of GQDs is asymmetric, uniform, porous, has good liquid flow, and can be used as an effective carrier of buprenorphine into cells. Inflammation and inflammatory cell infiltration, including macrophages, lymphocytes, and neutrophils, were not observed in the GQD-Dex/PNIPAM treatment group. The results showed that buprenorphine hydrogel improved anti-inflammatory efficiency and pain management[180] Figure 31. Different graphene hydrogels and release profile list in Table 4, It is helpful to observe the sustained release effect of different graphene-based hydrogels

In summary, graphene can enhance aromatic hydrophobicity and a large specific surface area through hydrophobic interactions and π-π stacking, significantly improve the drug loading capacity, and facilitate the targeted release of drugs. At the same time, the presence of oxygen-containing functional groups on graphene further improves drug loading efficiency and stability. The recent research hotspot, GQD, has a high specific surface area, is easy to surface modify, does not require toxic organic solvents, and has little environmental pollution. Applying GQD to drug delivery can achieve real-time monitoring of the biodistribution and drug release of nanoparticles. Therefore,

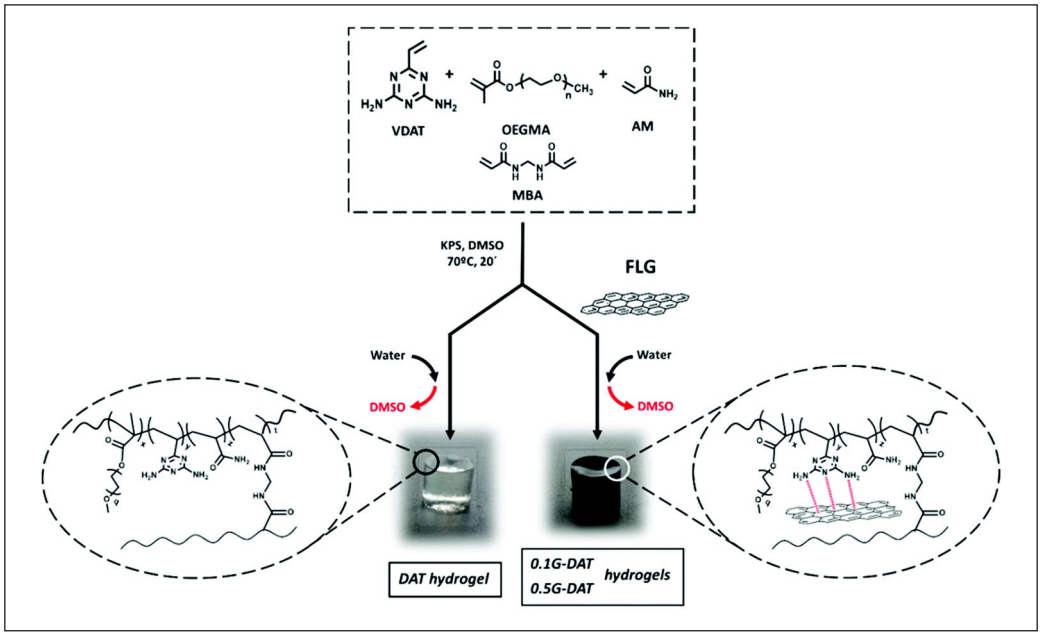

Figure 30. Synthesis of DAT and G-DAT hydrogels.[177]

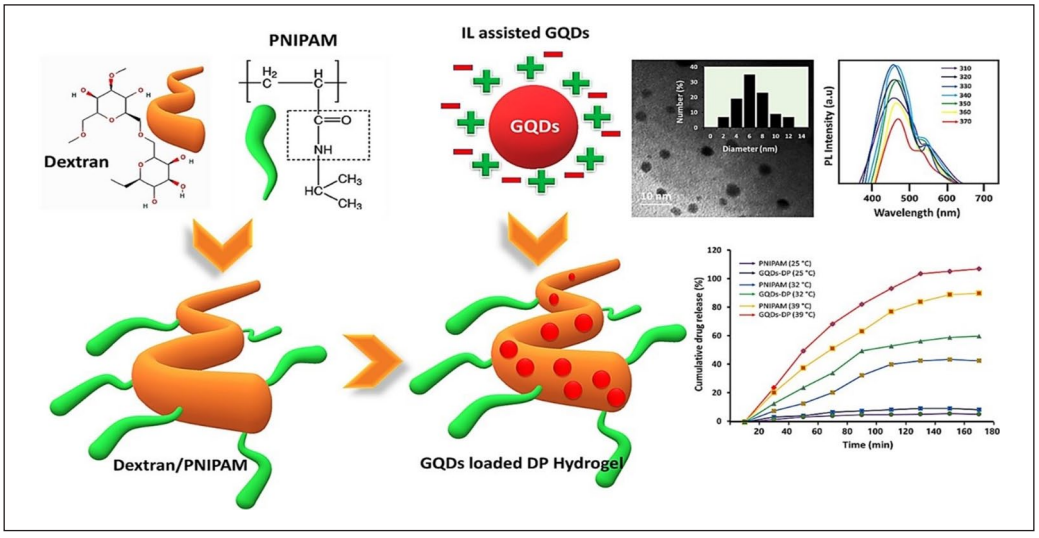

Figure 31. Schematic diagram of DP hydrogel formation loaded with GQDs.[180]

the potential of GQDs in the field of drug delivery should be further exploited in the future. At present, drug loading research on graphene derivative hydrogels mainly focuses on tumor drugs. In the future, it is also necessary to study the sustained release effect of other drugs, such as BMP2 that promotes bone healing and VEGF that promotes angiogenesis. At the same time, before the graphene hydrogel drug delivery system can be used in clinical applications, research on its behavior, toxicity, biodistribution and elimination methods in the body is still a big challenge, and the sustained release time of specific drugs also needs to be further improved. We firmly believe that graphene hydrogels will have greater performance and wider biomedical applications in the field of drug delivery.

Antibacterial

Antibacterial materials are recognized as important biomaterials because they can effectively inhibit bacterial infections. At present, hydrogels with antibacterial functions are the main focus of biomedical research. At present, antibacterial hydrogels are divided into three categories: 1.

Table 4. Different graphene hydrogels and release profile in section 4.5.

Graphene derivative based hydrogels	Condition of drug release	Release profile	References
GO-CMC/DOX	pH 6.8 and 7.4 in PBS solution	The maximum DOX release (35%) was achieved in 24 h in pH 6.8 solution while in pH 7.4 solution is 20%	Rasoulzadeh and Namazi[148]
GO-Ag-CH/DOX	pH 1.2 in the acid buffer medium pH 6.8 in PBS solution	The maximum DOX release (50%) was achieved in 24 h in pH 1.2 acid buffer medium while in pH 6.8 solution is 25%	Rasoulzadehzali and Namazi[149]
GO-alginate/DOX	pH1.2 6.8 and 7.4 in PBS solution	The maximum DOX release (88%) was achieved in 12 h in pH 7.4 while in pH 6.8 solution is 80%, in pH 1.2 is 35%	Rehman et al.[151]
GO-sodium alginate/Lidocaine hydrochloride	pH7.4 in PBS solution	The maximum LH release (51.1%) was achieved in 120 h in PBS solution	Luu et al.[152]
GO-SenA-HA hydrogels	pH7.4 in PBS solution	The maximum SenA release (100%) was achieved in 22 day in PBS solution	Maturavongsadit et al.[153]
GO-DMA-EGDMA-HEMA	In STF	The maximum cyclosporine (50%) was achieved in72h in STF	Desai et al.[154]
MPDA@GO/CNF-tetracycline hydrochloride (TH)	pH5 and 7.4 in PBS solution	The maximum DOX release (78%) was achieved in 24 h in pH 5 while in pH 7.4 solution is 48%	Liu et al.[156]
PS@GO-PNIPAm PCHs-Moxifloxacin	In water	The maximum MOX (65%) was achieved in 1h in water	Shen et al.[158]
GO/pNIPAM/PEGDA-Dextran	pH7.4 in PBS solution	The maximum dextran (80%) was achieved in 14 min	Sun et al.[159]
PVA/GO-VB12	pH1.2 HCL and 7.4 in PBS solution	The maximum VB12 release (55%) was achieved in 12 h in pH 1.2 while in pH 7.4 solution is 12% in 5h	Luo et al.[160]
GO/PVA-Curcumin	PH1.2 6.8 and 7.4 in PBS solution	The maximum Curcumin release (50%) was achieved in 24 h in pH 7.4 while in pH 6.8 solution is 20% in 7h, pH 1.2 is 12% in 3h	Hou et al.[161]
GO/gum tragacanth-Rivastigmine	pH1.2 simulated gastric and 7.4 Simulated intestinal	The maximum RIV release (100%) was achieved in 6 h in pH 7.4 while in pH 1.2 is 50%	Rahmani et al.[162]
FLGO-5-Fluorouracil	PH5 7.4 and 9 in PBS solution	The maximum 5-FU release (59%) was achieved in 7 day in pH 5 while in pH 7.4 solution is 43% in 7 day, pH 9 is 41% in 7 day	Li P et al.[163]
XG-g-PAA/GO-Diclofenac potassium	In artificial intestinal fluid and in Artificial gastric fluid	The maximum DCFP release (68.41%) was achieved in 96 h in artificial intestinal fluid while in artificial gastric fluidn is 34.57% in 96 h	Li et al.[164]
Pluronic® F127/rGO-Cyclosporine	pH7.4 in PBS solution	The maximum Cyc release (66.2%) was achieved in 24 h in pH 7.4 PBS solution	Li et al.[166]
Pluronic® F127/rGO-Tulobuterol	pH7.4 in PBS solution	The maximum TB release (89.5%) was achieved in 24 h in pH 7.4 PBS solution	Luo et al.[167]

(Continued)

Table 4. (Continued)

Graphene derivative based hydrogels	Condition of drug release	Release profile	References
Pluronic® F68/rGO-Lidocaine	pH7.4 in PBS solution	The maximum Lidocaine release (91%) was achieved in 10 h in pH 7.4 PBS solution	Li et al.[168]
Pluronic® F68/rGO-Triptolide	Using goat skin	The maximum Triptolide release (96.78%) was achieved in 10 h in goat skin	Guo et al.[169]
Pluronic® F68/rGO-Flurbiprofen	Using rat skin	The maximum Flurbiprofen release (94.94%) was achieved in 72 h in rat skin	Yang and Li[170]
rGO/hyaluronic acid- Paclitaxel	pH7.4 in PBS solution	The maximum PLX release (92%) was achieved in 80 h in pH 7.4 PBS solution	Patil et al.[171]
rGO-COOH gel-metformin	pH7.4 in PBS solution	The maximum metformin release (64%) was achieved in 24 h in pH 7.4 PBS	Chengnan L et al.[172]
CMC-rGO/CHO-PEG-DOX	PH 6.5 and 7.4 in PBS solution	The maximum DOX release (100%) was achieved in 20 h in pH 7.4 or pH 6.5	Liu et al.[173]
Chitosan/Graphene-Methotrexate	pH7.4 in PBS solution	The maximum MTX release (18%) was achieved in 170 h in pH 7.4	Saeednia et al.[174]
PAA/Graphene-Diclofenac	pH7.4 in PBS solution	The maximum Diclofenac release (100%) was achieved in 6 h in pH 7.4	Mauri et al.[175]
PNIPAM-GO/PDA-NPs-EGF	pH7.4 in PBS solution	The maximum EGF release (45%) was achieved in 16 Ddy in pH 7.4	Leganés J et al.[177]
Graphene/diaminotriazine-Imipramine	pH7.4 in PBS solution and pH1.2 SGF media	The maximum Imipramine release (90%) was achieved in 24 h in pH 1.2 while in pH 7.4 solution is 80% in 24 h	Zhu Y et al.[176]
CMC/GQD-DOX	pH7.4 in PBS solution and pH4.5 SAB media	The maximum DOX5 release (60%) was achieved in 400 h in pH 4.5 while in pH 7.4 solution is 50% in 400 h	Yue et al.[180]
GQDs-Dex/PNIPAM	pH7.4 in PBS solution	The maximum Dex release (60%) was achieved in 3h in pH 7.4	Javanbakht and Namazi[179]

Hydrogels containing inorganic nanoparticles, 2. Hydrogels containing antibiotics, and 3. Hydrogels with inherent antibacterial properties. Due to its photothermal properties, graphene can be used as a photothermal agent to combine with hydrogels to cause the high temperature to denature the proteins on the bacterial cell membrane. The graphene sheets wrap the bacteria or use their sharp edges to penetrate the bacteria, rather than a purely molecular mechanism. This physical interaction means that bacteria are less likely to develop resistance to graphene. Graphene can also enhance the bodys immunity and improve the bodys resistance to bacteria. Therefore, graphene-based hydrogels have great prospects in antibacterial properties.

GO. Studies have shown that GO exhibits good antimicrobial activity. GO hydrogel can mimic the cancerous pagurus carapace, which is an antibacterial cloak. The hydrogel reduced the colony areas of Staphylococcus aureus, Escherichia coli, and Candida albicans by approximately 70%, 65%, and 45%, respectively. First, the sharp GO flakes cut the bacterial membranes, leading to nucleic acid leakage. Secondly, GO embedded in the folded structure decreases cell metabolism. Although the GO edges could not cleave fungi protected by thicker cell walls, they slowed colony growth and cell metabolism. Thus, S. aureus is more sensitive to GO because it lacks the outer membrane that protects Gram-negative E. coli. Finally, C. albicans is a fungus with a thick and complex cell wall structure, resulting in limited antifungal efficacy.[181] An antibacterial hydrogel was prepared using O-chitosan quaternary ammonium salt (O-HACC), polyvinyl alcohol, and GO (O-HACC/PVA/GO). It was shown that -HACC, which introduces a quaternary ammonium group on the hydroxyl group, can interact with negative residues on the bacterial cell surface to inhibit bacterial reproduction. The introduction of GO increased the antibacterial activity of the O-HACC/PVA hydrogel by a factor of two because of the destruction of bacterial RNA by the membrane stress caused by the sharp edges of GO. Moreover, the quaternary ammonium salt group had a synergistic effect with GO, and the hydrogel exhibited a strong inhibitory effect on S. aureus and E. coli.[182] Some studies have found that the specific antibacterial mechanism of GO-containing chitosan hydrogels is due to the interaction of the positively charged amino groups in chitosan with the negatively charged phospholipids and lipopolysaccharides on the bacterial surface, resulting in bacterial death. Alternatively, direct contact of sharp GO nanosheets with bacteria leads to membrane stress and subsequent superoxide anion-independent oxidation, which in turn leads to the oxidation of proteins, lipids, and nucleic acids, ultimately leading to membrane damage and bacterial death[183–185] Figures 32 and 33. GO-embedded sodium deoxycholate (NaDC) hydrogels also exhibited synergistic antibacterial

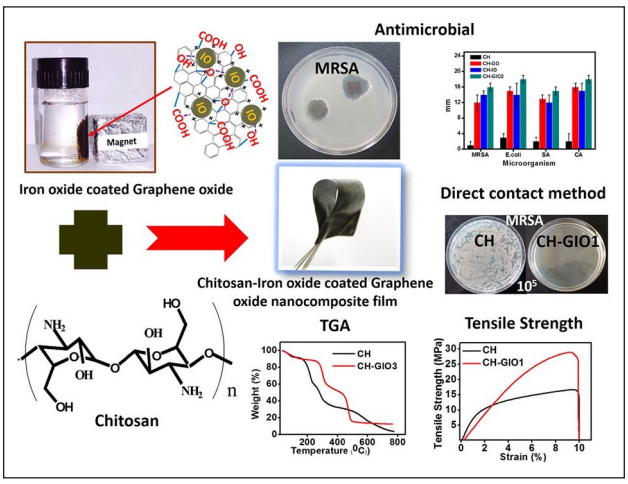

Figure 32. Schematic of the formation of the chitosan−GIO hydrogel nanocomposite film.[183]

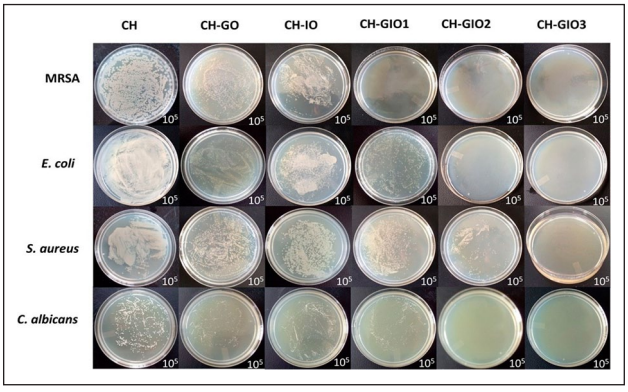

Figure 33. Typical photographs of recultivated microorganism colonies for methicillin-resistant Staphylococcus aureus (MRSA), Escherichia coli (E. coli), Staphylococcus aureus (S. aureus), and Candida albicans (C. albicans) on agar culture plates, where the concentrations of bacteria seeded onto the graphene films were 105 CFU/mL.[183]

effects. Compared to pure gels, GO-NaDC showed significant selectivity against E. coli and S. aureus. Co-culturing for 22 h significantly inhibited the growth of E. coli and S. aureus.[186] GO hydrogels loaded with antisense DNA oligonucleotides can inhibit the transcription of the drug resistance gene YycFG, thereby inhibiting the growth of S. aureus, whereas GO induces oxidative stress in the bacterial outer cell wall, which inhibits biofilm formation by S. aureus and plays a synergistic role.[187]

The characteristics of GO under near-infrared light also play a bactericidal role. The hydrogel polymerized by vinylglucan (DexIEM), vinylgraphene oxide (GM), and laponite, and the adequate cross-linking of GM and laponite improved the drug-loading performance of the hydrogel. Meanwhile, GM as a photothermal agent gives the hydrogel excellent photothermal conversion ability,

and the surface temperature can be increased from 26.8°C to 55.5°C under near-infrared irradiation, thereby enabling the material to inactivate bacteria.[188] β-cyclodextrin-functionalized GO also has near-infrared light response functions and combines with NO donor BNN6 to form a composite hydrogel. GO itself has an antibacterial effect, and its photothermal effect enhances the release of NO, which can have a synergistic antibacterial effect. Under infrared laser irradiation, the inactivation rates of S. aureus and E. coli are 97.6% and 95.5%, respectively.[189]

rGO. rGO-containing hyaluronic acid graft dopamine (HA-DA/rGO) hydrogel exhibits a good near-infrared photothermal effect. Studies have shown that when the temperature exceeds 50°, bacteria are killed due to the destruction of certain enzymes and proteins. When the irradiation time was increased to 10 min, the HA-DA/rGO group showed an almost complete killing effect on E. coli and S. aureus. The survival rates of the two bacteria decreased to 74.1% and 62.9%, respectively, which also indicated that the bactericidal performance of HA-DA/rGO was derived from the photothermal effect provided by rGO. rGO-containing butyl methacrylate (BuMA) and polyethylene glycol methyl methacrylate (PEGMEMA) also released loaded cefepixime "on demand" under near-infrared light activation without photothermal activation, and no antibiotic release was observed. The addition of rGO further enhanced the current density of the composite hydrogel and induced more carbon-centered free radicals, thereby enhancing its antibacterial activity. This was verified for the CuI-BiOI/rGO and CuI-BiOI hydrogels; however, only a small number of E. coli and S. aureus were killed in the latter.[141,190,191] The study showed that the hydrogel formed by combining rGO with sodium carboxymethyl cellulose (NaCMC) showed a synergistic effect. The XTT assay confirmed that the hydrogel reduced the colony formation of S. aureus (81%–84%) and Pseudomonas aeruginosa (50%–62%). Bacteria were encapsulated and deposited in the aggregated structure of rGO.[192] Another study found that a hydrogel formed by lignan nanoparticles (LNP) and rGO also possessed synergistic antibacterial activity, and the antibacterial effect of the composite hydrogel was enhanced compared to that of bare LNP or rGO. LNP have significant antibacterial activity against Klebsiella pneumoniae and Enterococcus faecalis, which is due to the mechanical stress caused by rGO as the main factor leading to cell membrane rupture. In contrast, the lignin side chain structure and functional groups impart LNP with antibacterial properties.[193] However, some studies have found that rGO components alone do not exhibit antibacterial effects, and that the antibacterial property of the rare-earth terbium ion (Tb3+) is due to its strong synergistic interaction with the carboxyl and carbonyl groups of the bacterial peptidoglycan, which destroys the integrity of the bacterial cell wall. The addition of rGO to the Tb3+-containing hydrogel further increased its killing efficacy against S. aureus and P. aeruginosa by 1.5 and 2 orders of magnitude, respectively. This synergistic bactericidal effect between Tb3+ and rGO is due to the increased loading and release of Tb3+ resulting from the rGO-induced loosening of the hydrogel network, leading to an enhanced bactericidal effect.[194] Similarly, rGO exhibits a high surface-to-volume ratio. Silver sulfadiazine and silver nanoparticles on the hydrogel scaffold are encapsulated in the cavity or surface of rGO, which exert synergistic antibacterial effects through π-π stacking interactions between drugs and rGO aromatic rings. It has antibacterial activity against P. aeruginosa, S. aureus, E. faecalis, and E. coli[195,196] Figures 34 and 35.

GQDs. Some studies have found that GQD-ε-PL hydrogel has a photothermal effect. First, the composite hydrogel can be rapidly heated. Second, high temperatures can directly damage the bacterial cell membrane, change the permeability of the bacterial cell membrane, and lead to leakage of the bacterial cytoplasm and death. Results showed that the viabilities of E. coli, S. aureus, and P. aeruginosa in the simple hydrogel were 66.5%, 42%, and 80.8%, respectively. The viabilities in GQD-ε-PL significantly decreased to 10.2%, 11.8%, and 19.0%, respectively. After activating the photothermal effect, bacterial viability continued to decrease to 3.4%, 2.9%, and 2.0%, respectively[197] Figure 36.

In summary, current research shows that graphene mainly uses the following three pathways: 1. Physical cutting pathway, that is, after bacteria come into direct contact with graphene-based materials, the sharp sheets of the material pierce the bacterial cell membrane, causing the outflow of cell contents and killing the bacteria. Graphene wraps the bacteria to isolate them from the external environment and prevent them from absorbing nutrients, thereby inhibiting the growth of bacteria. 2. Oxidative stress pathway, that is, after the cell membrane comes into direct contact with graphene-based materials, the free radical reaction is stimulated through charge transfer or ROS generation, thereby destroying the membrane structure and important biological macromolecules of the bacteria and causing death. 3. Lipid molecule destruction pathway, that is, graphene nanosheets can be inserted into the bacterial cell membrane in a short time, extracting the phospholipid components therein, or directly spread on the cell membrane surface to cause lipid molecule flipping, ultimately leading to bacterial lysis and death.[198] In the process of hydrogel preparation, graphene antibacterial components are added by doping or chemical bonding, so that it has the functions of both gel and graphene, so that the two have a synergistic effect. However, how to maximize the antibacterial effect is the focus of future research. The toxicity of biomaterials to the human body is a difficult problem that can never be avoided. The research on

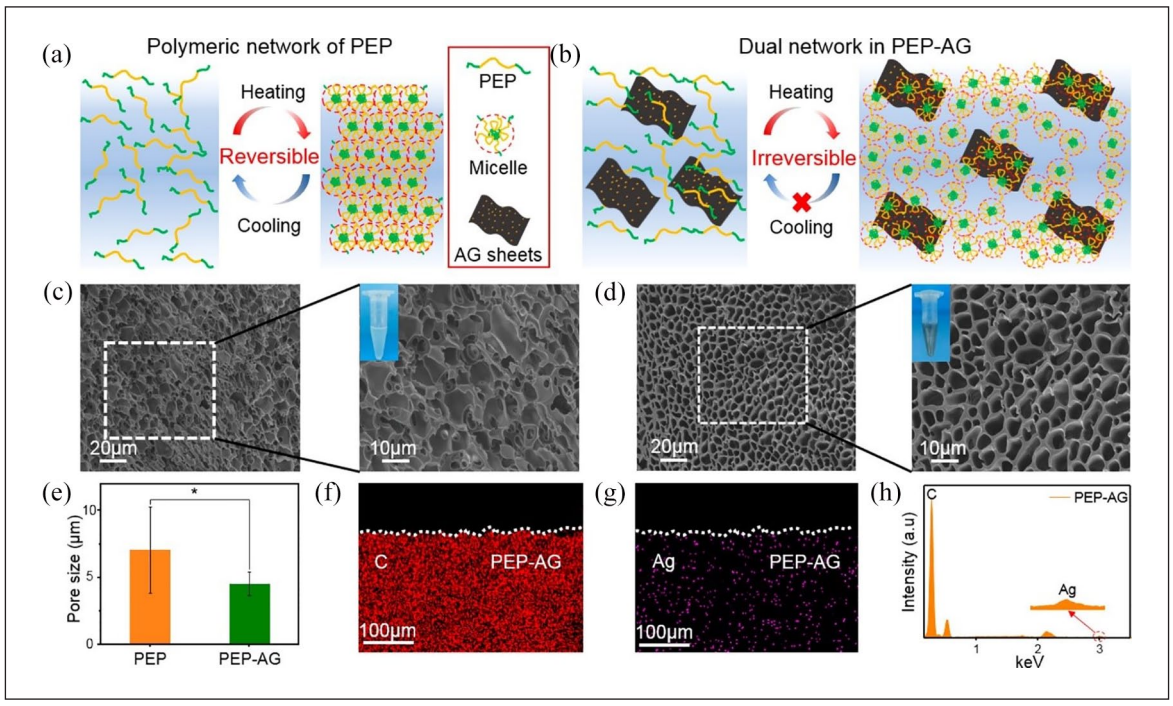

Figure 34. Characterization of PEP and PEP-AG hydrogels. Schematic structures in (a) the PEP hydrogel and (b) the PEP-AG composite hydrogel. Low- and high-resolution SEM images of porous structures in (c) the PEP hydrogel and (d) the PEP-AG hydrogel. (e) Pore size distributions of PEP and PEP-AG hydrogels. (f and g) EDS mapping of C and Ag elements in the PEP-AG hydrogel and (h) the relative spectrum.[196]

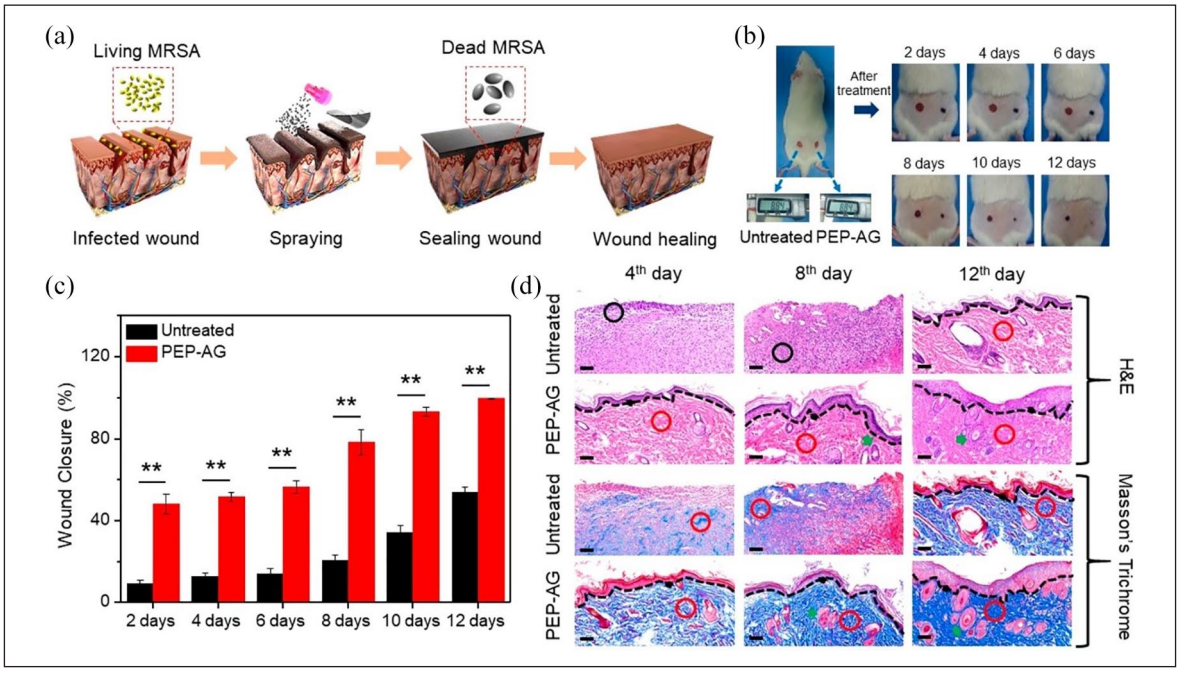

Figure 35. PEP-AG hydrogel-accelerated healing of a MRSA-infected wound on rats. (a) Illustration of the PEP-AG hydrogel as an antibacterial dressing by spray procedure onto the MRSA-infected wound. (b) Two round MRSA-infected wounds were made on the two sides of depilated back skin of the hip on each rat. The left wound remained untreated, while the right wound was covered by the PEP-AG hydrogel, and pictures were collected on the second, fourth, sixth, eighth, 10th, and 12th days in the wound healing process. (c) Wound closure rate in untreated group and PEP-AG group (error bars are standard deviation, $n = 5$). (d) Pathological examination of a skin section collected from the wound areas in the untreated group and PEP-AG group on the fourth, eighth, and 12th days. Black circle, red circle, black arrow, green arrow, and black dashed line indicate inflammatory cells, collagen fibers, epidermis, hair follicles, and boundary of epithelium and dermis, respectively.[196]

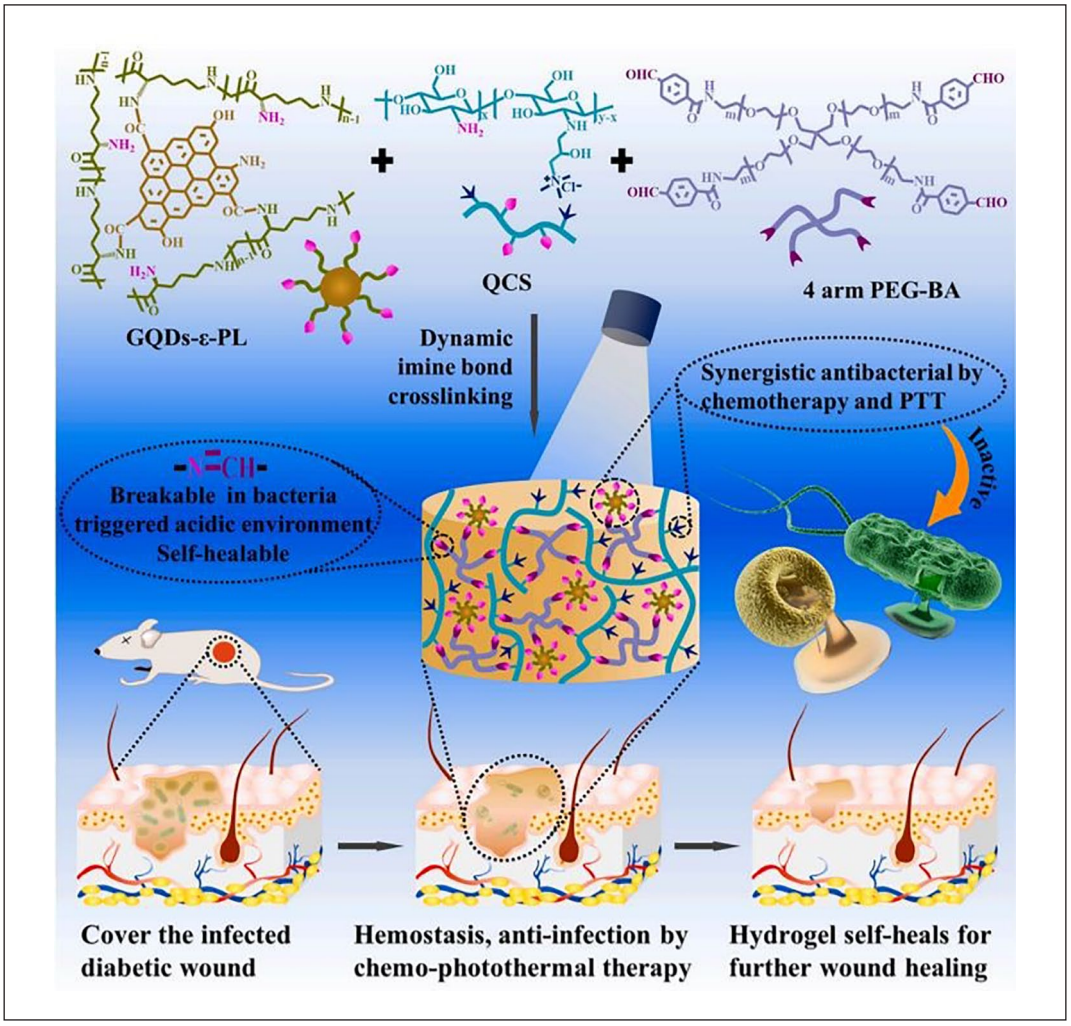

Figure 36. Schematic diagram of GQDs-ε-PL/QCS/4 arm PEG-BA hydrogel and the hemostasis, the chemo-photothermal synergistic anti-infection and self-healing functions of the hydrogel for accelerating the healing of the infected diabetic wounds.[197]

the mechanism of interaction between graphene materials and the human body is still in its initial stage, and the relevant literature is limited. Despite this, people can still use surface modification and other means to maintain the excellent performance of the graphene material itself and avoid inducing its biological toxicity, so that it can be more safely and widely used in various fields. In addition, the study of the preparation process and antibacterial mechanism of graphene-based hydrogel antibacterial materials is also of great reference significance for the study of other functional composite materials. In the future, with the trend of antibacterial materials developing in the direction of green and environmental protection, graphene-based hydrogel antibacterial materials will also gain broader development and application.

Cardiac repair

Heart dysfunction is one of the leading causes of death worldwide, and existing treatments such as drug therapy, heart transplantation, and cell therapy still have limitations. As a 3D scaffold material, hydrogel can be used to deliver cells to damaged myocardial tissue and promote heart regeneration. Its properties are close to those of the extracellular matrix, with good biocompatibility and cell adhesion, while graphene and its derivatives give hydrogels better biocompatibility, biodegradability, mechanical strength, and conductivity. In particular, excellent conductivity is important for cardiac tissue engineering applications, because good conductivity is conducive to cell activity and the recovery of myocardial function. Therefore, it is urgent to develop a conductive cardiac tissue engineering material.

GO. Studies have found that an appropriate concentration of GO can produce hydrogel scaffolds with a stiffness similar to that of natural hearts and provide suitable mechanical properties for the growth and development of cardiomyocytes. The addition of GO to gelatin hydrogels significantly enhanced the arrangement and beating speed

of cardiomyocytes and cardiac gene expression; therefore, GO-containing hydrogels may be used for the treatment of damaged myocardium.[199] In the early stage of myocardial infarction, myocardial cell necrosis activates the inflammatory response, and the ROS content increases. The mechanical strength of the novel GO lithium silicate-gelatin composite hydrogel was improved by the addition of GO. The interconnected porous structure of the composite hydrogel allowed the exchange of nutrients and metabolites to promote cell growth, whereas the potential antioxidant properties and cytocompatible release of GO enabled the composite hydrogel to inhibit H_2O_2-induced oxidative stress. Clinical studies have shown that the direct injection of WJ-MSCs into the infarcted myocardial region reduces apoptosis and fibrosis. In an in vitro oxidative stress model, a composite hydrogel containing WJ-MSCs reduced inflammation and apoptosis and improved the viability of cardiomyocytes under oxidative stress.[200] The addition of GO to Alg-GO composite hydrogels improved cell adhesion and spreading. The hydrogel promoted the differentiation of rMSCs into cardiomyocyte-like cells expressing the cardiac markers troponin T and GATA4.[201] After myocardial infarction, both the inflammatory response and the presence of scar tissue lead to ventricular dysfunction. Therefore, the application of conductive hydrogels can not only provide mechanical support to the infarct area but also synchronize contraction and restore ventricular function by electrically connecting isolated cardiomyocytes and intact tissues. The novel composite hydrogel composed of GO and oligo(poly(ethylene glycol) fumarate) (OPF) exhibits electrical conductivity. The conductive network formed by GO in the OPF hydrogel improves the microenvironment of the infarct area. HE and immunofluorescence staining showed that GO was in close contact with the heart tissue in and around the infarct area, and that GO interacted with cardiomyocytes. Compared with OPF alone, OPF/GO enhanced Ca2+ signal transduction in myocardial cells in the infarcted area 4 weeks after myocardial infarction. In addition, OPF/GO injection into the infarct area enhances the generation of cytoskeletal structures that provide mechanical support and electrical connections between healthy myocardium and cardiomyocytes in the scar.[202] Therefore, GO-containing hydrogels have promising prospects for applications in cardiac tissue engineering Figures 37 and 38.

rGO. By incorporating conductive amine-rGO nanosheets into the structure of a hydrogel, and by varying the concentration of amine-rGO, the hydrogel can maintain a suitable cardiac scaffold conductivity range (10^{-6}–10^{-2} S/m), which is sufficient to induce spontaneous beating of cardiomyocytes.[203] The addition of collagen-coated rGO to the alginate hydrogel increased the conductivity of the alginate, and the lowest impedance modulus and highest specific capacitance were obtained. This greatly facilitates their

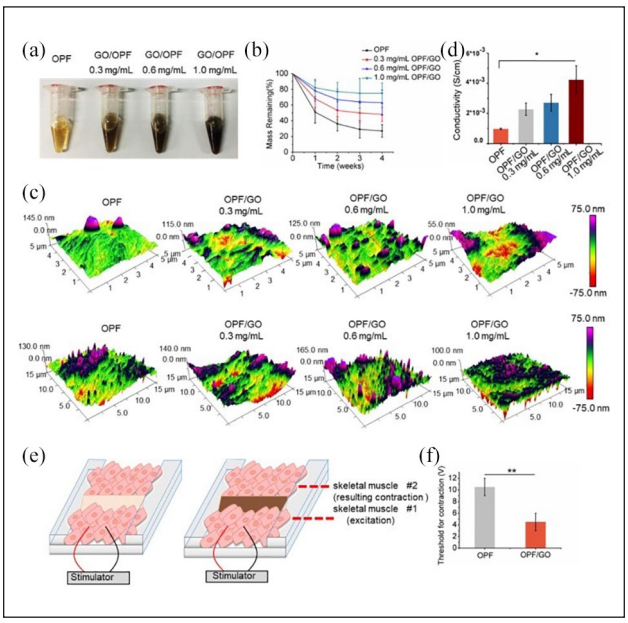

Figure 37. Synthesis and characterization of OPF/GO conductive hydrogel. (a) Photographs of OPF and OPF/GO hydrogels with various concentrations. (b) Degradation behavior of OPF and OPF/GO hydrogels ($n = 3$/group). (c) Spatial topography of OPF and OPF/GO hydrogels measured by AFM. (d) Conductivity of OPF and OPF/GO with various concentrations ($n = 3$/group). (e) A schematic illustration of the ex vivo setup used for measuring excitation threshold of muscle tissue. One muscle was electrically stimulated while the beating or contraction of the other muscle was monitored. (f) Excitation threshold of muscle tissue connected by pure OPF and OPF/GO hybrid gels, demonstrating that OPF/GO hybrid gels gave rise to the lowest excitation threshold, which was due to the conductivity of the OPF/GO hybrid gels.[202]

application in cardiomyocyte regeneration.[204] An ideal scaffold material should have characteristics similar to those of the ECM of natural myocardial tissue. The addition of rGO to a GelMA composite hydrogel significantly improved the conductivity and mechanical properties of the material. Compared with the GelMA hydrogel sheets, the rGO/GelMA hydrogel had more organized cardiomyocytes, enhanced cell-cell coupling, and exhibited stronger contractility and faster spontaneous beat rates. Further studies revealed that the GelMA/rGO hydrogel promoted the growth and proliferation of umbilical cord mesenchymal stem cells UCMSCs, improved the myocardial differentiation ability of UCMSCs, and upregulated the expression of cTnI and Cx43. An in-depth study showed that, compared with the PBS group, the GelMA/rGO/UCMSC hydrogel significantly improved the ejection fraction, significantly reduced myocardial infarct size and myocardial fibrosis, increased the ventricular ejection fraction, and increased the expression levels of cTnI and Cx43, and decreased caspase-3 expression in rats with myocardial infarction[205,206] Figures 39 and 40. The

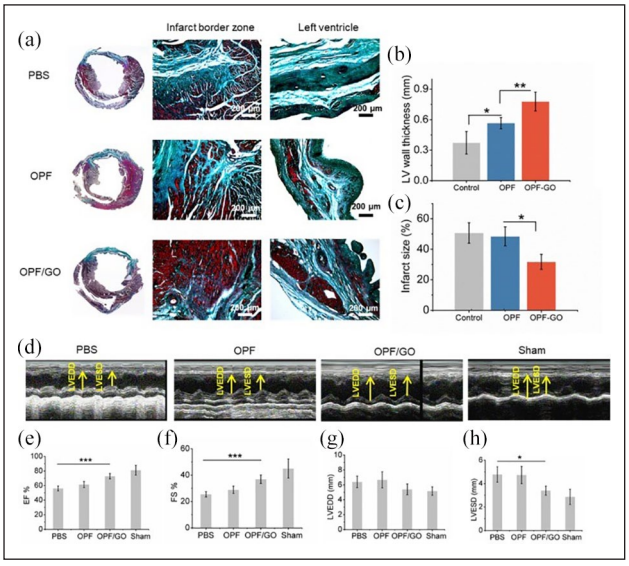

Figure 38. Masson's trichrome staining and echocardiographic measurements represent the effects of OPF/GO hydrogel on the morphology and myocardial functional recovery of infarcted hearts. (a) Masson trichrome staining of PBS-, OPF- or OPF/GO-injected heart 4 weeks post injection. Four weeks after injection, hearts were excised and left ventricle wall thickness (b) and infarct size (c) were measured. (d) Systolic ventricular function was improved after OPF/GO hydrogel injection into the border zone. Echocardiography (ECHO) was performed at 4 weeks post injection. Quantification of the parameters reflecting blood pumping function, including ejection fraction (EF) (e) and fractional shortening (FS) (f) 6 weeks after MI. Quantification of the parameters reflecting ventricular filling function, including left ventricular end-diastolic dimension (LVEDD) (g) and left ventricular end-systolic dimension (LVESD) (h).[202]

diagnosis and treatment of acute myocardial infarction is a very difficult problem in the clinic. The development of therapeutic drugs and treatment technologies in the cardiovascular field is still a daunting challenge. In this study, given the good conductivity of rGO, rGO was incorporated into GelMA to improve the mechanical and electrical properties of the hydrogel. The myocardial cell network on the rGO-GelMA hydrogel was more evenly distributed. The evenly distributed cell network had evenly distributed cell-cell connections between adjacent myocardial cells, providing a suitable environment for the propagation of action potentials, thereby achieving the synchronous beating of myocardial cells on the entire cell membrane. In addition, the conductive rGO network in the GelMA hydrogel may provide an additional pathway for the flow of direct current, thereby reducing the impedance of charge redistribution and action potential propagation. In recent years, conductive hydrogels have shown ideal therapeutic effects in the reconstruction of cardiac function after myocardial infarction. However, under the complex microenvironment of the heart and the limited regenerative capacity of myocardial cells, how to optimize the preparation of hydrogel patches with good biocompatibility, conductivity and stable mechanical properties is still the main challenge we face. The research on hydrogels for cardiac repair is still in its infancy. The future material direction should be able to better promote membrane potential polarization and be closer to the electrophysiological and mechanical properties of myocardial tissue. At the same time, more in-depth research is needed to gain a more detailed understanding of the specific molecular mechanisms that control the cardiomyocyte growth pathway. The future requires the joint efforts of academic laboratories, the biotechnology and pharmaceutical industries, and government agencies to help solve the difficult problems in this field and ultimately contribute to drug discovery and the development of new treatment strategies.

Similarly, a composite hydrogel of dopamine-rGO (PDA-rGO) and GelMA was conductive and mechanical, and cardiomyocytes cultured on the composite hydrogel were more cytocompatible than those cultured on GelMA alone. Higher cell survival rates, significant upregulation of cardiac-related proteins, and faster maturation were observed. In addition, compared to the pure GelMA, the composite hydrogel improved the orientation of sarcomeres and increased the expression of CX43, which promoted the propagation of pacing signals between cells. This conductive hydrogel exhibits synergistic effects when combined with electrical stimulation to construct more functionally mature cardiac muscle layers.[24] The study found that cardiomyocytes cultured with dECM-rGO continuously generated a strong contraction force, and the conduction velocity was significantly greater than that of the corresponding dECM hydrogel, which was close to the average conduction velocity of an isolated human left ventricular myocardium. The transmission of electrical signals between cardiomyocytes is closely related to the formation of gap junction protein 43(CX43), and the gene encoding this protein is highly expressed in dECM-rGO tissues. Meanwhile, the dECM-rGO hydrogel exhibited shear-thinning behavior, making it suitable for 3D bioprinting. In conclusion, rGO hydrogels can provide an ideal scaffold for cardiac tissue engineering applications and have great potential in cardiac therapy.[207]

GQDs. Composite hydrogels made of GQDs exhibit electrical conductivity and have good micro- and macro-permeability for natural biomolecules and nutrients, which provides an ideal microenvironment for cell colonization and vascularization during heart repair. A hydrogel combined with hBMSCs improved angiogenesis in the myocardial tissue. It reduced myocardial cell necrosis in the area of acute myocardial infarction, had significant cardiac regenerative activity, and improved the vascular density and ejection fraction at the site of myocardial infarction. These results provide a new approach for the treatment of

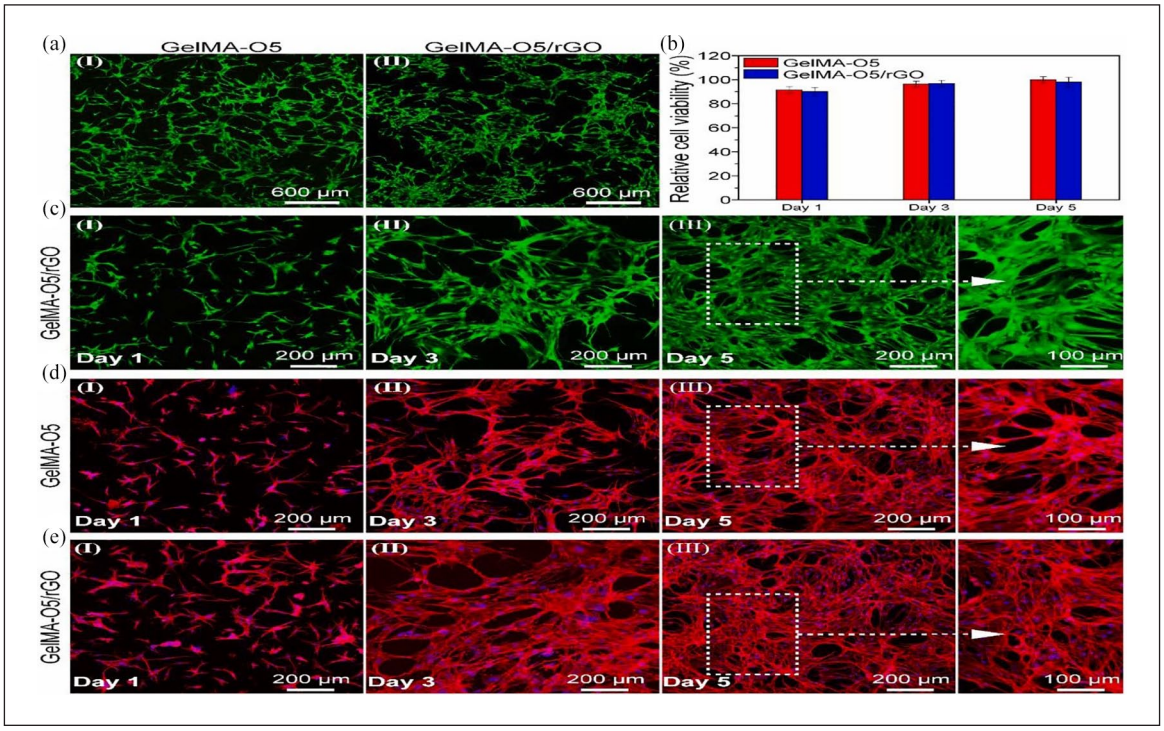

Figure 39. (a) Live/dead staining images of UCMSCs cultured on GelMA-O5 (I) and GelMA-O5/rGO (II) hydrogels at day 3 (The green fluorescence represents living cells and the red fluorescence means dead cells). (b) Cell viability of UCMSCs cultured on hydrogels versus different culture times by CCK-8 assay. (c) Live/dead staining images of UCMSCs cultured on GelMA-O5/rGO hydrogels at day 1, day 3 and day 5. (d) Cell morphology of Umbilical cord mesenchymal stem cells (UCMSCs) in GelMA-O5 hydrogel. (e) Cell morphology of Umbilical cord mesenchymal stem cells (UCMSCs) in on GelMA-O5/rGO hydrogel.[206]

cardiac remodeling after acute myocardial infarction[208] Figure 41. The specific mechanism may be after acute myocardial infarction, mitochondrial ROS production damages myocardial cells and the area of infarction increases excessively. ROS accelerates ventricular hypertrophy and heart failure by inducing the production of matrix metalloproteinases (MMPs) and destroying the hemostatic effect of Ca^{2+}. On the one hand, GQDs can regulate the production of ROS. GQDs reduce cardiac oxidative stress by increasing the GSH/GSSG ratio, promote the recovery of myocardial cells and angiogenesis in the damaged area, and reduce the area of infarction.[209] On the other hand, the antioxidant activity of GQDs is due to the interaction between reactive oxygen free radicals and the electrons in their conjugated ring structure, which reduces the expression of proinflammatory factors by removing ROS. And GQDs have the characteristics of high conductivity due to the presence of π-π bonds. Therefore, GQDs can be used as electrochemical biosensors to improve the electrical conduction of the heart to alleviate cardiac electrocardiographic dysfunction.[210]

In summary, hydrogel, as a three-dimensional scaffold material, can be used to deliver cells to damaged myocardial tissue and promote heart regeneration. Graphene-based hydrogel is close to the extracellular matrix, and its application potential in cardiac tissue engineering includes: 1. It has excellent mechanical properties and excellent electrical conductivity. 2. It has good flexibility and can adapt to the flexibility required by heart tissue. 3. It has good biocompatibility and can significantly support cell proliferation and adhesion. The conductive microenvironment of the infarcted myocardium can be reconstructed and neovascularization improved.[211] Research shows that graphene hydrogel can not only be used to repair damaged myocardium but can also be used for artificial heart valves. Functionalized GO nanocomposites can be used to manufacture artificial heart valves, which have excellent mechanical and blood compatibility. and anti-calcification properties.[212] At present, there are relatively few graphene hydrogel materials used for heart repair. This may be due to the continuous beating of the heart itself, which requires high adhesion, tensile resistance and wear resistance of the material. At the same time, the cardiomyocytes themselves It is difficult to regenerate, which makes material development difficult. The electrical conductivity and mechanical properties of graphene itself are an excellent heart tissue engineering repair material. Heart repair materials of the future should be developed with a focus on both the material properties and the heart's physiological characteristics. We believe that graphene-based hydrogels have significant potential in the field of cardiac repair.

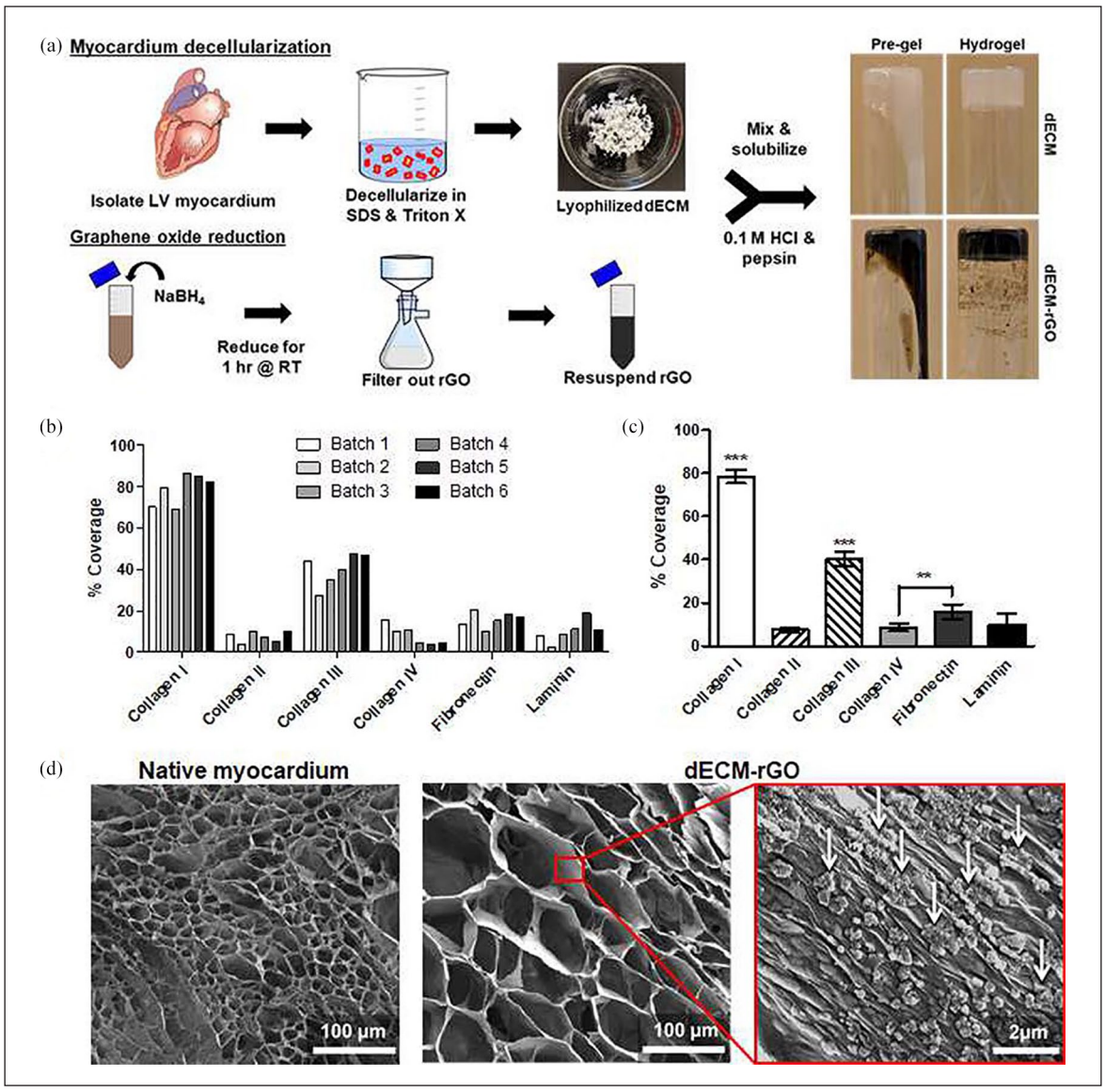

Figure 40. Materials synthesis and structural-biochemical characterization. (a) Composite hydrogels are synthesized using a parallel process. dECM (top) is produced by first isolating and mincing left ventricular myocardium from freshly-harvested porcine hearts. Minced tissue is decellularized using a combination of detergents before being lyophilized. rGO (bottom) is produced by reducing GO with NaBH4 for 1 h before filtration and resuspension in dH2O. The two components are combined with HCl and pepsin to form a pre-gel solution that can then be formed into hydrogels by incubation at 37°C. (b) LC/MS analysis of dECM indicates that while some batch-to-batch variation occurs, (c) overall protein composition is relatively well maintained across produced batches. $^{**}p < 0.01$, $^{***}p < 0.001$ (One way ANOVA with a Tukey's post-hoc test, $n = 6$). (d) SEM imaging of dECM-rGO hydrogels reveals a porous structure similar to that of decellularized myocardium. Deposition of rGO flakes (white arrows) on the pore walls can be observed.[207]

Conclusions and prospect

Graphene and its derivatives have good electrical conductivity, porosity, photothermal effect, pH stability, structural stability and biocompatibility, and have attracted extensive attention from researchers. Hydrogels have been widely studied and applied in the biomedical field due to their adjustable physical and chemical properties and high biocompatibility. At present, the application of hydrogels is mainly concentrated in the fields of wound repair, eye diseases, drug release, etc. In recent years, graphene-based hydrogels have shown many excellent properties such as high surface area, porosity, surface functionalization and adjustable pore size distribution, high electrical conductivity, photothermal conversion efficiency and good toughness, mechanical strength and stiffness, making them very attractive in tissue engineering applications. At present, graphene hydrogels show great potential in various biomedical

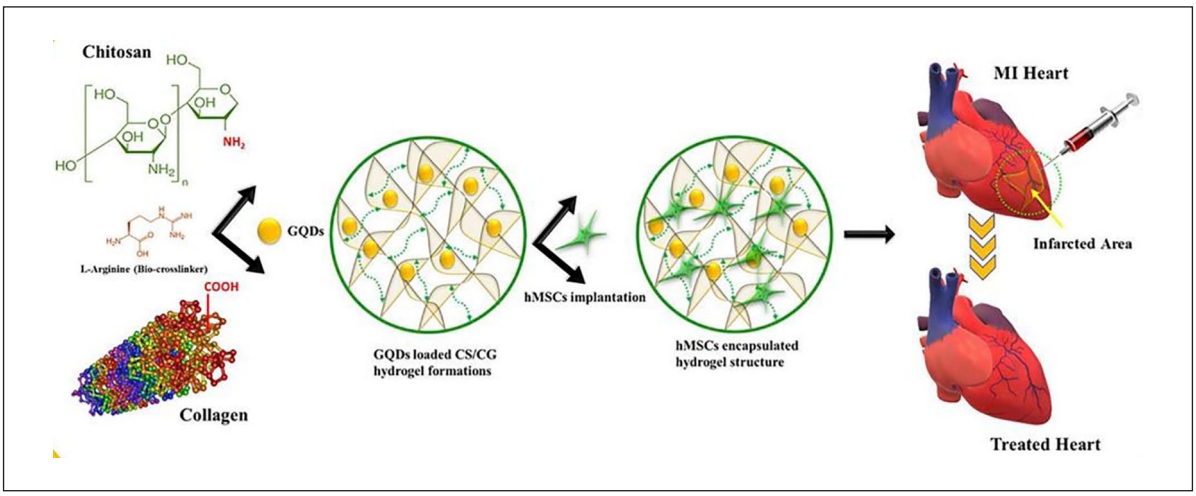

Figure 41. Schematic representations of the hydrogel GCC hydrogel formation and the demonstration of the scope of the work.[208]

and pharmaceutical applications, such as drug release, anticancer treatment, wound healing and bone regeneration.[213] At the same time, graphene and its derivative hydrogels have been widely studied in 3D printing technology because they meet the basic requirements of bioinks such as shear thinning properties, viscoelastic behavior, sol-gel transformation, and cell compatibility. This article reviews the latest research progress of graphene and its derivatives and different hydrogel composites in medical applications.

Consistent with many research conclusions, the combination of hydrogel and graphene is a green, sustainable, and more efficient composite material with better physical and chemical properties and biological activity. The incorporation of hydrogel into graphene can minimize the potential cytotoxicity of graphene, while graphene and its derivatives can more effectively promote cell proliferation, differentiation and migration by providing cell binding sites, further improving the biocompatibility of hydrogels, and the two can play a synergistic enhancement effect. Unfortunately, however, there have been no clinical trials on the application of graphene-based hydrogel products so far, so there is still a long way to go to achieve the transformation from laboratory to clinic. Although graphene-based hydrogels have shown good application prospects in the biomedical field, the clinical application of graphene-based hydrogels needs to overcome some challenges, such as potential side effects such as inflammation, swelling, pain, etc, biological toxicity in vivo, thermal damage to normal tissues, and insufficient therapeutic effects. However, its behavior in the body and its interaction mechanism with various biomolecules need to be further studied, and most of the research on graphene-based hydrogels is still in the experimental stage. The long-term potential toxicity of graphene-based hydrogels is still unclear, which requires us to increase our research efforts.

In summary, how to develop safe, reliable, efficient, and low-toxic graphene-based hydrogels and transform them into clinical use requires the advancement of modern biological technology and the collaboration of multiple disciplines. As research continues to deepen, we expect that graphene-based hydrogels can become a good treatment method to relieve patients pain and bring good news.

Acknowledgements

Feifei Ni and Yangyang Chen contributed equally to this work.

Abbreviations

2D: Two-dimensional, 3D: Three-dimensional, GQDs: Graphene quantum dots, CS: chitosan, CAD: computer-aided design, rGO: reduced graphene oxide, Alg: alginate, HOS: human osteosarcoma, GH: gelatin, ECM: extracellular matrix, NIPAM: N-isopropyl acrylamide, PEG: polyethylene glycol, TMSCs: Tonsil-Derived Mesenchymal Stem Cells, PAAm: polyacrylamide, m-rGO: modified reduced graphene oxide, GF: graphene foam, hMSCs: human bone marrow mesenchymal stem cells (hMSCs), GelMA: Gelatin methacryloyl alcohol, GHPA: Phenol-rich gelatin, SISMA: small intestinal submucosa, SGOB: silk graphene oxide bioink, SB: silk fibroin, ChiMA: methacrylate chitosan, NSCs: neural stem cell, CNCs: cellulose nanocrystals, PNIPAAm: isopropylacrylamide, SerMA: sericin methacryloyl, CMC: carboxymethyl chitosan, PEGDA: polyethylene glycol diacrylate, HAP: hydroxyapatite, GelMA/PEGDA: gelatin polyethylene glycol diacrylic acid, GM: Gelatin methacrylate, Ac-CD: acryloyl β-cyclodextrin, β-CD:β-cyclodextrin, SGH: self-supporting graphene hydrogel, hADSCs: human adipose-derived stem cells, PDLLA: poly-D, l-lactic acid/polyethylene glycol, PSBMA: poly-sulfobetaine methacrylate, IVD: Intervertebral disc, NP: nucleus pulposus, PVA: polyvinyl alcohol, GEH: graphene elastic hydrogel, PAM: polyacrylamide, CFGO: Acetylcholine-functionalized GO,CS/OHEC: Chitosan oxidized hydroxyethyl cellulose, NGCs: Nerve-guided conduits,

BDNF: brain-derived neurotrophic factor, GR-SA: graphene and sodium alginate, BNC: bacterial nanocellulose, P(AA): poly(acrylicacid), BPEI: branched-chain-polyethylenimine, DEX: dextran, CGCD: chitosan oligosaccharide-modified GO (CG), calcium alginate foam gel dressing (CD),CEO: chick embryo angiogenesis, CF: ciprofloxacin, TA: Tannic acid, KA: Keratin, DOX: doxorubicin, MPDA: mesoporous polydopamine, CNF: cellulose nanofibril, PS: Polystyrene, PCHs: photonic crystal hydrogels, PNIPAm: poly(N-isopropylacrylamide), CUR: curcumin, XG: xanthan gum, DCFP: diclofenac potassium, MTX: methotrexate, PDANPs: polydopamine nanoparticles, G-DAT: Graphene-diaminotriazine, Dex/PNIPAM: dextran/polyisopropyl acrylamide, O-HACC: O-chitosan quaternary ammonium salt, NaDC: sodium deoxycholate, DA: dopamine, BuMA: butyl methacrylate, PEGMEMA: polyethylene glycol methyl methacrylate, NaCMC: sodium carboxymethyl cellulose, LNP: lignan nanoparticles, OPF: oligo(poly(ethylene glycol) fumarate), UCMSC: umbilical cord mesenchymal stem cells

Authors' contributions

The manuscript was mainly designed by H Wang and ZW Shao. FF Ni and YY Chen wrote the manuscript. F Gao revised the content of the manuscript. Z Wang, X Zhang contributed to the collection of data and composition of the review. All authors read and approved the final manuscript.

Availability of data and materials

Not applicable.

Declaration of conflicting interests

The author(s) declared no potential conflicts of interest with respect to the research, authorship, and/or publication of this article.

Funding

The author(s) disclosed receipt of the following financial support for the research, authorship, and/or publication of this article: This work was supported by the National Natural Science Foundation of China (81672166).

Ethics approval and consent to participate

Not applicable.

Consent for publication

Not applicable.

ORCID iD

Hong Wang https://orcid.org/0009-0008-9983-3825

References

1. Baniasadi H, Abidnejad R, Fazeli M, et al. Innovations in hydrogel-based manufacturing: a comprehensive review of direct ink writing technique for biomedical applications. *Adv Colloid Interface Sci* 2024; 324: 103095.
2. Hao H, Wu S, Lin J, et al. Immunization against Zika by entrapping live virus in a subcutaneous self-adjuvanting hydrogel. *Nat Biomed Eng* 2023; 7(7): 928–942.
3. Peng Y, Liang S, Meng QF, et al. Engineered bio-based hydrogels for cancer immunotherapy. *Adv Mater* 2024; 36(21): e2313188.
4. Zhou W, Lei S, Liu M, et al. Injectable and photocurable CAR-T cell formulation enhances the anti-tumor activity to melanoma in mice. *Biomaterials* 2022; 291: 121872.
5. Smith TT, Moffett HF, Stephan SB, et al. Biopolymers code livering engineered T cells and STING agonists can eliminate heterogeneous tumors. *J Clin Investig* 2017; 127(6): 2176–2191.
6. Abolpour Moshizi S, Moradi H, Wu S, et al. Biomimetic ultraflexible piezoresistive flow sensor based on graphene nanosheets and PVA hydrogel. *Adv Mater Technol* 2022; 7(1): 2100783.
7. Lu Y, Yang G, Wang S, et al. Stretchable graphene–hydrogel interfaces for wearable and implantable bioelectronics. *Nat Electron* 2023; 7(1): 51–65.
8. Weng T, Zhang W, Xia Y, et al. 3D bioprinting for skin tissue engineering: current status and perspectives. *J Tissue Eng* 2021; 12: 20417314211028574.
9. Alonzo M, AnilKumar S, Roman B, et al. 3D bioprinting of cardiac tissue and cardiac stem cell therapy. *Transl Res* 2019; 211: 64–83.
10. Tavafoghi M, Darabi MA, Mahmoodi M, et al. Multimaterial bioprinting and combination of processing techniques towards the fabrication of biomimetic tissues and organs. *Biofabrication* 2021; 13(4): 042002.
11. Zhang Y, Wang B, Hu J, et al. 3D composite bioprinting for fabrication of artificial biological tissues. *Int J Bioprinting* 2021; 7(1): 299.
12. Dey M and Ozbolat IT. 3D bioprinting of cells, tissues and organs. *Sci Rep* 2020; 10(1): 14023.
13. Sekar MP, Budharaju H, Zennifer A, et al. Current standards and ethical landscape of engineered tissues-3D bioprinting perspective. *J Tissue Eng* 2021; 12: 20417314211027677.
14. Ghidini T. Regenerative medicine and 3D bioprinting for human space exploration and planet colonisation. *J Thorac Dis* 2018; 10(Suppl 20): S2363–S2375.
15. Panda S, Hajra S, Mistewicz K, et al. A focused review on three-dimensional bioprinting technology for artificial organ fabrication. *Biomater Sci* 2022; 10(18): 5054–5080.
16. Li S, Tian X, Fan J, et al. Chitosans for tissue repair and organ three-dimensional (3D) bioprinting. *Micromachines* 2019; 10(11): 765.
17. Song D, Xu Y, Liu S, et al. Progress of 3D bioprinting in organ manufacturing. *Polymers* 2021; 13(18): 3178.
18. Rastin H, Zhang B, Mazinani A, et al. 3D bioprinting of cell-laden electroconductive mxene nanocomposite bioinks. *Nanoscale* 2020; 12(30): 16069–16080.
19. Martin JH, Yahata BD, Hundley JM, et al. 3D printing of high-strength aluminium alloys. *Nature* 2017; 549(7672): 365–369.
20. Tuli NT, Khatun S and Rashid AB. Unlocking the future of precision manufacturing: a comprehensive exploration of 3D printing with fiber-reinforced composites in aerospace, automotive, medical, and consumer industries. *Heliyon* 2024; 10(5): e27328.
21. Grajek H, Jonik J, Witkiewicz Z, et al. Applications of graphene and its derivatives in chemical analysis. *Crit Rev Anal Chem* 2020; 50(5): 445–471.

22. Yang Y, Wei Y, Guo Z, et al. From materials to devices: graphene toward practical applications. *Small Methods* 2022; 6(10): e2200671.
23. Liu G, Yang Y, Liu Y, et al. Injectable and thermosensitive hydrogel with platelet-rich plasma for enhanced biotherapy of skin wound healing. *Adv Healthc Mater* 2024; 13(12): e2303930.
24. Li XP, Qu KY, Zhou B, et al. Electrical stimulation of neonatal rat cardiomyocytes using conductive polydopamine-reduced graphene oxide-hybrid hydrogels for constructing cardiac microtissues. *Colloids Surf B Biointerfaces* 2021; 205: 111844.
25. Park J, Jeon N, Lee S, et al. Conductive hydrogel constructs with three-dimensionally connected graphene networks for biomedical applications. *Chem Eng J* 2022; 446: 137344.
26. Wang Z, Li S, Wu Z, et al. Pulsed electromagnetic field-assisted reduced graphene oxide composite 3D printed nerve scaffold promotes sciatic nerve regeneration in rats. *Biofabrication* 2024; 16(3): 035013.
27. Lee S, Lee J and Jeon S. Aggregation-induced emission of matrix-free graphene quantum dots via selective edge functionalization of rotor molecules. *Sci Adv* 2023; 9(7): eade2585.
28. Zmejkoski DZ, Marković ZM, Mitić DD, et al. Antibacterial composite hydrogels of graphene quantum dots and bacterial cellulose accelerate wound healing. *J Biomed Mater Res B Appl Biomater* 2022; 110(8): 1796–1805.
29. Patil R, Bahadur P and Tiwari S. Dispersed graphene materials of biomedical interest and their toxicological consequences. *Adv Colloid Interface Sci* 2020; 275: 102051.
30. Zhao H, Ding R, Zhao X, et al. Graphene-based nanomaterials for drug and/or gene delivery, bioimaging, and tissue engineering. *Drug Discov Today* 2017; 22(9): 1302–1317.
31. Chen Z, Meng C, Wang X, et al. Ultrasensitive DNA origami plasmon sensor for accurate detection in circulating tumor DNAs. *Laser Photonics Rev* 2024; 2400035: 1–12.
32. Zheng F, Chen Z, Li J, et al. A highly sensitive CRISPR-empowered surface plasmon resonance sensor for diagnosis of inherited diseases with femtomolar-level real-time quantification. *Adv Sci* 2022; 9(14): e2105231.
33. Chen Z, Li J, Li T, et al. A CRISPR/Cas12a-empowered surface plasmon resonance platform for rapid and specific diagnosis of the omicron variant of SARS-CoV-2. *Natl Sci Rev* 2022; 9(8): nwac104.
34. Chen Z, Wu C, Yuan Y, et al. CRISPR-Cas13a-powered electrochemical biosensor for the detection of the L452R mutation in clinical samples of SARS-CoV-2 variants. *Nanobiotechnol* 2023; 21(1): 141.
35. Srimaneepong V, Skallevold HE, Khurshid Z, et al. Graphene for antimicrobial and coating application. *Int J Mol Sci* 2022; 23(1): 499.
36. Ławkowska K, Pokrywczyńska M, Koper K, et al. Application of graphene in tissue engineering of the nervous system. *Int J Mol Sci* 2021; 23(1): 33.
37. Lu R, Zhang W, He Y, et al. Ferric ion crosslinking-based 3D printing of a graphene oxide hydrogel and its evaluation as a bio-scaffold in tissue engineering. *Biotechnol Bioeng* 2021; 118(2): 1006–1012.
38. Xavier Mendes A, Moraes Silva S, O'Connell CD, et al. Enhanced electroactivity, mechanical properties, and printability through the addition of graphene oxide to photo-cross-linkable gelatin methacryloyl hydrogel. *ACS Biomater Sci Eng* 2021; 7(6): 2279–2295.
39. Jiang Y, Zhou D and Yang B. 3D bioprinted GelMA/GO composite induces osteoblastic differentiation. *J Biomater Appl* 2022; 37(3): 527–537.
40. Kang MS, Kang JI, Le Thi P, et al. Three-dimensional printable gelatin hydrogels incorporating graphene oxide to enable spontaneous myogenic differentiation. *ACS Macro Lett* 2021; 10(4): 426–432.
41. Rueda-Gensini L, Serna JA, Cifuentes J, et al. Graphene oxide-embedded extracellular matrix-derived hydrogel as a multiresponsive platform for 3D bioprinting applications. *Int J Bioprinting* 2021; 7(3): 353.
42. Olate-Moya F, Arens L, Wilhelm M, et al. Chondroinductive alginate-based hydrogels having graphene oxide for 3D printed scaffold fabrication. *ACS Appl Mater Interfaces* 2020; 12(4): 4343–4357.
43. Cheng Z, Landish B, Chi Z, et al. 3D printing hydrogel with graphene oxide is functional in cartilage protection by influencing the signal pathway of Rank/Rankl/OPG. *Mater Sci Eng C Mater Biol Appl* 2018; 82: 244–252.
44. Zhang J, Eyisoylu H, Qin XH, et al. 3D bioprinting of graphene oxide-incorporated cell-laden bone mimicking scaffolds for promoting scaffold fidelity, osteogenic differentiation and mineralization. *Acta Biomater* 2021; 121: 637–652.
45. Zorba Yildiz AP, Darici H, Yavuz B, et al. Preparation and characterization of graphene-based 3D biohybrid hydrogel bioink for peripheral neuroengineering. *J Vis Exp* 2022; 183: e63622.
46. Marapureddy SG, Hivare P, Sharma A, et al. Rheology and direct write printing of chitosan - graphene oxide nanocomposite hydrogels for differentiation of neuroblastoma cells. *Carbohydr Polym* 2021; 269: 118254.
47. Choe G, Oh S, Seok JM, et al. Graphene oxide/alginate composites as novel bioinks for three-dimensional mesenchymal stem cell printing and bone regeneration applications. *Nanoscale* 2019; 11(48): 23275–23285.
48. Li J, Liu X, Crook JM, et al. Development of 3D printable graphene oxide based bio-ink for cell support and tissue engineering. *Front Bioeng Biotechnol* 2022; 10: 994776.
49. Ding X, Yu Y, Shang L, et al. Histidine-triggered GO hybrid hydrogels for microfluidic 3D printing. *ACS Nano* 2022; 16(11): 19533–19542.
50. Ajiteru O, Sultan MT, Lee YJ, et al. A 3D printable electroconductive biocomposite bioink based on silk fibroin-conjugated graphene oxide. *Nano Lett* 2020; 20(9): 6873–6883.
51. Zhu W, Harris BT and Zhang LG. Gelatin methacrylamide hydrogel with graphene nanoplatelets for neural cell-laden 3D bioprinting. In: *2016 38th Annual international conference of the IEEE engineering in medicine and biology society*, 2016, pp. 4185–4188.
52. Sayyar S, Gambhir S, Chung J, et al. 3D printable conducting hydrogels containing chemically converted graphene. *Nanoscale* 2017; 9(5): 2038–2050.
53. Huang Ct Kumar Shrestha L, Ariga K, et al. A graphene-polyurethane composite hydrogel as a potential bioink for 3D bioprinting and differentiation of neural stem cells. *J Mater Chem B* 2017; 5(44): 8854–8864.

54. Khabibullin A, Alizadehgiashi M, Khuu N, et al. Injectable shear-thinning fluorescent hydrogel formed by cellulose nanocrystals and graphene quantum dots. *Langmuir* 2017; 33(43): 12344–12350.
55. Patel M, Moon HJ, Ko DY, et al. Composite system of graphene oxide and polypeptide thermogel as an injectable 3D scaffold for adipogenic differentiation of tonsil-derived mesenchymal stem cells. *ACS Appl Mater Interfaces* 2016; 8(8): 5160–5169.
56. Lee WC, Lim CH, Shi H, et al. Origin of enhanced stem cell growth and differentiation on graphene and graphene oxide. *ACS Nano* 2011; 5(9): 7334–7341.
57. Marrella A, Giannoni P, Pulsoni I, et al. Topographical features of graphene-oxide-functionalized substrates modulate cancer and healthy cell adhesion based on the cell tissue of origin. *ACS Appl Mater Interfaces* 2018; 10(49): 41978–41985.
58. Ryu SB, Park KM and Park KD. In situ graphene oxide-gelatin hydrogels with enhanced mechanical property for tissue adhesive and regeneration. *Biochem Biophys Res Commun* 2022; 592: 24–30.
59. Shao C, Liu Y, Chi J, et al. Responsive inverse opal scaffolds with biomimetic enrichment capability for cell culture. *Research* 2019; 2019: 9783793.
60. Zhang L, Li X, Shi C, et al. Biocompatibility and angiogenic effect of chitosan/graphene oxide hydrogel scaffolds on EPCs. *Stem Cells Int* 2021; 2021: 1–17.
61. Zhang Y, Liu X, Michelson K, et al. Graphene oxide-based biocompatible 3D mesh with a tunable porosity and tensility for cell culture. *ACS Biomater Sci Eng* 2018; 4(5): 1505–1517.
62. Mokhtari H, Kharaziha M, Karimzadeh F, et al. An injectable mechanically robust hydrogel of Kappa-carrageenan-dopamine functionalized graphene oxide for promoting cell growth. *Carbohydr Polym* 2019; 214: 234–249.
63. Narayanan KB, Choi SM and Han SS. Biofabrication of Lysinibacillus sphaericus-reduced graphene oxide in three-dimensional polyacrylamide/carbon nanocomposite hydrogels for skin tissue engineering. *Colloids Surf B Biointerfaces* 2019; 181: 539–548.
64. Wang Y, Xiao Y, Gao G, et al. Conductive graphene oxide hydrogels reduced and bridged by l-cysteine to support cell adhesion and growth. *J Mater Chem B* 2017; 5(3): 511–516.
65. Santhosh M, Choi J-H and Choi J-W. Magnetic-assisted cell alignment within a magnetic nanoparticle-decorated reduced graphene oxide/collagen 3D nanocomposite hydrogel. *Nanomater* 2019; 9(9): 1293.
66. Kim S, Choi C and Cha C. Mechanotopography-driven design of dispersible nanofiber-laden hydrogel as a 3D cell culture platform for investigating tissue fibrosis. *Adv Healthc Mater* 2021; 10(21): e2101109.
67. Feng L, Hao Y, Zhu M, et al. Incorporation of laminarin-based hydrogel with graphene foam to enhance the toughness of scaffold and regulate the stem cell behavior. *ACS Biomater Sci Eng* 2019; 5(10): 5295–5304.
68. Hu X-B, Qin Y, Fan WT, et al. A three-dimensional electrochemical biosensor integrated with hydrogel enables real-time monitoring of cells under their in vivo-like microenvironment. *Anal Chem* 2021; 93(22): 7917–7924.
69. Saravanan S, Vimalraj S and Anuradha D. Chitosan based thermoresponsive hydrogel containing graphene oxide for bone tissue repair. *Biomed Pharmacother* 2018; 107: 908–917.
70. Pathmanapan S, Periyathambi P and Anandasadagopan SK. Fibrin hydrogel incorporated with graphene oxide functionalized nanocomposite scaffolds for bone repair - in vitro and in vivo study. *Nanomed* 2020; 29: 29.
71. Céspedes-Valenzuela DN, Sánchez-Rentería S, Cifuentes J, et al. Preparation and characterization of an injectable and photo-responsive chitosan methacrylate/graphene oxide hydrogel: potential applications in bone tissue adhesion and repair. *Polymers* 2021; 14(1): 126.
72. Qi C, Deng Y, Xu L, et al. A sericin/graphene oxide composite scaffold as a biomimetic extracellular matrix for structural and functional repair of calvarial bone. *Theranostics* 2020; 10(2): 741–756.
73. Khorshidi S and Karkhaneh A. Hydrogel/fiber conductive scaffold for bone tissue engineering. *J Biomed Mater Res A* 2018; 106(3): 718–724.
74. Liu S, Mou S, Zhou C, et al. Off-the-shelf biomimetic graphene oxide–collagen hybrid scaffolds wrapped with osteoinductive extracellular matrix for the repair of cranial defects in rats. *ACS Appl Mater Interfaces* 2018; 10(49): 42948–42958.
75. Zou M, Sun J and Xiang Z. Induction of M2-Type macrophage differentiation for bone defect repair via an interpenetration network hydrogel with a GO-based controlled release system. *Adv Healthc Mater* 2021; 10(6): e2001502.
76. Kolanthai E, Sindu PA, Khajuria DK, et al. Graphene oxide—a tool for the preparation of chemically crosslinking free alginate–chitosan–collagen scaffolds for bone tissue engineering. *ACS Appl Mater Interfaces* 2018; 10(15): 12441–12452.
77. Wang B, Yuan S, Xin W, et al. Synergic adhesive chemistry-based fabrication of BMP-2 immobilized silk fibroin hydrogel functionalized with hybrid nanomaterial to augment osteogenic differentiation of rBMSCs for bone defect repair. *Int J Biol Macromol* 2021; 192: 407–416.
78. Zhou C, Luo C, Liu S, et al. Pearl-inspired graphene oxide-collagen microgel with multi-layer mineralization through microarray chips for bone defect repair. *Mater Today Bio* 2022; 15: 100307.
79. Jiao D, Zheng A, Liu Y, et al. Bidirectional differentiation of BMSCs induced by a biomimetic procallus based on a gelatin-reduced graphene oxide reinforced hydrogel for rapid bone regeneration. *Bioact Mater* 2021; 6(7): 2011–2028.
80. Dong W, Ma W, Zhao S, et al. Multifunctional 3D sponge-like macroporous cryogel-modified long carbon fiber reinforced polyetheretherketone implants with enhanced vascularization and osseointegration. *J Mater Chem B* 2022; 10(28): 5473–5486.
81. Xie X, Hu K, Fang D, et al. Graphene and hydroxyapatite self-assemble into homogeneous, free standing nanocomposite hydrogels for bone tissue engineering. *Nanoscale* 2015; 7(17): 7992–8002.
82. Zhao C, Zeng Z, Qazvini NT, et al. Thermoresponsive citrate-based graphene oxide scaffold enhances bone regeneration from BMP9-stimulated adipose-derived mes-

enchymal stem cells. *ACS Biomater Sci Eng* 2018; 4(8): 2943–2955.
83. Pazarçeviren AE, Evis Z, Keskin D, et al. Resorbable PCEC/gelatin-bismuth doped bioglass-graphene oxide bilayer membranes for guided bone regeneration. *Biomed Mater* 2019; 14(3): 035018.
84. Kosowska K, Domalik-Pyzik P, Krok-Borkowicz M, et al. Synthesis and characterization of chitosan/reduced graphene oxide hybrid composites. *Materials* 2019; 12(13): 2077.
85. Chopra V, Thomas J, Sharma A, et al. A bioinspired, ice-templated multifunctional 3D cryogel composite crosslinked through in situ reduction of GO displayed improved mechanical, osteogenic and antimicrobial properties. *Mater Sci Eng C Mater Biol Appl* 2021; 119: 111584.
86. Qin H, Ji Y, Li G, et al. MicroRNA-29b/graphene oxide-polyethyleneglycol-polyethylenimine complex incorporated within chitosan hydrogel promotes osteogenesis. *Front Chem* 2022; 10: 958561.
87. Li Y, He J, Zhou J, et al. A conductive photothermal nonswelling nanocomposite hydrogel patch accelerating bone defect repair. *Biomater Sci* 2022; 10(5): 1326–1341.
88. Li D, Nie W, Chen L, et al. Self-assembled hydroxyapatite-graphene scaffold for photothermal cancer therapy and bone regeneration. *J Biomed Nanotechnol* 2018; 14(12): 2003–2017.
89. Lu J, Cheng C, He YS, et al. Multilayered graphene hydrogel membranes for guided bone regeneration. *Adv Mater* 2016; 28(21): 4025–4031.
90. Lyu CQ, Lu JY, Cao CH, et al. Induction of osteogenic differentiation of human adipose-derived stem cells by a novel self-supporting graphene hydrogel film and the possible underlying mechanism. *ACS Appl Mater Interfaces* 2015; 7(36): 20245–20254.
91. Tang C, Holt BD, Wright ZM, et al. Injectable amine functionalized graphene and chondroitin sulfate hydrogel with potential for cartilage regeneration. *J Mater Chem B* 2019; 7(15): 2442–2453.
92. Shen H, Lin H, Sun Ax, et al. Chondroinductive factor-free chondrogenic differentiation of human mesenchymal stem cells in graphene oxide-incorporated hydrogels. *J Mater Chem B* 2018; 6(6): 908–917.
93. Trucco D, Vannozzi L, Teblum E, et al. Graphene oxide-doped gellan gum-PEGDA bilayered hydrogel mimicking the mechanical and lubrication properties of articular cartilage. *Adv Healthc Mater* 2021; 10(12): e2001434.
94. Satapathy MK, Manga YB, Ostrikov KK, et al. Microplasma cross-linked graphene oxide-gelatin hydrogel for cartilage reconstructive surgery. *ACS Appl Mater Interfaces* 2020; 12(1): 86–95.
95. Shen H, Lin H, Sun AX, et al. Acceleration of chondrogenic differentiation of human mesenchymal stem cells by sustained growth factor release in 3D graphene oxide incorporated hydrogels. *Acta Biomater* 2020; 105: 44–55.
96. Wang Z, Li J, Jiang L, et al. Zwitterionic hydrogel incorporated graphene oxide nanosheets with improved strength and Lubricity. *Langmuir* 2019; 35(35): 11452–11462.
97. Zhang Y, Zhang M, Jiang H, et al. Bio-inspired layered chitosan/graphene oxide nanocomposite hydrogels with high strength and pH-driven shape memory effect. *Carbohydr Polym* 2017; 177: 116–125.
98. Ligorio C, Zhou M, Wychowaniec JK, et al. Graphene oxide containing self-assembling peptide hybrid hydrogels as a potential 3D injectable cell delivery platform for intervertebral disc repair applications. *Acta Biomater* 2019; 92: 92–103.
99. Ligorio C, Vijayaraghavan A, Hoyland JA, et al. Acidic and basic self-assembling peptide and peptide-graphene oxide hydrogels: characterisation and effect on encapsulated nucleus pulposus cells. *Acta Biomater* 2022; 143: 145–158.
100. Ligorio C, O–Brien M, Hodson NW, et al. TGF-β3-loaded graphene oxide - self-assembling peptide hybrid hydrogels as functional 3D scaffolds for the regeneration of the nucleus pulposus. *Acta Biomater* 2021; 127: 116–130.
101. Samadi N, Sabzi M and Babaahmadi M. Self-healing and tough hydrogels with physically cross-linked triple networks based on Agar/PVA/Graphene. *Int J Biol Macromol* 2018; 107(Pt B): 2291–2297.
102. Lyu C, Cheng C, He Y, et al. Graphene hydrogel as a porous scaffold for cartilage regeneration. *ACS Appl Mater Interfaces* 2022; 14(49): 54431–54438.
103. Fu R, Liu C, Yan Y, et al. Bone defect reconstruction via endochondral ossification: a developmental engineering strategy. *J Tissue Eng* 2021; 12: 20417314211004211.
104. Zhang C, Yuan Tj, Tan Mh, et al. Smart graphene-based hydrogel promotes recruitment and neural-like differentiation of bone marrow derived mesenchymal stem cells in rat skin. *Biomater Sci* 2021; 9(6): 2146–2161.
105. Li G, Zhao Y, Zhang L, et al. Preparation of graphene oxide/polyacrylamide composite hydrogel and its effect on Schwann cells attachment and proliferation. *Colloids Surf B Biointerfaces* 2016; 143: 547–556.
106. Zhao Y, Wang Y, Niu C, et al. Construction of polyacrylamide/graphene oxide/gelatin/sodium alginate composite hydrogel with bioactivity for promoting Schwann cells growth. *J Biomed Mater Res A* 2018; 106(7): 1951–1964.
107. Pradhan K, Das G, Khan J, et al. Neuro-regenerative choline-functionalized injectable graphene oxide hydrogel repairs focal brain injury. *ACS Chem Neurosci* 2019; 10(3): 1535–1543.
108. Zhang X, Khan S, Wei R, et al. Application of nanomaterials in the treatment of intracerebral hemorrhage. *J Tissue Eng* 2023; 14: 20417314231157004.
109. Aghajanian S, Taghi Doulabi A, Akhbari M, et al. Facial nerve regeneration using silicone conduits filled with ammonia-functionalized graphene oxide and frankincense-embedded hydrogel. *Inflamm Regen* 2021; 41(1): 13.
110. Zhao Y, Liu J, Gao Y, et al. Conductive biocomposite hydrogels with multiple biophysical cues regulate Schwann cell behaviors. *J Mater Chem B* 2022; 10(10): 1582–1590.
111. Wychowaniec JK, Litowczenko J, Tadyszak K, et al. Unique cellular network formation guided by heterostructures based on reduced graphene oxide - Ti3C2Tx MXene hydrogels. *Acta Biomater* 2020; 115: 104–115.
112. Zheng F, Li R, He Q, et al. The electrostimulation and scar inhibition effect of chitosan/oxidized hydroxyethyl cellulose/reduced graphene oxide/asiaticoside liposome based

hydrogel on peripheral nerve regeneration in vitro. *Mater Sci Eng C Mater Biol Appl* 2020; 109: 110560.
113. Chen X, Ranjan VD, Liu S, et al. In situ formation of 3D conductive and cell-laden graphene hydrogel for electrically regulating cellular behavior. *Macromol Biosci* 2021; 21(4): e2000374.
114. Hu Y, Chen Z, Wang H, et al. Conductive nerve guidance conduits based on morpho butterfly wings for peripheral nerve repair. *ACS Nano* 2022; 16(2): 1868–1879.
115. Amagat J, Su Y, Svejsø FH, et al. Self-snapping hydrogel-based electroactive microchannels as nerve guidance conduits. *Mater Today Bio* 2022; 16: 100437.
116. Arnaldi P, Di Lisa D, Maddalena L, et al. A facile approach for the development of high mechanical strength 3D neuronal network scaffold based on chitosan and graphite nanoplatelets. *Carbohydr Polym* 2021; 271: 118420.
117. Martín C, Merino S, González-Domínguez JM, et al. Graphene improves the biocompatibility of polyacrylamide hydrogels: 3D polymeric scaffolds for neuronal growth. *Sci Rep* 2017; 7(1): 10942.
118. Palejwala AH, Fridley JS, Mata JA, et al. Biocompatibility of reduced graphene oxide nanoscaffolds following acute spinal cord injury in rats. *Surg Neurol Int* 2016; 7: 75.
119. Jin Y, Zhang W, Zhang Y, et al. Multifunctional biomimetic hydrogel based on graphene nanoparticles and sodium alginate for peripheral nerve injury therapy. *Biomater Adv* 2022; 135: 212727.
120. McNamara MC, Aykar SS, Alimoradi N, et al. Behavior of neural cells post manufacturing and after prolonged encapsulation within conductive graphene-laden alginate microfibers. *Adv Biol* 2021; 5(11): e2101026.
121. Xiong Z, Huang W, Liang Q, et al. Harnessing the 2D structure-enabled viscoelasticity of graphene-based hydrogel membranes for chronic neural interfacing. *Small Methods* 2022; 6(11): e2201202.
122. Homaeigohar S, Tsai TY, Young TH, et al. An electroactive alginate hydrogel nanocomposite reinforced by functionalized graphite nanofilaments for neural tissue engineering. *Carbohydr Polym* 2019; 224: 115112.
123. Cai Y, Huang Q, Wang P, et al. Conductive hydrogel conduits with growth factor gradients for peripheral nerve repair in diabetics with non-suture tape. *Adv Healthc Mater* 2022; 11(16): e2200755.
124. Huang Q, Cai Y, Zhang X, et al. Aligned graphene mesh-supported double network natural hydrogel conduit loaded with netrin-1 for peripheral nerve regeneration. *ACS Appl Mater Interfaces* 2021; 13(1): 112–122.
125. Agarwal G, Kumar N and Srivastava A. Highly elastic, electroconductive, immunomodulatory graphene crosslinked collagen cryogel for spinal cord regeneration. *Mater Sci Eng C Mater Biol Appl* 2021; 118: 111518.
126. Wang L, Song D, Zhang X, et al. Silk-graphene hybrid hydrogels with multiple cues to induce nerve cell behavior. *ACS Biomater Sci Eng* 2019; 5(2): 613–622.
127. Chen XY, Low HR, Loi XY, et al. Fabrication and evaluation of bacterial nanocellulose/poly(acrylic acid)/graphene oxide composite hydrogel: characterizations and biocompatibility studies for wound dressing. *J Biomed Mater Res B Appl Biomater* 2019; 107(6): 2140–2151.
128. Wang Y, Liu S and Yu W. Functionalized graphene oxide-reinforced chitosan hydrogel as biomimetic dressing for wound healing. *Macromol Biosci* 2021; 21(4): e2000432.
129. Khalili R, Zarrintaj P, Jafari SH, et al. Electroactive poly (p-phenylene sulfide)/r-graphene oxide/chitosan as a novel potential candidate for tissue engineering. *Int J Biol Macromol* 2020; 154: 18–24.
130. Liang Y, Li M, Yang Y, et al. PH/glucose dual responsive metformin release hydrogel dressings with adhesion and self-healing via dual-dynamic bonding for athletic diabetic foot wound healing. *ACS Nano* 2022; 16(2): 3194–3207.
131. Zhang X, Tan B, Wu Y, et al. An injectable, self-healing carboxymethylated chitosan hydrogel with mild photothermal stimulation for wound healing. *Carbohydr Polym* 2022; 293: 119722.
132. Ding X, Yu Y, Yang C, et al. Multifunctional GO hybrid hydrogel scaffolds for wound healing. *Research* 2022; 2022: 9850743.
133. Feng W and Wang Z. Shear-thinning and self-healing chitosan-graphene oxide hydrogel for hemostasis and wound healing. *Carbohydr Polym* 2022; 294: 119824.
134. Al-Arjan WS, Khan MUA, Almutairi HH, et al. pH-Responsive PVA/BC-f-GO dressing materials for burn and chronic wound healing with curcumin release kinetics. *Polymers* 2022; 14(10): 1949.
135. ur Rehman SR, Augustine R, Zahid AA, et al. Graphene oxide loaded hydrogel for enhanced wound healing in diabetic patients. In: *2019 41st annual international conference IEEE engineering in medicine and biology society*, 2019, pp. 3943–3946.
136. Nguyen HT, Ho TL, Pratomo A, et al. Enzymatically triggered graphene oxide released from multifunctional carriers boosts anti-pathogenic properties for promising wound-healing applications. *Mater Sci Eng C Mater Biol Appl* 2021; 128: 112265.
137. Bai Q, Teng L, Zhang X, et al. Multifunctional single-component polypeptide hydrogels: the gelation mechanism, superior biocompatibility, high performance hemostasis, and scarless wound healing. *Adv Healthc Mater* 2022; 11(6): e2101809.
138. Xie F, Zou L, Xu Z, et al. Alginate foam gel modified by graphene oxide for wound dressing. *Int J Biol Macromol* 2022; 223(Pt A): 391–403.
139. Chen X, Peng Y, Xue H, et al. MiR-21 regulating PVT1/PTEN/IL-17 axis towards the treatment of infectious diabetic wound healing by modified GO-derived biomaterial in mouse models. *Nanobiotechnol* 2022; 20(1): 309.
140. Rehman SRU, Augustine R, Zahid AA, et al. Reduced graphene oxide incorporated GelMA hydrogel promotes angiogenesis for wound healing applications. *Int J Nanomedicine* 2019; 14: 9603–9617.
141. Liang Y, Zhao X, Hu T, et al. Adhesive hemostatic conducting injectable composite hydrogels with sustained drug release and photothermal antibacterial activity to promote full-thickness skin regeneration during wound healing. *Small* 2019; 15(12): e1900046.
142. Zhang H, Zheng S, Chen C, et al. A graphene hybrid supramolecular hydrogel with high stretchability, self-healable and photothermally responsive properties for wound healing. *RSC Adv* 2021; 11(11): 6367–6373.

143. Lužajić Božinovski T, Todorović V, Milošević I, et al. Macrophages, the main marker in biocompatibility evaluation of new hydrogels after subcutaneous implantation in rats. *J Biomater Appl* 2022; 36(6): 1111–1125.
144. Zhu L and Chen L. Facile design and development of nanoclustery graphene-based macromolecular protein hydrogel loaded with ciprofloxacin to antibacterial improvement for the treatment of burn wound injury. *Polym Bull* 2022; 79(9): 7953–7968.
145. Ren Y, Yu X, Li Z, et al. Fabrication of pH-responsive TA-keratin bio-composited hydrogels encapsulated with photoluminescent GO quantum dots for improved bacterial inhibition and healing efficacy in wound care management: in vivo wound evaluations. *Photochem Photobiol* 2020; 202: 111676.
146. Zhang J, Zheng Y, Lee J, et al. A pulsatile release platform based on photo-induced imine-crosslinking hydrogel promotes scarless wound healing. *Nat Commun* 2021; 12(1): 1670.
147. Zhou S, Xie M, Su J, et al. New insights into balancing wound healing and scarless skin repair. *J Tissue Eng* 2023; 14: 20417314231185848.
148. Rasoulzadeh M and Namazi H. Carboxymethyl cellulose/graphene oxide bio-nanocomposite hydrogel beads as anticancer drug carrier agent. *Carbohydr Polym* 2017; 168: 320–326.
149. Rasoulzadehzali M and Namazi H. Facile preparation of antibacterial chitosan/graphene oxide-Ag bio-nanocomposite hydrogel beads for controlled release of doxorubicin. *Int J Biol Macromol* 2018; 116: 54–63.
150. Singh B and Singh B. Influence of graphene-oxide nanosheets impregnation on properties of sterculia gum-polyacrylamide hydrogel formed by radiation induced polymerization. *Int J Biol Macromol* 2017; 99: 699–712.
151. Rehman S, Madni A, Jameel QA, et al. Natural polymer-based graphene oxide bio-nanocomposite hydrogel beads: superstructures with advanced potentials for drug delivery. *AAPS PharmSciTech* 2022; 23(8): 304.
152. Luu CH, Nguyen G, Le TT, et al. Graphene oxide-reinforced alginate hydrogel for controlled release of local anesthetics: synthesis, characterization, and release studies. *Gels* 2022; 8(4): 246.
153. Maturavongsadit P, Wu W, Fan J, et al. Graphene-incorporated hyaluronic acid-based hydrogel as a controlled Senexin A delivery system. *Biomater Transl* 2022; 3(2): 152–161.
154. Desai DT, Maulvi FA, Desai AR, et al. In vitro and in vivo evaluation of cyclosporine-graphene oxide laden hydrogel contact lenses. *Int J Pharm* 2022; 613: 121414.
155. Maulvi FA, Soni PD, Patel PJ, et al. Controlled bimatoprost release from graphene oxide laden contact lenses: in vitro and in vivo studies. *Colloids Surf B Biointerfaces* 2021; 208: 112096.
156. Liu Y, Fan Q, Huo Y, et al. Construction of a mesoporous polydopamine@go/cellulose nanofibril composite hydrogel with an encapsulation structure for controllable drug release and toxicity shielding. *ACS Appl Mater Interfaces* 2020; 12(51): 57410–57420.
157. Gosecka M, Gosecki M and Urbaniak M. Composite dynamic hydrogels constructed on boronic ester cross-links with NIR-enhanced diffusivity. *Biomacromolecules* 2022; 23(3): 948–959.
158. Shen H, Lin Q, Tang H, et al. Fabrication of temperature- and alcohol-responsive photonic crystal hydrogel and its application for sustained drug release. *Langmuir* 2022; 38(12): 3785–3794.
159. Sun X, Liu L, Zou H, et al. Intelligent drug delivery microparticles with visual stimuli-responsive structural color changes. *Int J Nanomedicine* 2020; 15: 4959–4967.
160. Luo Q, Shan Y, Zuo X, et al. Anisotropic tough poly(vinyl alcohol)/graphene oxide nanocomposite hydrogels for potential biomedical applications. *RSC Adv* 2018; 8(24): 13284–13291.
161. Hou L, Shi Y, Jiang G, et al. Smart nanocomposite hydrogels based on azo crosslinked graphene oxide for oral colon-specific drug delivery. *Nanotechnol* 2016; 27(31): 315105.
162. Rahmani Z, Sahraei R and Ghaemy M. Preparation of spherical porous hydrogel beads based on ion-crosslinked gum tragacanth and graphene oxide: study of drug delivery behavior. *Carbohydr Polym* 2018; 194: 34–42.
163. Li P, Dai X, Sui Y, et al. Thermally induced and physically cross-linked hydrogel doped with graphene oxide for controlled release. *Soft Matter* 2021; 17(13): 3664–3671.
164. Li L, Zheng X, Pan C, et al. A pH-sensitive and sustained-release oral drug delivery system: the synthesis, characterization, adsorption and release of the xanthan gum-graft-poly(acrylic acid)/GO-DCFP composite hydrogel. *RSC Adv* 2021; 11(42): 26229–26240.
165. Li H, Jia Y and Liu C. RETRACTED: pluronic® F127 stabilized reduced graphene oxide hydrogel for transdermal delivery of ondansetron: ex vivo and animal studies. *Colloids Surf B Biointerfaces* 2020; 195: 111259.
166. Li Q, Li F, Qi X, et al. RETRACTED: pluronic® F127 stabilized reduced graphene oxide hydrogel for the treatment of psoriasis: in vitro and in vivo studies. *Colloids Surf B Biointerfaces* 2020; 195: 111246.
167. Luo S, Jin S, Yang T, et al. Sustained release of tulobuterol from graphene oxide laden hydrogel to manage asthma. *J Biomater Sci Polym Ed* 2021; 32(4): 524–535.
168. Li W, Zhang G and Wei X. Lidocaine-loaded reduced graphene oxide hydrogel for prolongation of effects of local anesthesia: in vitro and in vivo analyses. *J Biomater Appl* 2021; 35(8): 1034–1042.
169. Guo B, Qiao F, Liao Y, et al. Triptolide laden reduced graphene oxide transdermal hydrogel to manage knee arthritis: in vitro and in vivo studies. *J Biomater Sci Polym Ed* 2021; 32(10): 1288–1300.
170. Yang C and Li T. RETRACTED: transdermal delivery of flurbiprofen from polyoxypropylene-polyoxyethylene block copolymer stabilized reduced graphene oxide to manage pain in spondylitis: in vitro and in vivo studies. *Eur J Pharm Sci* 2021; 165: 105929.
171. Patil R, Kansara V, Ray D, et al. Slow degrading hyaluronic acid hydrogel reinforced with cationized graphene nanosheets. *Int J Biol Macromol* 2019; 141: 232–239.
172. Chengnan L, Pagneux Q, Voronova A, et al. Near-infrared light activatable hydrogels for metformin delivery. *Nanoscale* 2019; 11(34): 15810–15820.

173. Liu W, Zhang X, Zhou L, et al. Reduced graphene oxide (rGO) hybridized hydrogel as a near-infrared (NIR)/pH dual-responsive platform for combined chemo-photothermal therapy. *J Colloid Interface Sci* 2019; 536: 160–170.
174. Saeednia L, Yao L, Berndt M, et al. Structural and biological properties of thermosensitive chitosan-graphene hybrid hydrogels for sustained drug delivery applications. *J Biomed Mater Res A* 2017; 105(9): 2381–2390.
175. Mauri E, Salvati A, Cataldo A, et al. Graphene-laden hydrogels: a strategy for thermally triggered drug delivery. *Mater Sci Eng C Mater Biol Appl* 2021; 118: 111353.
176. Zhu Y, Zeng Q, Zhang Q, et al. Temperature/near-infrared light-responsive conductive hydrogels for controlled drug release and real-time monitoring. *Nanoscale* 2020; 12(16): 8679–8686.
177. Leganés J, Sánchez-Migallón A, Merino S, et al. Stimuli-responsive graphene-based hydrogel driven by disruption of triazine hydrophobic interactions. *Nanoscale* 2020; 12(13): 7072–7081.
178. Leganés Bayón J, Sánchez-Migallón A, Díaz-Ortiz, et al. On-demand hydrophobic drug release based on microwave-responsive graphene hydrogel scaffolds. *Chemistry* 2020; 26(71): 17069–17080.
179. Javanbakht S and Namazi H. Doxorubicin loaded carboxymethyl cellulose/graphene quantum dot nanocomposite hydrogel films as a potential anticancer drug delivery system. *Mater Sci Eng C Mater Biol Appl* 2018; 87: 50–59.
180. Yue J, He L, Tang Y, et al. Facile design and development of photoluminescent graphene quantum dots grafted dextran/glycol-polymeric hydrogel for thermoresponsive triggered delivery of buprenorphine on pain management in tissue implantation. *Photochem Photobiol* 2019; 197: 111530.
181. Papi M, Palmieri V, Bugli F, et al. Erratum: Biomimetic antimicrobial cloak by graphene-oxide agar hydrogel. *Sci Rep* 2017; 7(1): 2779.
182. Cao J, He G, Ning X, et al. Preparation and properties of O-chitosan quaternary ammonium salt/polyvinyl alcohol/graphene oxide dual self-healing hydrogel. *Carbohydr Polym* 2022; 287: 119318.
183. Konwar A, Kalita S, Kotoky J, et al. Chitosan-iron oxide coated graphene oxide nanocomposite hydrogel: a robust and soft antimicrobial biofilm. *ACS Appl Mater Interfaces* 2016; 8(32): 20625–20634.
184. Khan MUA, Yaqoob Z, Ansari MNM, et al. Chitosan/poly vinyl alcohol/graphene oxide based pH-responsive composite hydrogel films: drug release, anti-microbial and cell viability studies. *Polymers* 2021; 13(18): 3124.
185. Hanif W, Hardiansyah A, Randy A, et al. Physically crosslinked PVA/graphene-based materials/aloe vera hydrogel with antibacterial activity. *RSC Adv* 2021; 11(46): 29029–29041.
186. Biswas S, Chatterjee U, Sarkar S, et al. Fabrication of morphologically modified strong supramolecular nanocomposite antibacterial hydrogels based on sodium deoxycholate with inverted optical activity and sustained release. *Colloids Surf B Biointerfaces* 2020; 188: 110803.
187. Wu S, Gan T, Xie L, et al. Antibacterial performance of graphene oxide/alginate-based antisense hydrogel for potential therapeutic application in Staphylococcus aureus infection. *Biomater Adv* 2022; 141: 213121.
188. Luo J, Ma Z, Yang F, et al. Fabrication of laponite-reinforced dextran-based hydrogels for NIR-responsive controlled drug release. *ACS Biomater Sci Eng* 2022; 8(4): 1554–1565.
189. Huang S, Liu H, Liao K, et al. Functionalized GO nanovehicles with nitric oxide release and photothermal activity-based hydrogels for bacteria-infected wound healing. *ACS Appl Mater Interfaces* 2020; 12(26): 28952–28964.
190. Rosselle L, Cantelmo AR, Barras A, et al. An 'on-demand' photothermal antibiotic release cryogel patch: evaluation of efficacy on anex vivomodel for skin wound infection. *Biomater Sci* 2020; 8(21): 5911–5919.
191. Ma X, Wang Z, Yang H, et al. Enhanced bacterial disinfection by cui-bioi/rgo hydrogel under visible light irradiation. *RSC Adv* 2021; 11(33): 20446–20456.
192. Ali NH, Amin MCIM and Ng SF. Sodium carboxymethyl cellulose hydrogels containing reduced graphene oxide (rGO) as a functional antibiofilm wound dressing. *J Biomater Sci Polym Ed* 2019; 30(8): 629–645.
193. Sohni S, Hassan T, Khan SB, et al. Lignin nanoparticles-reduced graphene oxide based hydrogel: a novel strategy for environmental applications. *Int J Biol Macromol* 2023; 225: 1426–1436.
194. Wang Y, Lu Y, Zhang J, et al. A synergistic antibacterial effect between terbium ions and reduced graphene oxide in a poly(vinyl alcohol)–alginate hydrogel for treating infected chronic wounds. *J Mater Chem B* 2019; 7(4): 538–547.
195. Khan MUA, Haider S, Raza MA, et al. Smart and pH-sensitive rGO/arabinoxylan/chitosan composite for wound dressing: in-vitro drug delivery, antibacterial activity, and biological activities. *Int J Biol Macromol* 2021; 192: 820–831.
196. Yan X, Fang WW, Xue J, et al. Thermoresponsive in situ forming hydrogel with Sol-gel irreversibility for effective methicillin-resistant Staphylococcus aureus infected wound healing. *ACS Nano* 2019; 13(9): 10074–10084.
197. Cheng C, Zhong H, Zhang Y, et al. Bacterial responsive hydrogels based on quaternized chitosan and GQDs-ε-PL for chemo-photothermal synergistic anti-infection in diabetic wounds. *Int J Biol Macromol* 2022; 210: 377–393.
198. Gungordu Er S, Edirisinghe M and Tabish TA. Graphene-based nanocomposites as antibacterial, antiviral and antifungal agents. *Adv Healthc Mater* 2023; 12(6): e2201523.
199. Zhang F, Zhang N, Meng HX, et al. Easy applied gelatin-based hydrogel system for long-term functional cardiomyocyte culture and myocardium formation. *ACS Biomater Sci Eng* 2019; 5(6): 3022–3031.
200. Cheng YH, Cheng SJ, Chen HH, et al. Development of injectable graphene oxide/laponite/gelatin hydrogel containing Wharton's jelly mesenchymal stem cells for treatment of oxidative stress-damaged cardiomyocytes. *Colloids Surf B Biointerfaces* 2022; 209(Pt 2): 112150.
201. Soltani S, Emadi R, Haghjooy Javanmard S, et al. Development of an injectable shear-thinning nanocomposite hydrogel for cardiac tissue engineering. *Gels* 2022; 8(2): 121.
202. Zhou J, Yang X, Liu W, et al. Injectable OPF/graphene oxide hydrogels provide mechanical support and enhance cell electrical signaling after implantation into myocardial infarct. *Theranostics* 2018; 8(12): 3317–3330.
203. Mousavi A, Mashayekhan S, Baheiraei N, et al. Biohybrid oxidized alginate/myocardial extracellular matrix injectable

hydrogels with improved electromechanical properties for cardiac tissue engineering. *Int J Biol Macromol* 2021; 180: 692–708.
204. Raslan A, Ciriza J, Ochoa de, Retana AM, et al. Modulation of conductivity of alginate hydrogels containing reduced graphene oxide through the addition of proteins. *Pharmaceutics* 2021; 13(9): 1473.
205. Shin SR, Zihlmann C, Akbari M, et al. Reduced graphene oxide-GelMA hybrid hydrogels as scaffolds for cardiac tissue engineering. *Small* 2016; 12(27): 3677–3689.
206. Zhu S, Yu C, Liu N, et al. Injectable conductive gelatin methacrylate / oxidized dextran hydrogel encapsulating umbilical cord mesenchymal stem cells for myocardial infarction treatment. *Bioact Mater* 2022; 13: 119–134.
207. Tsui JH, Leonard A, Camp ND, et al. Tunable electroconductive decellularized extracellular matrix hydrogels for engineering human cardiac microphysiological systems. *Biomaterials* 2021; 272: 120764.
208. Si R, Gao C, Guo R, et al. Human mesenchymal stem cells encapsulated-coacervated photoluminescent nanodots layered bioactive chitosan/collagen hydrogel matrices to indorse cardiac healing after acute myocardial infarction. *Photochem Photobiol* 2020; 206: 111789.
209. Rostamzadeh F, Jafarinejad-Farsangi S, Ansari-Asl Z, et al. Treatment for myocardial infarction: in vivo evaluation of curcumin-loaded PEGylated-GQD nanoparticles. *J Cardiovasc Pharmacol* 2023; 81(5): 361–372.
210. Rostamzadeh F, Najafipour H, Jafarinejad-Farsangi S, et al. Beneficial effects of PEGylated graphene quantum dot on arrhythmias induced by myocardial infarction. *Biotechnol Appl Biochem* 2022; 69(5): 2222–2228.
211. Zhang X, Song C, Nong H, et al. Development of an asymmetric hydrophobic/hydrophilic ultrathin graphene oxide membrane as actuator and conformable patch for heart repair. *Adv Funct Mater* 2023; 33(32): 2300866.
212. Ovcharenko EA, Seifalian A, Rezvova MA, et al. A new nanocomposite copolymer based on functionalised graphene oxide for development of heart valves. *Sci Rep* 2020; 10(1): 5271.
213. Yang H, Zheng H, Duan Y, et al. Nanocellulose-graphene composites: preparation and applications in flexible electronics. *Int J Biol Macromol* 2023; 253(Pt 3): 126903.